UNIVERSITY OF THE
WITWATERSRAND,
JOHANNESBURG

Prediction of Ground Instability for Coinciding Mining Operations

Prosper Munemo

A research report submitted to the Faculty of Engineering and the Built Environment, University of the Witwatersrand, Johannesburg, in partial fulfilment of the requirements for the degree of Master of Science in Engineering.

Johannesburg, 2021

DECLARATION

I declare that this research report is my own, unaided work. It is being submitted for the degree of Master of Science in Engineering in the University of the Witwatersrand, Johannesburg. It has not been submitted before for any degree or examination in any other University.

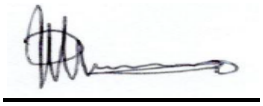

Prosper Munemo

8th day of July 2021

ABSTRACT

It is common knowledge that mining activities bring about instabilities in the rock mass. These ground instabilities are excessive when the mining operations involve interacting underground and surface mining excavations. This can be attributed to strata relaxation which induces tensile stresses around excavations. This research focused on predicting the behaviour of the rock mass upon which the underground excavations were interacting with a mined out open pit. The research was based on a case study mining operation situated along the Great Dyke of Zimbabwe.

Rock mass characterisation using the Q-system was used to show the quality of the rock mass intermediate the underground and pit excavations. Finite Element Analysis (FEA) was used to model the excavations both in 2D and 3D with the purpose of predicting the stress distributions and deformations around the mining excavations. Three-dimensional modelling was done to give an insight on how the stresses were distributed in the third dimension. Thus, 3D modelling allowed for effective determination of the average pillar stress on the in-panel pillars. The 2D model was also used in the stability analysis of the intermediate pillar created between the underground and pit excavations.

The rock mass characterisation showed that the rock mass was fairly intact basing on the considerably high RQD values. However, the resultant Q-values were considerably low due to the low J_w values assigned to the rock mass. The low J_w values corroborated well with what was observed in the field survey whereby water could be seen dripping from the support boreholes. The 2D maximum principal stress analysis, showed that the zone of very low compressive stresses and tensile stresses was larger in the hanging wall of the panel in the close proximity to the intermediate pillar. The total displacements predicted by the 2D model were very small (≤4mm) thereby implying some linear elastic behaviour in the rock mass. The 3D model predicted an average pillar stress of 20MPa, whereas the 2D model predicted an average pillar stress of 6MPa. This showed that the 2D model underestimated the pillar stresses. This is attributed to the fact that 3D analysis effectively considers the tributary load imposed on the in-panel pillars which is not the case with 2D analysis.

From the stability analysis of the intermediate pillar, it was observed that the strength factor of the rock mass decreases with a decrease in the pillar width. Zones of low strength factor (SF ≤1) in the rock mass surrounding the pit highwall side were common especially on the model with an intermediate pillar width of 6m. Analysis of the minor principal stresses in the

hanging walls of the underground panels showed that the rock mass was subjected to tensile stresses with the tensile zone enlarged on the panel in the close proximity to the intermediate pillar. Usually, plastic deformation happens due to these tensile stresses. Thus, it can be concluded that in shallow excavations, the size of the plastic zone around underground panels is not only dependent on the mechanical properties of the rock but also on the position of the panels relative to other nearby excavations.

It is recommended that if underground excavations are interacting with a mined-out pit, it is prudent to backfill the pit in order to increase the rock mass confinement. However, there is potential of accumulation of water in the backfill which can adversely affect the rock mass stability. Therefore, a dewatering system must be put in place to control the water accumulations on the pit. This will reduce the risk of water inrushes into the underground workings. With the likely emergency of more such mining operations along the Great Dyke of Zimbabwe, this research equips the rock engineers and planning engineers to come up with designs of mining excavations which are economically viable and guaranteed of stability.

ACKNOWLEDGEMENTS

I would like to start by thanking my employer, Manicaland State University of Applied Sciences, for the financial assistance throughout my studies. I would also like to express my sincere gratitude to Zimplats Holdings Limited for allowing me to make use of their geotechnical database to carry out this research. The rest of the staff at Zimplats Mines Rock Engineering Division is sincerely appreciated for their unparalleled support and special mention goes to the rock engineering manager, Eng. Patrick Mushangwe.

To my supervisor, Prof. Rudrajit Mitra, I would like to offer my sincere gratitude and appreciation for your guidance throughout this research, without which the substance of this research would not have been of this high quality. Special thanks also go to my lecturer, Prof. Thomas Richard Stacey, for inspiring me to have passion for rock engineering. Your zeal to impart rock engineering knowledge to your students inspired me to strive for academic excellence.

To my classmates, thank you so much for the teamwork and fun that we had during our group discussions.

And lastly, to my wife, Caroline and my mother, Margaret, surely words cannot rightfully express how grateful am I to the love and encouragement that you proffered throughout my studies.

TABLE OF CONTENTS

LIST OF FIGURES

LIST OF TABLES

NOMENCLATURE

Acronyms	Description
COP	Code of Practice
DEM	Discrete Element Method
DFN	Discrete Fracture Network
DRMS	Design Rock Mass Strength
FDM	Finite Difference Method
FEA	Finite Element Analysis
FEM	Finite Element Method
GCD	Ground Control District
GDP	Gross Domestic Product
GPR	Ground Penetrating Radar
GPS	Global Positioning System
GSI	Geological Strength Index
InSAR	Interferometric Synthetic-Aperture Radar
IRS	Intact Rock Strength
MOSHAB	Mines Occupational Safety and Health Advisory Board
MRMR	Mining Rock Mass Rating
MSZ	Main Sulphide Zone
PGM	Platinum Group of Metals
RGA	Regional Geotechnical Areas
RMS	Rock Mass Strength
RQD	Rock Quality Designation
UCS	Uniaxial Compressive Strength

1 INTRODUCTION

1.1 General Overview

Mining activities, whether surface or underground, are always bound to disturb the stability of rock masses such that if they are not properly managed, the consequences can be catastrophic. In most mining operations which are associated with deposits which outcrop to the surface, it is a general norm that open pit mining is initially employed to exploit the deposits. However, as the depth increases, the operations become uneconomically viable. When the operations are no longer viable, transition to underground mining is usually opted for whereby the underground operations operate directly underneath the open pits. In some instances, the underground operations do not start directly below the open pit but can approach from a certain lateral direction such that the excavations will eventually coincide with the open pit floor. As these underground activities approach the vicinity of the open pit bottom, there is an increase in ground instability which can adversely influence the stability of the open pit slopes. Swindells et al. (2000) argued that this influence is very difficult to predict with the use of standard equilibrium methods since they fail to account for stress concentrations due to underground excavations. The use of numerical modelling codes to simulate the mining operations enhances the prediction of the rock mass behaviour in these typical mining operations.

1.2 Research Background

Platinum Group of Metals (PGM) mining in Zimbabwe is concentrated on the magma sub-chambers found on the Great Dyke. The sub-chambers host the Main Sulphide Zone (MSZ) which is highly mineralised with PGMs. Generally, this MSZ is a continuous layer forming an elongated basin which dips fairly shallow on the limbs and is relatively flatter near the centre of the basin as shown in Figure 1.1. The limb parts of the deposit outcrops on the surface therefore, making them compatible to be mined by open pit method. However, the flatter portions are situated relatively deeper from the surface, thus allowing the use of underground room and pillar mining method to exploit them. The use of both mining methods on the same deposit therefore entails that there is always potential for interactions between the underground and surface excavations which are highly likely to produce adverse effects on the ground stability.

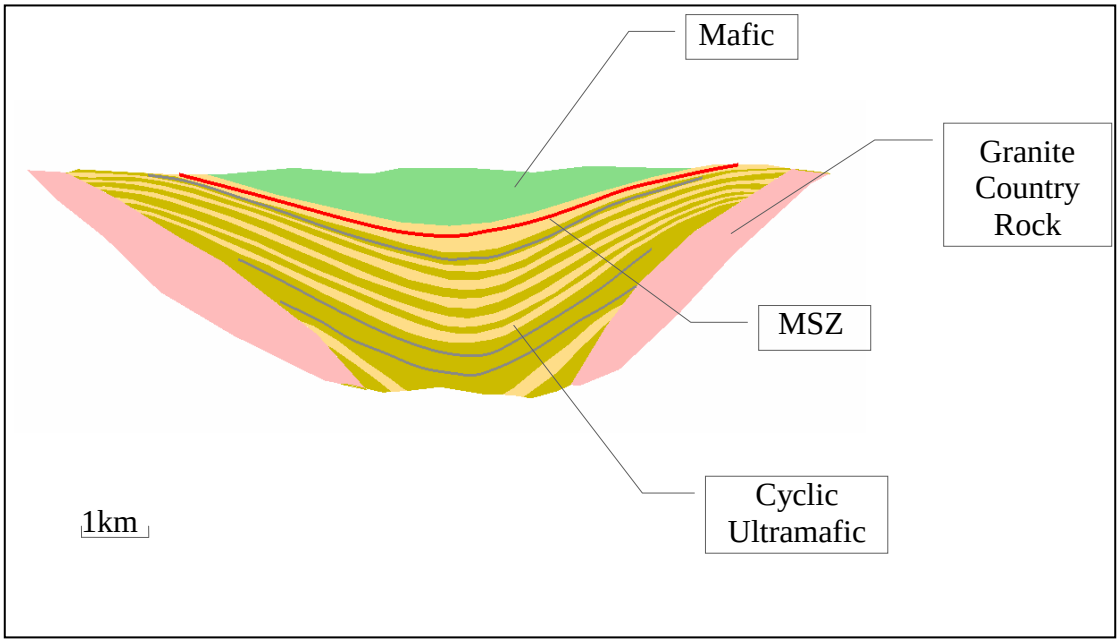

Figure 1.1: Great Dyke cross section (Zimplats Holdings Limited, 2012)

Some of these PGM mines in Zimbabwe have opted to start by mining the flatter portions of the deposits by room and pillar method and plans are underway to find efficient and safe methods to extract the minerals in the limb parts of the deposits. This research however, looks at a case study mine whereby the limb parts of the deposit have been initially exploited by open pit and underground excavations are proceeding in the direction towards the mined out open pit and eventually these excavations will coincide. It is highly expected that as the underground excavations approach the zones which have previously been influenced by the foregoing open pit operations, adverse ground stability issues will be prevalent. This then prompts the desire to predict the behaviour of the rock mass beforehand thereby creating a foundation for crafting mitigatory measures to ensure safety in the mining operations.

1.3 Problem Identification

The creation of underground excavations below or in the proximity of an already existing open pit excavation is always likely to pose hazards to both personnel and equipment as the crown pillar or pit floor is highly likely to succumb. The rock mass separating the pit bottom and underground excavations (inter-burden) is subjected to excessive stress redistributions as well as blast induced damage thereby posing a danger of weakening it. Sepehri et al. (2017) argued that, *"Redistribution of these stresses due to the mining activities causes the development of mining-induced stresses which ultimately can lead to deformation and failure of the ground"*. Deterioration of the inter-burden due to penetration of water in the rock mass discontinuities necessitated by a high influx of rainfall water in the open pit is inevitable. The

open pit slopes situated on the side from which the underground workings are approaching, are likely to have frequent failures due to blast induced vibrations. When these pit slopes continue to experience failure there will be progressive extension of the pit beyond the planned limits thereby damaging the surface environment. The need to drive underground mining excavations in these weakened rock masses therefore requires a holistic approach on the design of the support systems. Adoption of good support systems helps to prevent catastrophic cases of fall of ground which could cause loss of human life, mineral resources as well as mining equipment. Ground failures can also result in major sterilisation of the mineral resource as was experienced by Zimplats in 2014 whereby one of its portals, Portal 4 (Bimha Mine), had 50% of its mining area being sterilised due to ground failure. Zimplats Holdings Limited (2014) highlighted that the group's overall production was adversely affected by approximately 70,000 ounces of platinum as a result of the closure of Bimha Mine. Fall of ground still remain a major cause for injuries in these underground mining activities as is indicated in the chart shown in Figure 1.2.

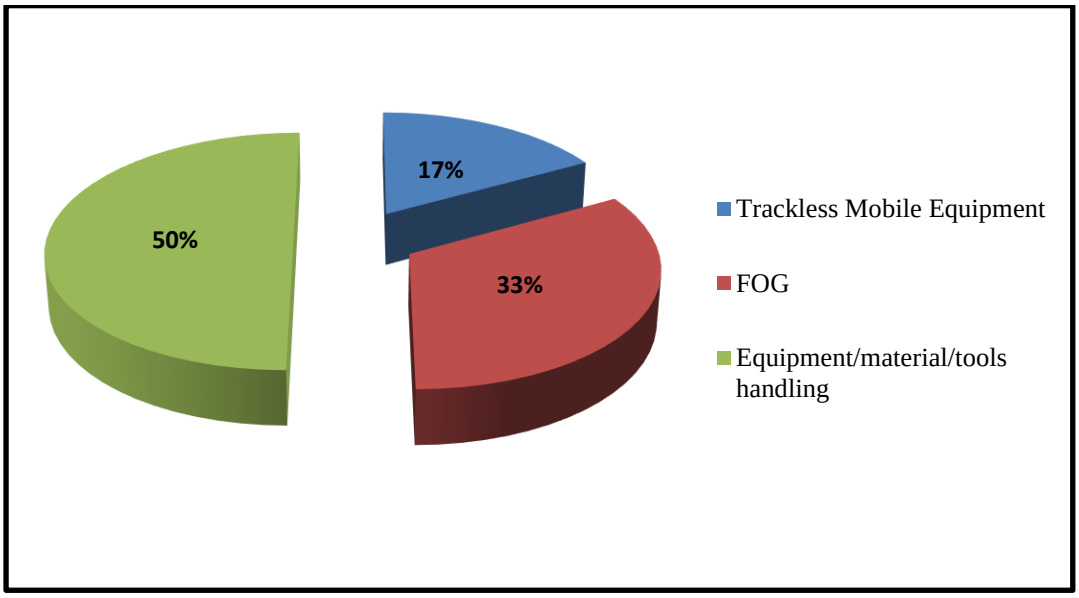

Figure 1.2: Injury causation agents (Zimplats Holdings Limited, 2017)

Figure 1.2 above shows that fall of ground (FOG) causes a lot of injuries in mining environments, hence the need to plan on how to navigate mining activities through these weakened rock masses. The simulation of these interacting mining activities through the use of numerical modelling codes therefore makes it possible to predict ground behaviour and plan, beforehand, on how to deal with these possible ground failures.

1.4 Rationale and Motivation

Mineral resources, if well managed, can aid in the growth of a country's Gross Domestic Product (GDP). Hence there is need to extract them in an efficient and safe manner so that their exploitation can contribute towards the betterment of humankind. The major challenge is that some of these natural resources exist in complex distributions which are predefined by nature such that there is a need for devising safe and economical ways to extract them. The use of finite element numerical modelling codes RS2 Version 10.0 by Rocscience (2019a) and RS3 Version 3.0 by Rocscience (2019b), facilitated for the prediction of the behaviour of the rock mass. This will highlight important information which can then be used as a benchmark for other similar operations which are certainly going to come up in the near future. The highlighting of these ground stability issues will benefit mining activities in the following ways:

- Minimisation or eradication of the sterilisation of mineral resources due to massive ground failure since design of appropriate ground support and reinforcements is planned in advance;
- Improved worker moral as they are assured of a safe working environment since systems to combat ground failures which can result in human fatalities and/or injuries would have been put in place; and
- Foreknowledge on how to deal with adverse ground stability enhances the viability of the mining project as the risk is better managed.

Extensive research has been done focusing on how to deal with ground stability in mines which are in transition from open pit mining to underground mining in steeply dipping ore bodies. However, there is still little information covering ground stability issues when dealing with flat or shallow dipping deposits that are exploited by the method of room and pillar mining advancing towards a mined out open pit mine. Hence, this research is an attempt to further expand some understanding on ground stability issues associated with interacting mining excavations.

1.5 Research Scope

This research will focus on predicting the influence of stress redistributions around excavations as they are mined through a disturbed rock mass. The stress redistributions are considered to have been induced by the foregoing open pit mining activities. Therefore, it is expected that the use of numerical analysis methods will depict the portions of the excavations that are prone to failure. The first stage is the characterisation of the rock mass

between the approaching underground mining activities and the mined out open pit so as to take into consideration the extent to which the rock mass strength parameters have been altered. This characterisation is based on the data collected from exploration core logs and structural mapping done on the pit and underground walls. Numerical analysis is then used to model and simulate the mining activities so that predictions are made on how stresses are redistributed around excavations and how displacements are exhibited as the underground mining operations approach the pit floor. The simulations also take into consideration the influence of water accumulations on ground stability in the open pit as well as the impact of backfilling the open pit. The research will be limited to a case study mine, Portal 2 (Rukodzi Mine), which falls under Zimplats Mines, which presents a typical scenario whereby underground mining activities are advancing towards a mined out open pit.

1.6 Research Objectives

The objectives of this research are as follows:

- To characterise the rock mass through the use of the rock mass classification systems by taking into consideration the disturbances induced by the open pit operations;
- To generate a numerical model of the mine and simulate mining operations that will be used to predict highly stressed areas, around excavations, which are prone to fail; and
- To carry out a stability analysis of the pillar intermediate the underground and pit excavations.

1.7 Structure of the Report

This first chapter highlights the background of the research which is mainly focused on the ground instability issues associated with the exploitation of near-surface PGM deposits in Zimbabwe. The exploitation of such type of deposits is likely to be widespread in the near future along the Great Dyke. All of these PGM deposits are situated along the Great Dyke hence; they all have similar deposit geometry as described earlier. This implies that mining operations which involves the interactions of open pit and underground excavations are more likely to be implemented. This chapter also clearly lays down the problem definition which highlights the ground instability issues associated with interacting open pit and underground operations and has provided a clear justification of the need to have this research. The research objectives are also brought out in this chapter and the remaining portions of the research are structured as described below and depicted in Figure 1.3.

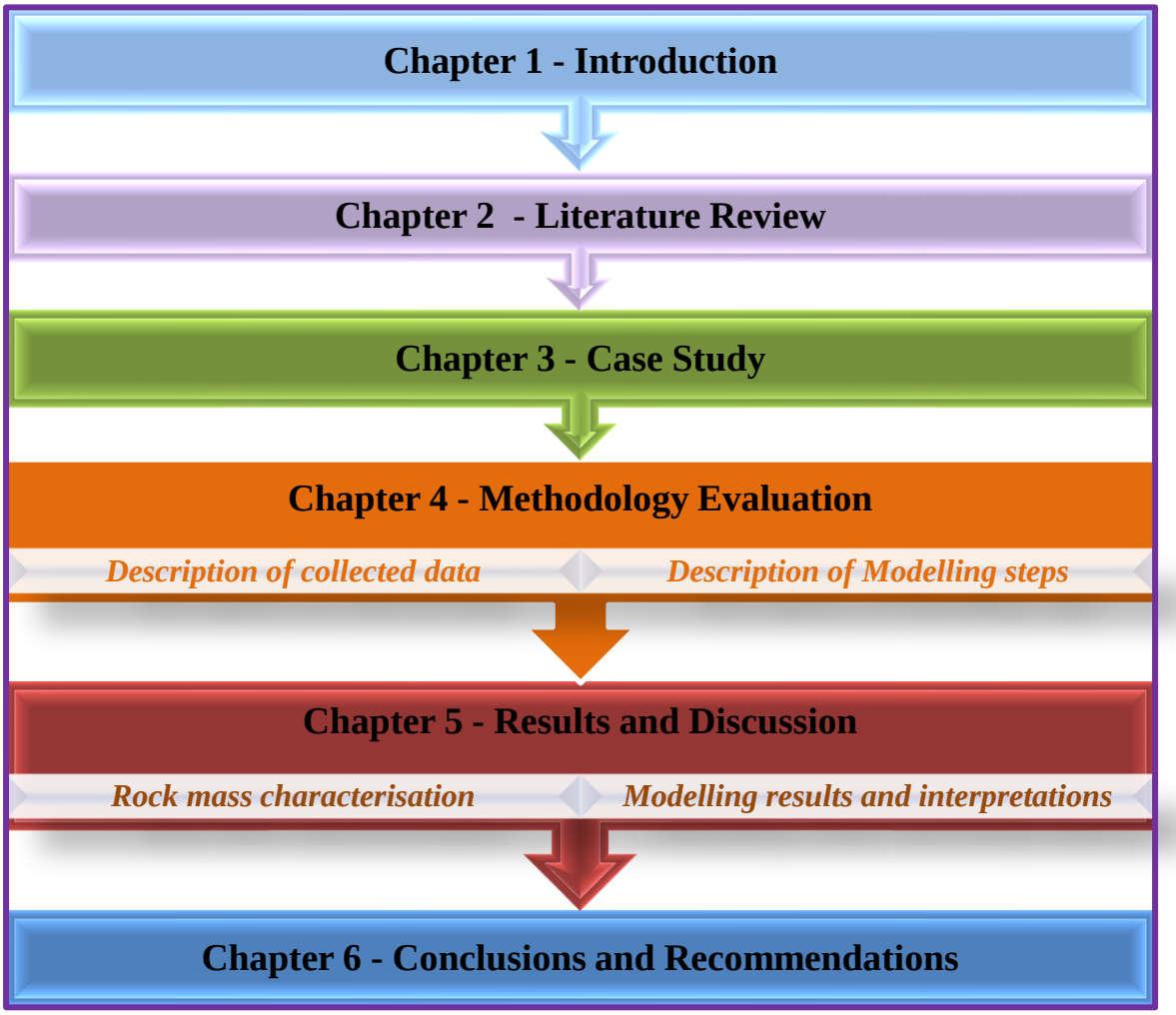

Figure 1.3: Structure of research report

The second chapter gives attention to the review of literature with the major focus on how rock masses are characterised using the various rock mass classification systems. In the same chapter, concepts of numerical modelling applications in rock masses are also explored. An emphasis is put on describing the concepts of the Finite Element Method (FEM) which is the underlying technique in the Rocscience RS2 and RS3 modelling packages. This chapter also carries the description of the various approaches which are used to determine the stable crown pillar thickness. Ground stability issues associated with coinciding mining operations are also looked into in this chapter.

The third chapter gives an overview of the Zimplats Mines group of mining operations. The focus is then narrowed down to the specific mine, Portal 2 (Rukodzi Mine), which has been used as a case study in this research. Portal 2 is a very suitable case study since it is comprised of underground mining operations interacting with a mined out open pit, which is the centre of attention of this research. The mine geometry, common geological structures and the prevailing mining parameters are also presented in this chapter. Descriptions of the

regional and local geology as well as climatic conditions of the area are also highlighted in this third chapter.

The fourth chapter is basically made up of two major parts. The first part deals with the description of the collected data as well as assumptions to which the validity of the use of the data in this research is based upon. The second part of this chapter focuses on describing how the mine geometry has been incorporated into the modelling packages RS2 and RS3. A description of the modelling steps from the stage of model set-up up to running of various analyses is also highlighted in this chapter. Furthermore, the chapter gives an insight of the various analyses carried out to bring out results presented in the fifth chapter.

The fifth chapter underlines the results from the rock mass classifications used to characterise the rock mass. Modelling results and their interpretations are presented in this chapter. The predicted stable crown pillar thickness is also presented in this fifth chapter. Chapter six provides the conclusions and recommendations arising from this research.

2. LITERATURE REVIEW

2.1 Introduction

Mining of most of the ore bodies which outcrops to the surface is usually achieved by initially employing surface mining methods then later on migrate to underground mining. Transition from surface to underground mining operations has mainly been practised on steeply dipping deposits. These deposits usually have a greater depth of continuity such that the surface mining method will reach a point where it is rendered uneconomic. In such typical deposits, when open pit mining method reaches its limit, underground access excavations such as shafts or ramps are usually sunk within the open pit to minimise mining development costs that could be incurred if these excavations were to be sunk from the surface.

One such typical mine which has successfully transitioned from open pit mining to underground sublevel stoping is Freda Rebecca Mine in Zimbabwe. Edison Investment Research (2012) confirmed the transition of mining operations that have happened at Freda Rebecca Mine when they pointed out that, *"Reserves are located in three principal areas of the mine, namely the 7, 12 and 6 areas, down to a depth of 1,040m and accessed via two single entry twin ramps driven from portals developed in both the Freda and Rebecca former open pits and mined by mechanised sub-level open stoping".*

Zimplats Mine took a similar approach at one of its portals, Portal 2 (Rukodzi Mine), where a decline was sunk inside the western pit to develop an underground room and pillar mine. However, the underground mining activities are now advancing towards a mined out eastern open pit such that these underground excavations will eventually coincide with the eastern pit bottom. The major difference between Freda Rebecca Mine and Zimplats Mines is that the former involves transition from open pit mining to steeply dipping sublevel open stoping operations, whereas the later involves transition to shallow and flat dipping room and pillar mining.

2.1.1 Underground Mining at Shallow Depths

Swart et al. (2000) defined near surface mining operations as those which happen at depths less than 100m below surface, whereas shallow mining involves mining at depths less than 1000m below surface. Ground instability in room and pillar mines at shallow depths is mainly controlled by geological structures which manifests as block and wedge failures as well as beam failure in stratified and bedded rocks (Swart et al., 2000). Generally, shallow

mining operations are associated with an influx of ground failures due to presence of discontinuities such as faults, shear zones, bedding planes and low angled joints. Intersections of these structures cause the release of blocks or wedges which can fall or slide from the excavations. These geological structures can also create domes in the panel hanging wall and when the dome weight exceeds the strength of the joint surface then failure occurs. Dome fallouts are more prevalent in shallow mining operations where clamping stresses are significantly low (Swart et al., 2000).

2.1.2 Hazards Associated with Coinciding Mining Operations

Normally, transitions in mining operations are associated with adverse ground stability concerns which, if not well managed, can lead to loss of human life, equipment and mineral resources. In addition to exercising caution, Holley et al. (2006) argued that, it is important to recognise that mining costs within areas that are in the immediate vicinity of abandoned underground workings are often much higher due to a requirement for additional safety and operational procedures, and also the different breakage (blasting) characteristics of the rock. The principal factors influencing the stability of the development slope is the geology, the physic-mechanical properties of the soil and rock in the slope, and the groundwater hydrology (He et al., 2007).

In the case of underground operation located below the open pit, slope strain can be expected as a result of subsidence induced by underground exploitation (Nguyen and Niedbalski, 2016). The underground operations may cause changes in the rock mass mechanical properties, ground water levels and the state of stress which may lead to slope deformation. If the pits are still being worked upon or have been mined out and are left not backfilled, there are high chances of massive slope failure due to underground operations. Such failures where there was influence by underground operations were once experienced at Palabora Mine and Ernest Henry Mine in 2004 and 2014 respectively (Nguyen and Niedbalski, 2016).

Swindells et al. (2000) argued that there is considerable amount of literature describing excavation interactions between abandoned underground mines and new open pit mines, rather than the impact of new underground excavations on an existing open pit slope. There is still little information specifically dealing with a typical scenario such as the one being focused on in this research. According to the MOSHAB (2000), the hazards associated with mining through abandoned or operating underground workings include:

- sudden and unexpected collapse of the open pit floor and/or open pit walls;

- the loss of people and/or equipment into unfilled or partially filled underground workings;
- loss of explosives from charged blast holes that have broken through into the underground workings;
- overcharging of blastholes where explosives have filled cavities connected to the blasthole; and
- risk of flyrock from cavities close to the pit floor and adjacent blast holes, particularly when explosives have entered the cavity from the blasthole during charging and the loss is not detected.

In general, the hazards mentioned above are significantly increased when the underground workings have not been backfilled with waste rock, sand fill, etc (MOSHAB, 2000). In addition to the above-mentioned hazards, MOSHAB (2000) also argues that when open pit mine excavations approach current operating mines, further hazards include:

- flooding of the underground workings;
- instability of the open pit walls and surrounding surface areas; and
- adverse effects on the underground mine ventilation system.

Ideally, this is true especially when the open pit excavations create sink holes which allow easy passage of water (for example, rainfall) into the underground workings. Furthermore, as the open pit deepens approaching the underground workings, the open pit floor is bound to fail and fall into underground excavations thereby blocking the ventilation airways.

2.2 Ground Instability

Ground instability is one of the major hazards associated with mining operations. It is brought about by either natural or artificial external factors or could be due to a combination of factors. British Geological Survey (2011) defined natural ground instability as the propensity for upward, lateral or downward movement of the ground that can be caused by a number of natural geological hazards. WorkSafe New Zealand (2016) in its Code of Practice (COP) identified that ground instability in mining operations is caused by several factors including:

- inadequately designed ground support;
- poor quality of ground support consumables;
- poorly installed ground support;
- deteriorated ground support;
- mining induced seismicity;

- natural seismicity;
- excessive compressive stress around excavations;
- excessive shear stress on discontinuities;
- tensile forces around excavations resulting from strata relaxation;
- ground water or artificially introduced water;
- presence of adverse geological structures in immediate vicinity of excavation;
- inappropriate choice of excavation or mining method;
- loose blocks due to poor rock mass quality in the perimeter of the excavation;
- collapse from localised or general thawing, or ineffective freeze due to moving ground water (ground freezing);
- excessive blast damage to the perimeter of the excavation;
- inappropriate shape and size of pillars, roadways or roadway alignment;
- pillar failure or collapse due to undersized pillars or poor mine layout; and
- load transfer, abutment stress, periodic weighting, face slabbing.

2.2.1 Ground Failure Mechanisms

The causes of ground instability mentioned above usually manifest in various types of ground failure mechanisms in underground mining operations. Figure 2.1 depicts the type of failures experienced in underground excavations due to the influence of in-situ stress and rock mass structure. When excavations are driven in a low stress mining environment, failure is mainly due to continuity and distribution of natural fractures in a brittle rock mass. Low stresses also allow the unraveling of blocks from the excavation surfaces if the rock mass is highly fractured as shown in Figure 2.1.

However, in high stress environments, new stress-induced fractures are created and usually these are parallel to the excavation boundary (Martin et al., 1999). Failure manifests as squeezing and swelling of rocks in high stresses. Stress induced failure in brittle rock masses are associated with slabbing and spalling and the failure zone exhibit a notched-shape regardless of the excavation shape. The far field stress coupled with excavation geometry and the rock mass strength also influences the depth of failure significantly. According to Castro and McCreath (1997), in intermediate stress environments rectangular shaped excavations with a flat roof are more stable than those with arched roofs.

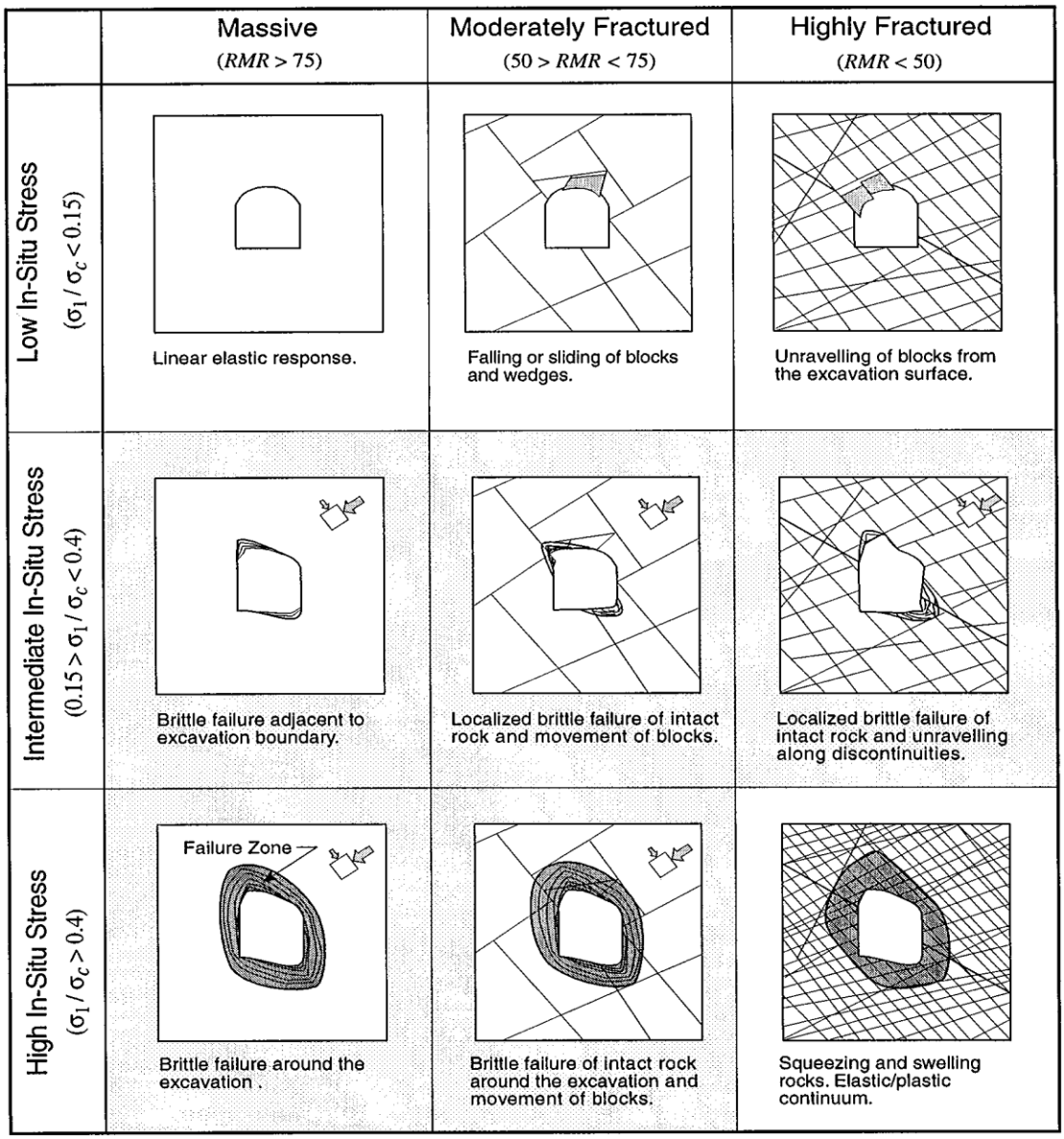

Figure 2.1: Ground failures in varying levels of stress and rock structures (after Martin et al., 1999)

2.2.1.1 Intact Rock Failure

According to Stacey and Swart (2001), this is a type of failure which takes place through intact rock material and it manifests differently in various rock types. Slabbing and spalling of excavation surfaces is exhibited in brittle rock, whereas in other rock types, shearing is exhibited.

2.2.1.2 Structural Failure

This is failure induced by the high prevalence of structural weakness planes such as joints, faults and bedding planes. The rock mass is rendered weaker than its parent rock. Thus, the stability of excavations in such rock mass environments is dependent on factors such as water saturations, confining stress and intensity of joints and joint strength.

2.2.1.3 Composite Failure

Baczynski (2000) described composite failure mechanisms as those failures involving combinations of intact rock material fracture and shear movement on defects. Composite failure mechanisms are mainly influenced by changes in stress distributions as these increase the intensity of minor fractures within the intact rock mass.

2.2.2 Rock Mass Stresses

Rock masses are always subjected to some kind of stresses every time and these stresses vary depending on what would have caused them. The various types of stresses that can be induced in rock masses include virgin/in-situ, tectonic, residual and field stresses.

2.2.2.1 Virgin Stresses

These are natural stresses which exist in the rock mass before any excavation is made. The magnitude and direction of the stress are mainly controlled by overlying strata and geological history. They usually take up the orientation and relative magnitude of the stress that have caused the most recent deformations (Stacey, 2018). In numerical modelling, virgin stresses determine the boundary conditions for stress analyses and these guides the stresses and deformations that result from creating excavations in the model. If the rock mass is undisturbed (which must be the condition for them to be termed virgin/in-situ stresses), the vertical component, q_v, of the rock stresses is due to gravity and is given by Equation [2.1].

$$\boldsymbol{q_v = \rho g h} \qquad \textbf{[2.1]}$$

Where, $\boldsymbol{\rho}$ is the rock mass density (t/m^3);

$\boldsymbol{g}$ is the acceleration due to gravity (m/s^2); and

$\boldsymbol{h}$ is the depth below surface (m).

The corresponding horizontal virgin stresses, which are difficult to measure, are usually calculated as an average of the two components considered along the strike and dip of the deposit. The horizontal and vertical components are connected by the following relationship shown in equation [2.2].

$$\boldsymbol{q_h = k q_v} \qquad \textbf{[2.2]}$$

Where, $\boldsymbol{k}$ is the horizontal to vertical stress ratio

The k-value decreases with increasing depth but at shallow depths it is usually high thus implying that when mining is being done at shallow depths there are high possibilities that excavations will experience high horizontal stresses. Extreme values of k-ratio, that is, $k < 0.4$ *or* $k > 2.5$, increase the likely occurrence of seismic activity (Stacey, 2018). Stacey (2018) further emphasised that low k-values are associated with reduction in the resistance to stabilization of the pillars to foundation failure. However, high k-values are linked to damage of tunnels especially in shallow mining stations.

According to Stacey and Wesseloo (1998), in-situ stresses may have a beneficial influence to the stability of the excavations if they are of a high enough magnitude to cause the confinement of the rock mass. However, if the stresses are of low magnitudes, there are high chances of instability in the rock masses since the confinement effect is reduced. Stacey and Wesseloo (1998) went on to emphasise that if the stresses are too high, fractures and failure in the rock masses maybe induced thus causing instability. Substantial in-situ stress measurements have been carried out in several parts of the world which culminated in the release of an updated world stress map by Heidbach et al. (2016), as shown in Figure 2.2. However, not many sites have been measured in Zimbabwe. In the few measurements that have been done in Zimbabwe, most of the data has not been published and it is contained in the databases for those specific mines.

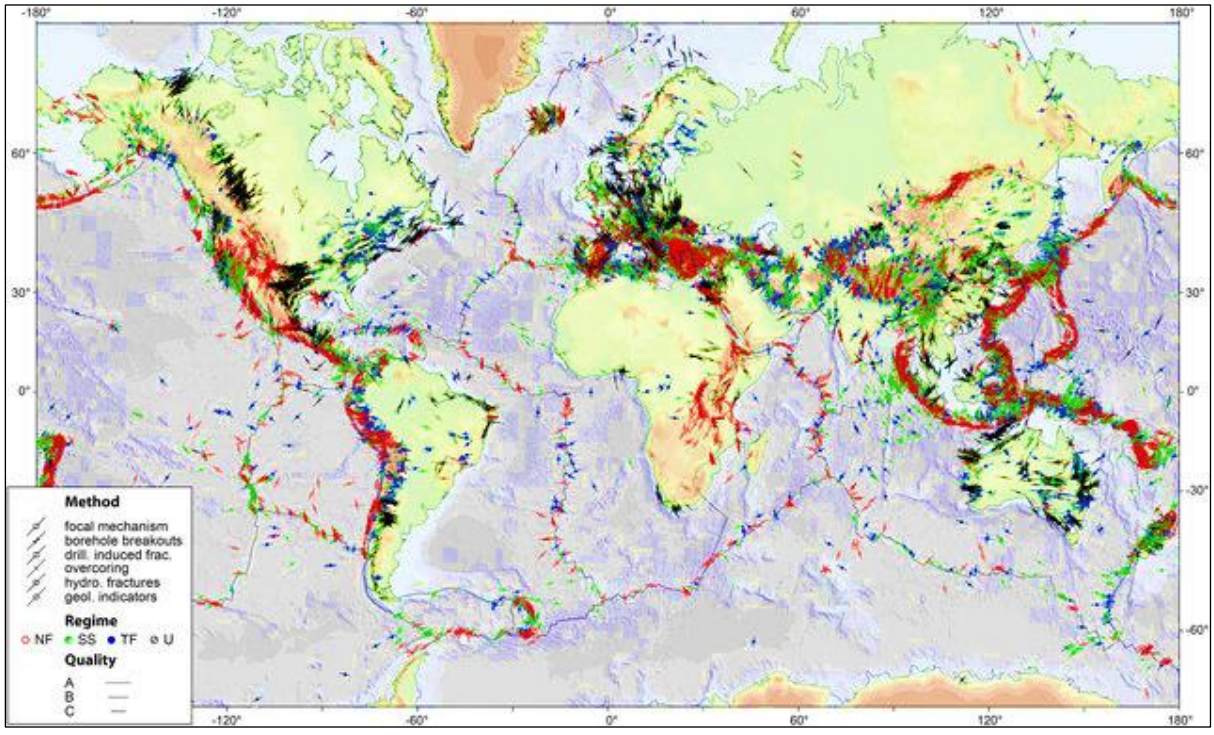

Figure 2.2: World stress map (after, Heidbach et al., 2016)

Figure 2.3 shows some of the measuring sites in the Southern Africa region with Zimbabwe having three sites. (i.e. those numbered 1-3). One of the measuring sites, numbered 1 on Figure 2.3, was at Shabani Mine at a depth of 350m below the surface. The site comprised of a dunite-serpentitite rock mass which has been folded and disrupted by shear zones, wrench and thrust faults (Gay, 1975).

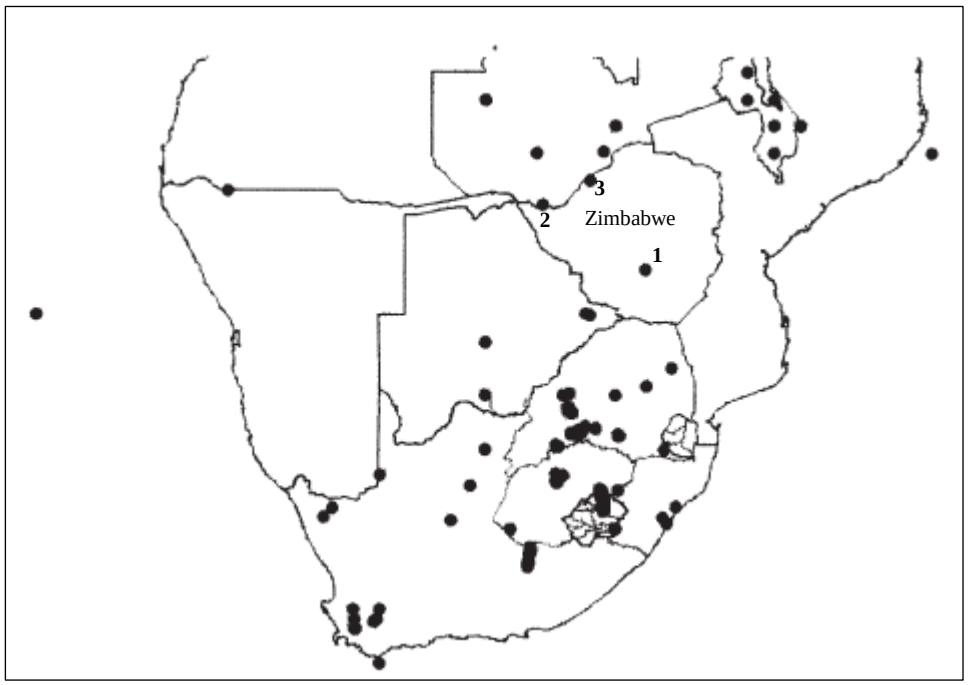

Figure 2.3: In-situ stress measuring sites in Southern Africa (after, Stacey and Wesseloo, 1998)

Gay (1975) mentions that Laubscher observed the presence of a strong near-horizontal compressive force which was sub-parallel to the large, present day intermediate stresses thereby suggesting that these forces influences the present-day stress field. Therefore, the high values of stresses measured at site 1 can be attributed to the presence of these compressive forces. Gay (1975) observed that the vertical stresses increase linearly with depth at a rate corresponding approximately to the increase of the overburden. He further observed that the horizontal stresses tend to be large at shallow depths where they are often larger than the vertical stress but less than the vertical stresses when depths get deeper. The major conclusion which was drawn by Gay (1975) from the measurements is that the principal stresses are inclined to the vertical, suggesting that the present-day state of stress includes components of both early as well as present-day tectonic and gravitational forces. It was observed that, there is no dominant trend in the orientation of the principal stresses over Southern Africa but rather the attitude of the stress ellipsoids changes over short distances depending on the local geologic structures.

2.2.2.2 Residual and Tectonic stresses

Residual stresses are also known as locked-in stresses which remain even after their causes have been removed. Tectonic stresses are due to the movement of the earth's crust over magma. They have a tendency of increasing the horizontal stresses significantly thereby causing the prevalence of high k-ratios at shallow depths.

2.2.2.3 Mining Induced Stresses

These are stresses that are superimposed onto the virgin stresses due to excavations created in the rock mass. Addition of the induced stresses to the virgin stresses result in stresses known as *resultant stresses*. Thus, the stability of excavations depends on the magnitude of the resultant stress, induced displacements as well as the strength of the rock mass surrounding the excavation.

2.2.2.4 Field Stresses

These are stresses which are experienced when an excavation is put closer to excavations that have been created before. A perfect example is that of interacting underground and open pit mining operations such as the one at Zimplats Mines, Rukodzi Mine where underground operations are being done in the vicinity of a mined out open pit. The resultant stresses from the open pit excavations become field stresses for the underground excavations. The new excavations will experience a resultant stress which is a combination of mining induced stress and field stress.

2.2.3 Ground Monitoring Tools

Nowadays, tools for monitoring ground behaviour in underground operations have been developed such as the Ground Penetrating Radar (GPR). A GPR is an electromagnetic signal that can penetrate through the surface in a non-destructive manner. Figure 2.4 shows a 3D simulation image of a GPR system in operation in an underground tunnel. In room and pillar mining, it is used as a probing method to establish the depth and extent of parting planes that might exist beyond the surfaces of the hanging wall and footwall in panels. It is now possible to drill boreholes for the purpose of installing borehole digital cameras. According to Paillet et al. (1990), a borehole digital camera is a device which works by continuously recording some colour images of the borehole walls. Figure 2.5 shows a sketch of the installation and connection of a typical borehole digital camera. This helps to give an understanding of the lithological changes and inherent fractures in the rock mass. Borehole imaging can also be used to observe crack development and fracture evolution around underground excavations thereby providing a basis for the establishment of the Excavation Damaged Zone (EDZ)

characteristics (Li et al., 2012). The system can also detect the stress induced damages in the boreholes thus enabling the estimation of in-situ stress orientations. Results obtained from these tools help to give insight to the rock engineer to come up with improved bolting supporting systems.

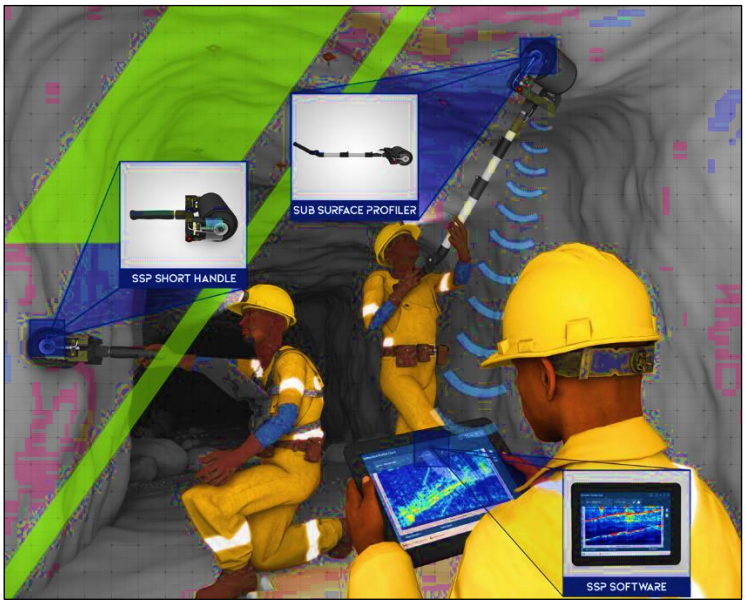

Figure 2.4: A 3D simulation image of GPR system (Reutech Mining, 2019)

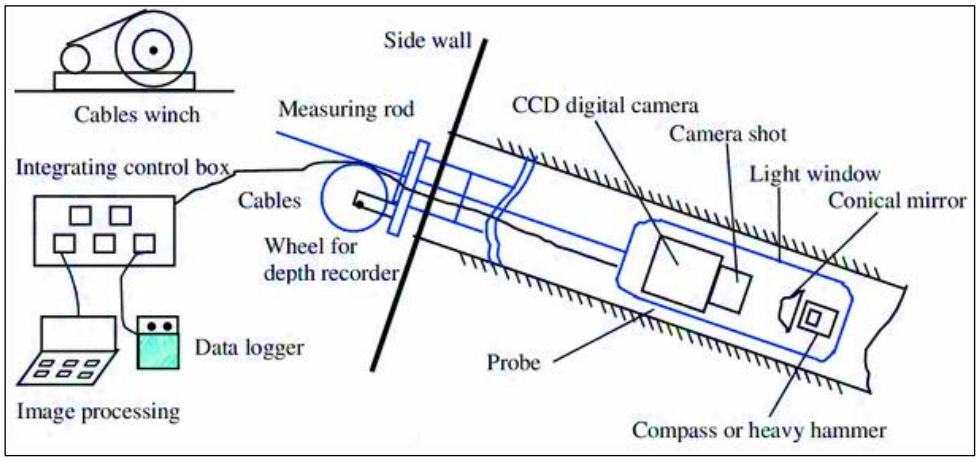

Figure 2.5: A sketch of installation and connection of a borehole digital camera (Li et al., 2012)

In surface mining operations, the existing ground monitoring systems can be divided into two categories which are surveying techniques and geotechnical methods. Survey techniques make use of survey instruments to establish the position and positional changes of any point on the surface, whereas geotechnical methods use specialised instruments to measure deformations (Jarosz and Wanke, 2003). Instruments used in surveying techniques include laser scanners, total stations, GPS receivers and photogrammetric cameras, whereas in geotechnical methods, instruments include piezometers, extensometers, tilt-meters, and

micro-seismic geophones. A survey technique that has gained more use in slope monitoring is the Interferometric Synthetic-Aperture Radar (InSAR). The use of InSAR provides an effective means to identify and map spatial movements across a large open pit and beyond the pit limits (Eberhardt et al., 2015). These monitoring tools can be used to identify high risk areas as well as providing early warnings of impending failures thereby giving ample time for evacuation of personnel and equipment from the working areas.

The data obtained from the monitoring tools can be used to validate the numerical analysis results. Although there might be a collection of vast data from some of these monitoring tools, it is seemingly that there is shortage of time and resources (in terms of personnel) to review the data in detail and to determine the significance of the data in respect with slope kinematics and mechanics of deformation (Severin et al., 2009). This challenge then calls for the need to use numerical analysis to predict rock behaviour thereby providing a warning of a change in behaviour and as a result enabling the possibility of restraining the impending damage.

2.3 Rock Mass Classification Systems

Rock mass classification systems have proved to be very important in the characterisation of rock masses as they provide a ready means of quantifying the quality of the rock mass. Geotechnical investigations are carried out on rock masses with the aim of determining parameters which influence the behavior of the rock mass. Rock mass classification systems are useful, in that they facilitate the combining of these parameters to quantitatively describe a given rock mass (Hume, 2011). Hume (2011) further reiterated that, *"The quantitative output provided is then used for further empirical design such as the support requirements, excavation methods and sequencing, or as input for use in numerical modelling programs".* A considerable number of these classification systems have evolved and some of them have been further modified in order to improve their limitations. Among these systems which are widely used in quantifying rock mass quality are the Rock Quality Designation (RQD), Rock Mass Rating (RMR), Rock Tunnelling Index (Q-system) and Mining Rock Mass Rating.

2.3.1 Rock Quality Designation (RQD)

The RQD system was developed by Deere et al. (1967) and is based on the results of drill core logs extracted from in-situ rock. It is defined as the percentage of intact core pieces longer than 100mm in the total length of core (Deere, 1988). Figure 2.6 shows how the value of RQD can be calculated if the data from drill core logs is available. RQD estimations are

entirely dependent upon the orientation of the drill core. This can be a problem especially in rock masses that are highly anisotropic with one dominant discontinuity set such as bedding planes, for which core oriented parallel to the bedding planes will estimate a higher RQD value than that oriented perpendicular (Hume, 2011).

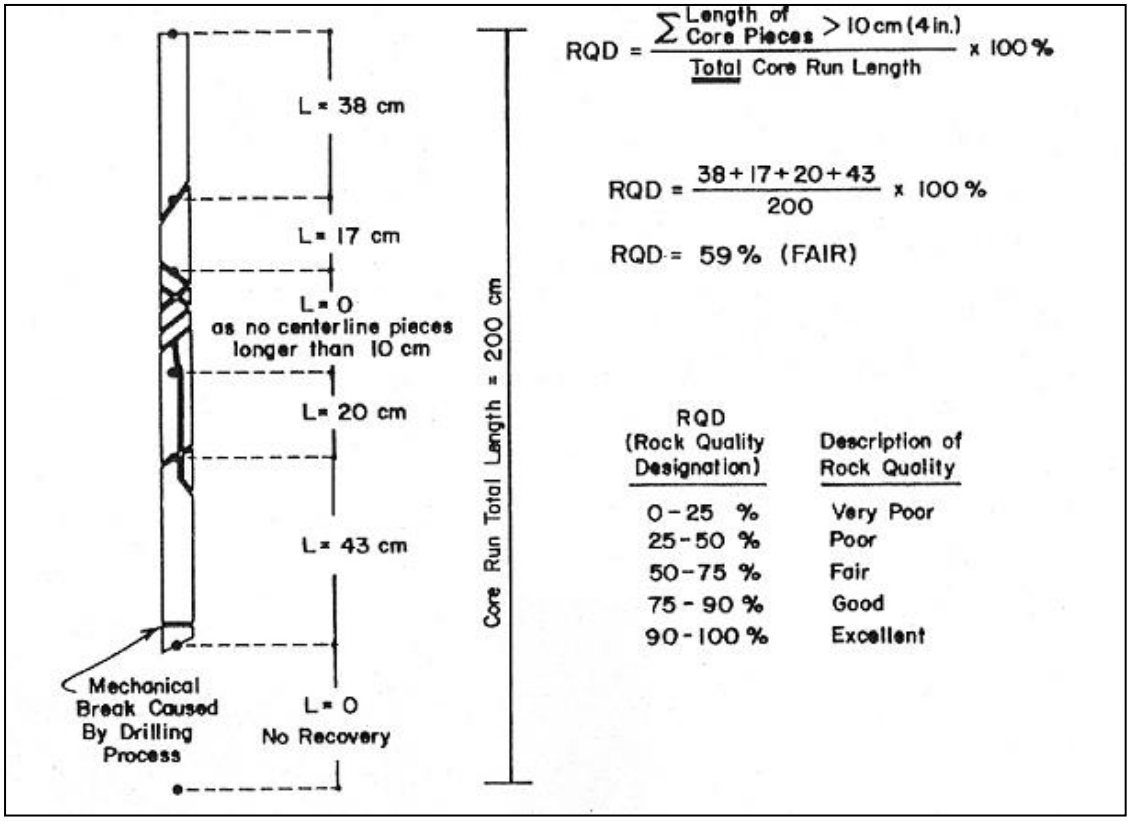

Figure 2.6: Procedure for measurement and calculation of RQD (after Deere, 1988)

Palmstrom (1982) proposed that, if the data from drill core logs is not available, RQD values for rock masses that are free from clayey material and have three or more joint sets can be determined based on the number of discontinuities per unit volume using Equation [2.3].

$$RQD = 115 - 3.3J_v \qquad [2.3]$$

Where, J_v is the total number of joints per unit length for discontinuity sets known as the volumetric joint count. The RQD ranges of values are correlated to particular rock mass quality as shown in Table 2.1.

The major limitation for RQD is that, it does not provide a comprehensive description as other geological parameters such as hydrological conditions, joint orientation and joint surface conditions are not included (Hume, 2011). Regardless of its limitations, the RQD has

proved to be quite an important parameter as it has been widely used in other classification systems.

Table 2.1: Correlation between RQD and Rock Mass Quality (after Deere, 1988)

RQD%	Rock Quality
<25	Very poor
25 – 50	Poor
50 – 75	Fair
75 – 90	Good
90 – 100	Excellent

2.3.2 Rock Quality Tunnelling Index (Q-system)

The Q-system has stood the test of time since its inception by Barton et al. (1974). The Q-system is a function made up of three quotients harbouring six parameters which describes the quality of the rock mass. The parameters are interrelated by the following Equation [2.4]:

$$\mathbf{Q} = {}^{\mathbf{RQD}}/_{\mathbf{J_n}} \times {}^{\mathbf{J_r}}/_{\mathbf{J_a}} \times {}^{\mathbf{J_w}}/_{\mathbf{SRF}} \qquad \textbf{[2.4]}$$

Where the parameters are defined as follows;

RQD - Rock Quality Designation

$\boldsymbol{J_n}$ - joint set number

$\boldsymbol{J_r}$ - joint roughness number

$\boldsymbol{J_a}$ - joint alteration number

$\boldsymbol{J_w}$ - joint water reduction factor

SRF - stress reduction factor

Each quotient represents an attribute of the rock mass, that is, (RQD/J_n) represents the relative block size or the degree of jointing. The relative frictional strength (J_r/J_a) represents the roughness and frictional characteristics of the joint walls or filling materials. (J_w/SRF) is the relative effect of water, faulting, squeezing, swelling and the strength to stress ratio (Hume, 2011).

The Q-system was developed from a civil engineering basis. Therefore, it provides a reasonable prediction for support requirements for civil excavations made by tunnel boring machines but it is too conservative for mining operations. Another limitation of the Q-system

is that it does not consider the orientation of the natural fractures in the rock mass. Thus, it does not give a reliable indication of rock mass behaviour in mining environments.

2.3.3 Rock Mass Rating

The RMR system was first developed by Bieniawski (1973) however; it has gone through various modifications in order that it would address facets encountered mainly in tunnelling. This system is composed of six parameters, which are combined to quantify the quality of the rock mass and these are:

i) Uniaxial compressive strength of rock material.
ii) Rock Quality Designation (RQD).
iii) Spacing of discontinuities.
iv) Condition of discontinuities.
v) Groundwater conditions.
vi) Orientation of discontinuities.

Each geological parameter is weighted according to its importance, and is assigned a maximum rating so that the total of all the parameters is 100 (Laubscher, 1990). For a particular rock mass, the summation of the rated parameters gives the final RMR value which is then used for design purposes. The classification categorises the quality of the rock mass in five groups of the same range of ratings and each group have subclasses A and B as shown in Table 2.2. The ratings range is 20 per class and the colours are used to represent the various classes on plans.

Table 2.2: RMR rock mass ratings (after Laubscher, 1990)

Meaning of the ratings					
	1	2	3	4	5
Class	A B	A B	A B	A B	A B
Rating	100 - 81	80 – 61	60 - 41	40 - 21	20 - 0
Description	Very good	Good	Fair	Poor	Very Poor
Colour	Blue	Green	Yellow	Brown	Red

The ratings from the RMR classification system are prone to distortions because they account for the joint frequency twice, that is, in RQD and joint spacing. Another limitation of the system is that, it does not consider the influence of mining induced stresses on the stability of the excavations.

2.3.4 Mining Rock Mass Rating (MRMR)

The Mining Rock Mass Rating (MRMR) was derived from the RMR system in 1974 to cater for the diverse mining environment. The fundamental difference was the recognition that in-situ rock mass ratings (RMR) had to be adjusted according to the mining environment so that the final ratings (MRMR) could be used for mine design (Laubscher, 1990). It is a very suitable classification system especially when dealing with the prediction of rock mass behaviour around an excavation because it takes into consideration the down rating of the rock mass parameters. The parameters which have to be adjusted are weathering, mining-induced stresses, joint orientation, and blasting effects and these are briefly discussed below.

Weathering significantly affects the intact rock strength (IRS) or value of the RQD percentage and the joint condition of the rock mass. The IRS is significantly decreased due to the chemical changes on the rock material due to weathering. In the case of RQD, weathering causes a drop in its percentage value since it induces numerous fractures in the rock mass. Furthermore, weathering causes alterations on the rock walls and washing away of joint filling. Weathering is time dependent, so the adjustment factors can take into consideration the period of excavation exposure such as shown in Table 2.3.

Table 2.3: Adjustments for weathering (after Laubscher, 1990)

Degree of Weathering	**Potential weathering and adjustments, %**				
	½ year	1 year	2 years	3 years	4+ years
Fresh	100	100	100	100	100
Slight	88	90	92	94	96
Moderate	82	84	86	88	90
High	70	72	74	76	78
Complete	54	56	58	60	62
Residual Soil	30	32	34	36	38

Joint orientation adjustments deal with the down rating of the rock mass stability on the basis of the attitude of the joints with respect to the vertical axis. The adjustment factors are highlighted in Table 2.4.

Table 2.4: Adjustments for Joint Orientations (after Laubscher, 1990)

No. of joints defining the block	No. of faces inclined away from the vertical				
	70%	**75%**	**80%**	**85%**	**90%**
3	3		2		
4	4	3		2	
5	5	4	3	2	1
6	6	5	4	3	2,1

Mining induced stresses are as a result of the redistribution of field stresses of some field stresses imposed by the development of mining excavations in the rock mass. This redistribution can cause spalling of walls, crushing of pillars and deformation of soft zones (Laubscher, 1990). If the stresses are compressive in nature, they can enhance the stability of the rock mass. The adjustments range from 60% to 120%.

Blasting is always bound to create fresh fractures in addition to the inherent ones in the rock mass. It also causes the widening up and movement of joints hence the need to carry out adjustments which cater for the variations in the excavation techniques. Rock walls that are poorly excavated are more likely to be unstable and usually these result from poor blasting practices. Excavation walls done by machines such as tunnel borers are usually stable. The blasting effect adjustments are depicted in Table 2.5.

Table 2.5: Blasting effect adjustments

Technique	**Adjustment, %**
Boring	100
Smooth-wall blasting	97
Good conventional blasting	94
Poor Blasting	80

Laubscher (1990) further reiterated that, “it is also possible to use the ratings (MRMR) in the determination of empirical rock-mass strength (RMS) and then in the application of the adjustments to arrive at a design rock mass strength (DRMS)”. According to Laubscher (1990), the RMS value is derived from downgrading the IRS value by a factor of 80%. A factor of 80% was reached upon from empirical data which showed that the IRS values obtained from laboratory testing of large specimens were always approximately 80% of those obtained from small specimens. Therefore, the RMS value for a rock mass with joints is given by Equation [2.5].

$$\mathbf{RMS} = \frac{(\mathbf{A}-\mathbf{B})}{\mathbf{80}} \times \mathbf{C} \times \frac{\mathbf{80}}{\mathbf{100}} \qquad \mathbf{[2.5]}$$

Where:

A – Total rating

B – IRS rating

C – IRS (MPa)

The DRMS, which is the unconfined rock mass strength, can then be derived by applying adjustments of weathering, joint orientation and blasting on the RMS. The DRMS is a very important input value in numerical modelling. The only major limitation of the MRMR classification is that it was mainly derived from cases involving the caving mining method therefore, its ratings for other mining methods maybe distorted.

2.3.5 Application of Rock Mass Classification Systems

In most of the room and pillar mines, the rock mass is delineated into geotechnical areas on a regional and/or local basis through the use of rock mass classification systems. Geotechnical areas are areas which exhibit specific rock mass behaviour and associated hazards in response to some mining activities where the same rock engineering strategies can be applied (Guler et al., 1998). Delineation of Regional Geotechnical Areas (RGA) can be accomplished by making use of information from exploration borehole core logs which gives insight on the depth of cover, stratigraphic structure of the rock mass, regional hydrology and geological discontinuities. The delineation involves the determination of the depth of cover where aspects of weathering at very shallow depths, low stress environments and influence of topography are considered. Regional hydrology assessment involves the identification of water tables, water bearing features and aquifers which are highly likely to adversely influence the mining excavations.

Delineation of local geotechnical areas usually known as Ground Control Districts (GCD) can be achieved through the use of information obtained from ongoing field observations and geotechnical mapping. This information involves the identification of geotechnical features such as parting planes, prevalent failure mechanisms as well as those parameters that are significantly contributing to instability.

The ratings obtained from these classification systems help in defining the strength of the rock material on various zones on which mining is going to take place. Communication

among mining personnel is enhanced through the use of ratings since the ratings assign numbers to describe the rock mass rather than sophisticated rock descriptions. The practical application of communicating the ratings derived from the classification systems is by colouring of the rated rock masses on mine plans and sections. The rock mass classification systems are a very good basis for predicting and analysis of rock mass stability around excavations. However, limitations are always inherent in each and every classification system. Thus, the use of more than one system to get an insight of the rock mass behaviour is always encouraged.

2.4 Numerical Modelling for Rock Masses

A model can be defined as a representation of a system that allows us to investigate the behaviour and attributes of the system and, sometimes, to predict outcomes of the system under different conditions (Hammah and Curran, 2009). Hammah and Curran (2009) argued that models come in two categories, that is, it can be a physical model or an abstraction. A physical model means a model built up of representative or equivalent material to portray the characteristics of a certain actual object, whereas an abstraction can be a set of equations or a computer program which follow some constitutive laws. Empirical methods fail to characterise the interaction between layers of rocks, thus they do not consider the geological structure, rock mass properties, presence of discontinuities and underground water (Nguyen and Niedbalski, 2016). Hence, their use in predicting the impact of underground operations on slope surface is limited when compared to numerical analysis.

Stacey (2018) argued that numerical modelling techniques are based on physical systems that are translated into a series of mathematical expressions. In rock engineering, numerical modelling is based on the principles of solid mechanics which deal with stress and strain relationship in both elastic and plastic materials. Stress and strain can cause deformation on the rock material and consequently, failure in the rock mass. Generally, underground excavations are in 2D due to the fact that they preserve their cross-sectional geometry in the third dimension. The presence of the rock in the third dimension prohibits strains in the third dimension and that is what is known as the “plane strain” condition.

If numerical models are well calibrated, they enhance the understanding and prediction of the behaviour of rock masses. The initial step in numerical modelling is the calibration of the model against the behaviour of the rock mass obtained from the field observations. This is then followed by running sensitivity analysis to test the model’s underlying principle and

finally comparisons of the results with the outcomes of alternative design methodologies (WorkSafe New Zealand, 2016).

2.4.1 Model Set-up and Simulations

In building up models, care must be taken in setting up the boundary and initial conditions accurately. For example, when modelling in RS2, a way to account for the continuous nature of the earth is by applying suitable boundary conditions to the sides of the model that simulate the larger extent of the rock mass in reality. Among these boundary conditions is the roller boundary condition where a model is allowed to move in a particular direction, that is, either along the x-direction or y-direction. Other than the roller boundary condition, there is also the fixed boundary condition which restricts movement in a particular direction. The external boundaries should not be set too close to the excavation boundaries since this can distort the results of the analyses that are to be carried out on the model. When external boundaries are too close to the excavation, the stress contours due to the boundary intersect the excavation boundary. Thus, the stresses that are predicted around the excavation are most likely to be incorrect. The general rule of thumb is that the external boundary should be 5 to 10 times the tunnel diameter away from the tunnel (Corkum, 2017). Basically, there are two categories of boundaries which are artificial and real boundaries. Artificial boundaries include truncated model domain, whereas real boundaries include free surfaces for example ground surface, tunnel, stope, loading etc.

Initial conditions, for example, in-situ stresses are set up in such a way that they point out the state of the model before any analysis is done on it. Corkum (2017) argued that when the excavation is very small in dimension, including the gradient due to gravitational loading is negligible relative to the overall stress at greater depths; a uniform field stress condition is used. The availability of rock mass mechanical properties data enables defining the initial state of the rock mass in numerical modelling. The rock mechanical properties serve as input data in the modelling software code and among these are rock density, elastic modulus, Poisson's ratio, UCS, tensile strength, cohesion and friction angle. The immediate step after inputting of parameter values in the model is to check whether the initial conditions are correct to the level to which they were intended to be. This can be done by running an analysis of the principal stresses and check whether they resemble the values that were input. Excavations created within the model serve to simulate the progressive mining operations thereby revealing the influences of these excavations on ground stability. The excavations in the model should be made in steps rather than once so as to avoid sudden load changes which

may cause artificial stress waves in the system to induce yield that might not have occurred had the loads been changed more gradually (Swindells et al, 2000).

The resultant models can then be analysed for the resultant changes in vertical and horizontal displacements as well as major vertical and horizontal stresses thus enabling the determination of the minimum stable pit floor or crown pillar thickness. The minimum open pit floor pillar thickness is defined as the minimum rock cover, measured vertically, above the highest point of the underground workings which provides an acceptable factor of safety against floor pillar failure during all mining activities (MOSHAB, 2000).

2.4.2 Model Calibration and Validation

Hammah and Curran (2009) argued that, "*The calibration process may include comparison of model results to measured stress and deformation and modifying the input parameters in a systematic manner to achieve a satisfactory agreement between the model results and measurements"*. Hoek and Brown (1980) pointed out that the most common calibration parameter in almost every engineering model is a factor to account for the rock strength reduction with increasing scale. On the other hand, model validation deals with comparing the calibrated model results to that of empirical data from case histories of in-situ rock mass monitoring. Diering and Stacey (1987) came up with a philosophy behind the application of numerical modelling in rock engineering. The concept behind the philosophy is the understanding that when applying stress analysis to mining problems, the actual numbers which result from these analyses must not be accorded too much credibility. Actually, what is important about these analyses are the trends and results of comparisons between a range of analyses. The philosophy highlights two approaches that can be used in the application of numerical modelling in rock engineering.

The first approach is that of having an initial analysis of a mining problem preferably modelling a geometry or situation in which the behaviour is known by back analysis (Diering and Stacey, 1987). This will allow the validity of the model to be established by comparing the observed results to the predicted behaviour. A well calibrated and validated model serves as a proper representative of the rock mass so the use of such a model to predict the rock mass behaviour can be well accepted as reliable.

The second approach is that of running a parametric study. In this case a general problem, rather than a specific one, is analysed for a range of parameters, for example material

properties and in-situ stresses (Diering and Stacey, 1987). Comparison of the results will then allow the identification of behavioural trends. It then becomes the onus of the engineer to determine whether a specific problem fits into the range of the general problem solutions in order to predict the behavioural trends.

2.4.3 Numerical Modelling Techniques

A number of numerical modelling techniques used in the modelling of rock masses have evolved; among the basic methods are Finite Element Method (FEM), Boundary Element Method (BEM) and Finite Difference Method (FDM). In the recent past, Discrete Element Method (DEM) and Discrete Fracture Networks (DFN) are now being incorporated in the modelling of rock masses to enhance the understanding of the rock mass behaviour. Hybrids of these techniques such as the FEM/DEM (ELFEN) have also been developed in order to capitalise the inherent capabilities in the individual techniques. FEM is discussed in detail in this literature review because it is the underlying technique in RS2 and RS3 modelling codes.

2.4.3.1 Finite Element Method (FEM)

This method has become an established technique which is widely used in structural and continuum mechanics. The technique is now being widely used in rock engineering where it can be used to model both elastic and non-elastic behaviour. The underlying concepts inherent in this technique are discussed in the following sections.

2.4.3.1.1 Finite Element Mesh

The model which is to be analysed is sub-divided into zones of similar geometry, i.e. triangles, rectangles etc, which are known as finite elements. The resultant model which has been discretized into finite elements is known as a finite element mesh. The rock mass is divided into finite elements and the commonly used type of such finite element is a triangular element because of its simplicity in creating a mesh. The more elements that are put into a mesh, the more computation time it takes to carry out the calculation. When the mesh is finely graded, the solution that is obtained in the analysis is more accurate. The concept of finite element stress analysis is best explained through the use of triangular finite elements such as shown in Figure 2.7. According to Stacey (2018), the method assumes that elements are connected at nodes and if a force is applied to the model, the elements will deform and the nodes will consequently be displaced from their original positions.

Assuming that the model is physically separated into triangular elements and joined at the nodes only, this model will exhibit behaviour such as that shown in Figure 2.8 if a load is

exerted on it. This behaviour will not represent the true behaviour of rock masses. Therefore, there is need to overcome this challenge when modelling rock masses. This is achieved by prescribing a way in which the elements may deform. A typical deformation prescribed for a triangular element is to have the displacement varying linearly across the element, for example, u and v displacements within the triangular element in the x and y directions respectively (Stacey, 2018). The u and v displacements are expressed by Equations [2.6] and [2.7] respectively.

$$\mathbf{u = a_1 + a_2x + a_3y} \qquad \textbf{[2.6]}$$

$$\mathbf{v = b_1 + b_2x + b_3y} \qquad \textbf{[2.7]}$$

Where, **a** and **b** are constant coefficients

By prescribing deformation to vary linearly, the displacement of any point along the interface of the elements A and B, Figure 2.9, must be identical for each element. This implies that the two elements will remain in contact and the displacements are continuous across the boundaries. It can be concluded that the basic principle of finite element analysis is that forces acting on the nodes will cause displacements of the nodes from their original positions (Stacey, 2018). The relationship between forces and displacements is provided by the stiffness of the model.

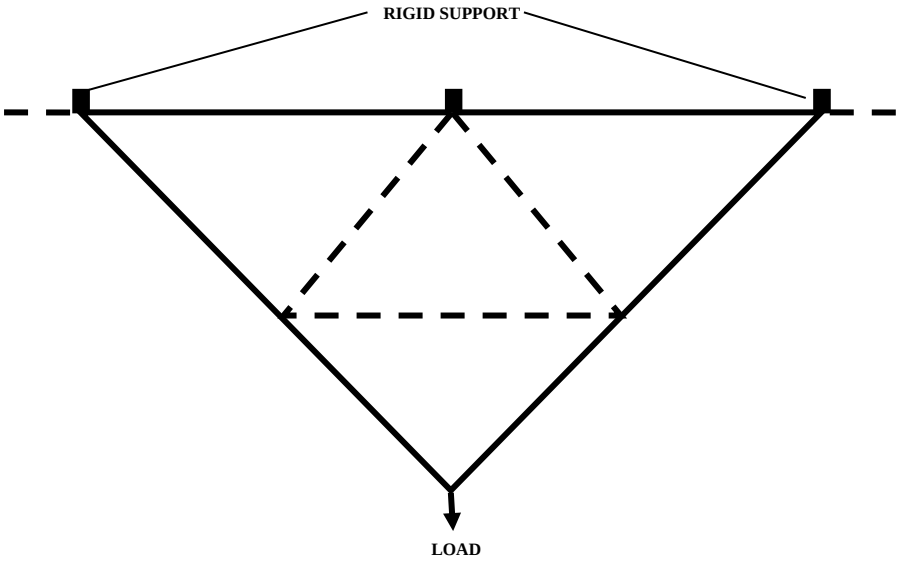

Figure 2.7: Triangular plate model (after Stacey, 2018)

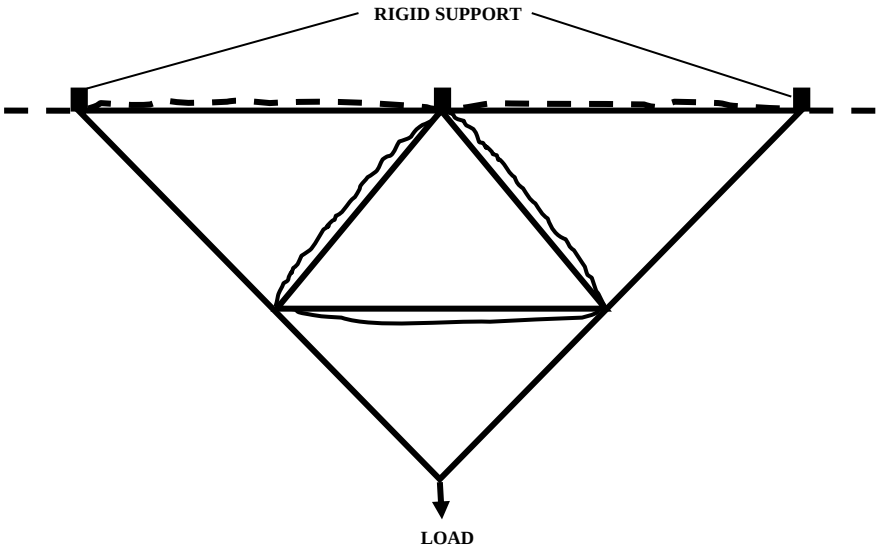

Figure 2.8: Deformation of triangular plate model (after Stacey, 2018)

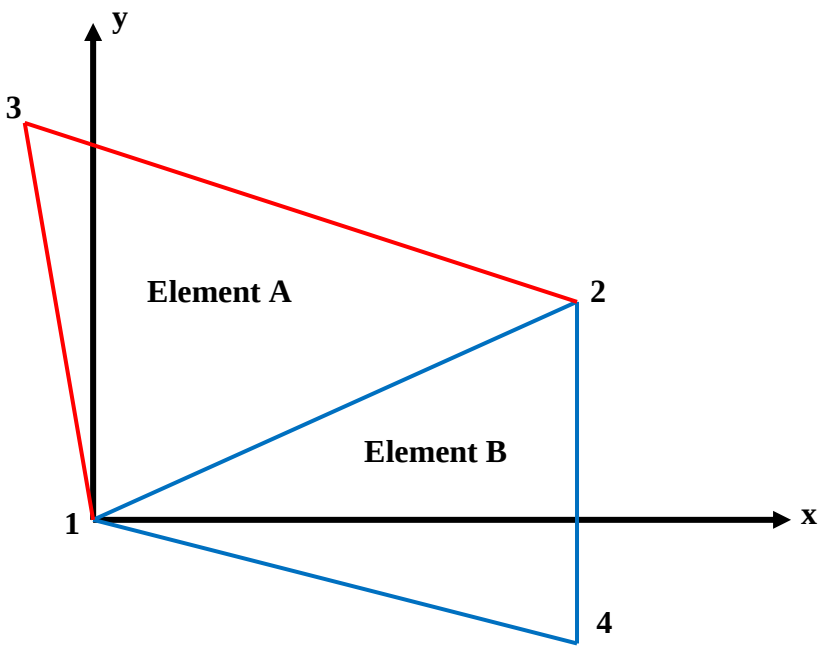

Figure 2.9: Two adjacent finite elements (after Stacey, 2018)

2.4.3.1.2 Model Stiffness

This is a combination of the stiffness of the components of the model, that is, the stiffness of the finite elements. Stiffness is incorporated in Equation [2.8] below, which relates to the acting force, F, and the corresponding distance, δ.

$$F = K\delta \qquad [2.8]$$

Where, K is the stiffness

This stiffness is influenced by the geometry and physical material properties of the model material. This implies that the magnitude of K varies with the length and cross-sectional area of the object as well as its elastic properties (Elastic modulus, E and Poisson's ratio, *v*). As have been highlighted earlier, if it is a 2D element, the displacements of the models occur in two directions x and y. Stiffness is directly related to the strains and stresses acting on the object. Stacey (2018) highlighted that the strains are given by solving the partial differentials of the displacements u and v in the x and y directions as shown in Equations [2.9], [2.10] and [2.11].

$$\boldsymbol{\varepsilon_x = {\partial u}/{\partial x} = a_2} \qquad \textbf{[2.9]}$$

$$\boldsymbol{\varepsilon_y = {\partial v}/{\partial y} = b_3} \qquad \textbf{[2.10]}$$

$$\boldsymbol{\tau = {\partial u}/{\partial y} + {\partial v}/{\partial x} = a_3 + b_2} \qquad \textbf{[2.11]}$$

These strains can be represented in a matrix form as shown in the matrix Equation [2.12].

$$\boldsymbol{\{\varepsilon\} = [A]\{\delta\}} \qquad \textbf{[2.12]}$$

These strains are linked to the stresses by elastic constants as shown in Equation [2.13].

$$\boldsymbol{\sigma = E\varepsilon} \qquad \textbf{[2.13]}$$

This can also be represented in a matrix form as shown in Equation [2.14].

$$\boldsymbol{\{\sigma\} = [C]\{\varepsilon\}} \qquad \textbf{[2.14]}$$

Where C is a matrix of E and v values

Knowing the geometry of the element, the stress highlighted above can be represented by a set of equivalent forces acting on each node of the element through the relation shown in Equation [2.15].

$$\boldsymbol{\{f\} = [B]\{\delta\}} \qquad \textbf{[2.15]}$$

Where {f} and [B] are matrices of forces and geometrical parameters respectively

By substituting Equations [2.12] and [2.14] into Equation [2.15], the relationship is shown in Equation [2.16].

$$\boldsymbol{\{f\} = [B][C][A]\{\delta\}} \qquad \textbf{[2.16]}$$

This implies that **K = [B][C][A]**

It can be concluded that the stiffness of the elements is derived from the material properties (elastic properties E and *v*) as well as the geometry of the element (defined by the model coordinates). The major advantage of finite element method is that the stiffness of each element is calculated individually thus making it so compatible to deal with heterogeneous material which is a realistic characteristic of rocks. The stiffness of the whole model is obtained from adding the appropriate element stiffness to form the equivalent nodal stiffness and this is represented by the matrix Equation [2.17]:

$$\{\mathbf{F}\} = \mathbf{K}\,[\mathbf{A}] \qquad \textbf{[2.17]}$$

2.4.3.1.3 Evaluation of Displacement and Stress using FEM

Generally, in geotechnical engineering the distribution of forces is usually known. Therefore, deduction of the corresponding displacements is easier. When determining the stresses, the theory of elasticity which links the strain and stress is used. As highlighted earlier, the strains are obtained from the partial differentials of the displacements. The stresses can then be calculated using the stress-strain relationship through the use of the modulus of elasticity and Poisson's ratio.

2.4.3.1.4 Types of Elements

There are various types of finite elements which can be used in rock mass modelling and these include triangular, rectangular and quadrilaterals. As mentioned earlier, the commonly used element is the triangular shaped finite element because of its simplicity in creating mesh. However, its main disadvantage is that the strains are considered to be constant throughout the element and consequently the stresses are also constant. This causes the need to have a large number of elements to model areas of high stresses which may become a challenge in data preparation when there is unavailability of high-powered computers. However, this large number of elements is preferred in the modelling of non-homogenous material if high powered computers are available. The other sophisticated elements such as rectangular and quadrilateral elements are good at modelling strain gradients. In three-dimensional modelling, the nodes on the finite elements will be having three degrees of freedom instead of two such as those experienced in 2-dimensional situation. Although three dimensional analyses give a close to reality analysis of rock masses, the only challenge is that of prolonged computing time. For example, when using a rectangular finite element in 2D analysis, stresses and displacements are calculated on four nodes in relation to x and y

directions thus forming 8 equations. In three dimensional analyses the equivalent will be a brick element having eight nodes upon which stresses and displacements are calculated relative to x, y and z directions thereby forming 24 equations.

2.4.3.1.5 Application of FEM to Non-linear Problems

In reality, rocks are non-linear in nature therefore there should be ways to take into consideration that nature in the finite element analyses. Continuum methods simulate the overall rock mass behaviour such that they do not allow shearing and opening up of joints. Stacey (2018) described the various approaches that are used to incorporate material non-linearity as follows.

1. Ubiquitous joint analysis

In this approach, the joints are assumed to be evenly distributed throughout the rock mass and in each element. Elastic analyses are then conducted for load or unload increments such that after each increment the calculated total stresses are used to determine normal and shear stresses on the ubiquitous joints. If shear and tensile criteria are used, failure of the joints is indicated in an element and the material elastic properties of the failed element are modified for the next load increment, for example, a low E-value for tensile failure and reduced E-value for shear failure.

2. The no-tension approach

This approach assumes that rock masses are weaker in tension. Thus, tensile stresses in elements are redistributed to other surrounding elements. The technique is best illustrated in iterative format, shown in Figure 2.10, in which two opposing forces are supported by three strands such that each strand supports a force of F/3. If, for example, the centre strand is cut such that the outer strands are left supporting the force F, the excessive force which was acting on the centre strand must therefore be relaxed. In finite element analysis, forces on the nodes of failed elements equivalent to the excessive stresses are calculated. The model is then analysed under the action of these forces only, which are then shared by the elements surrounding the failed elements. The approach can be combined with a shear failure criterion to allow for shear failure along joints as well as tensile opening of joints.

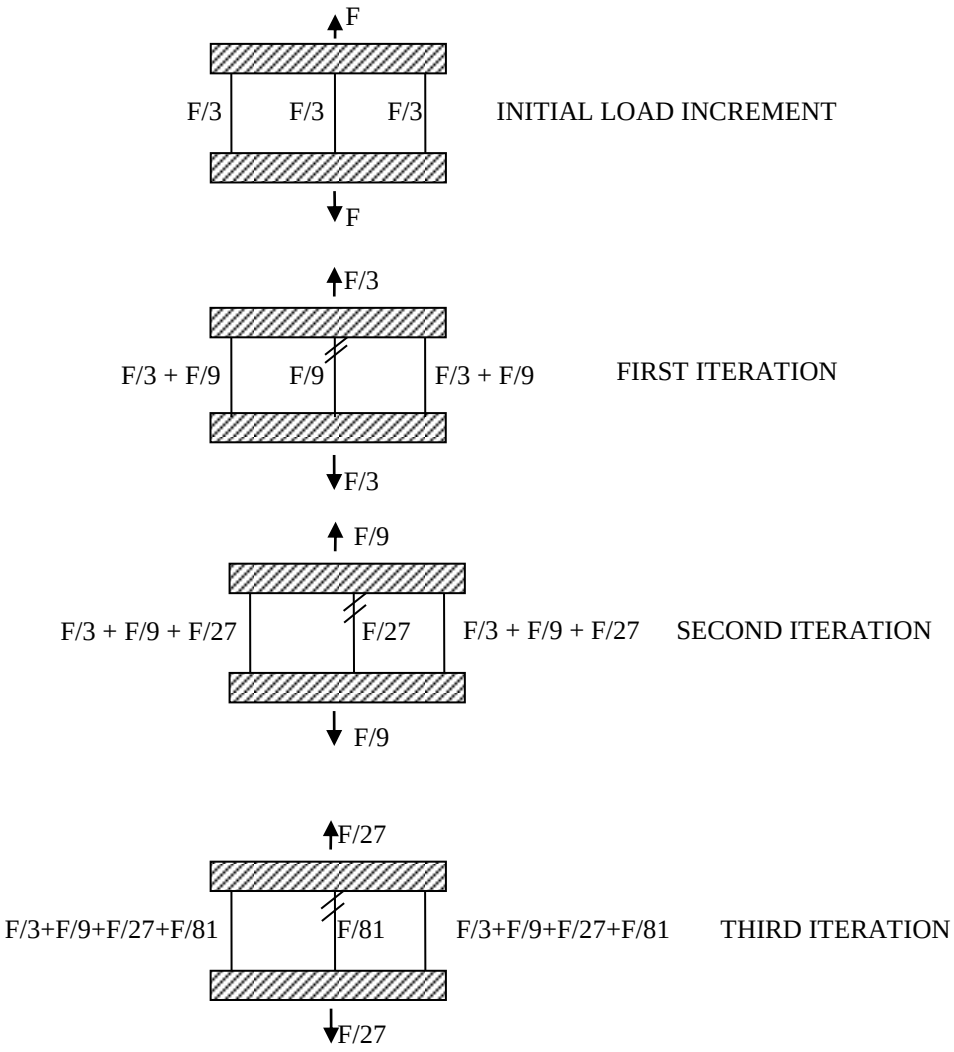

Figure 2.10: "No-tension" iteration procedure (after Stacey, 2018)

3. Joint elements

This approach allows the incorporation of joint elements in the model so as to allow the rock mass to be modelled as quasi-discontinuum. The technique accommodates both tensile and opening of joints as well as shear displacements along joints. The approach is most successful if the rock mass structure and joint properties are well known. It is very ideal for modelling large scale discontinuities such as faults, major joints or thin seams.

4. Plasticity

This approach can be used to determine the development of a failure zone around an excavation. This is achieved by having increments, either application or removal, of load to model the development of failure. The first concept in this approach is to have the stress conditions in each element after each increment being tested against the stress-strain curve.

The magnitude of 'failed' elements is then modified for the next increment. This concept is compatible to strain hardening materials. The second concept is to run elastic analysis for each increment of load. The stresses in the model are then tested against the stress-strain curve. If any elements have failed, the excessive stresses are redistributed by an iterative procedure equivalent to the no-tension approach. This reduces the stresses in the 'failed' elements, with a corresponding increase in deformation.

2.4.3.1.6 RS2 and RS3 Rocscience Software

For the purpose of this research RS2, a 2-dimensional finite element and RS3, a 3-dimensional finite element, programs with continuum modelling have been used. RS2 and RS3 are programs capable of analysing models involving excavations in soil and rock environments. RS2 (***Rock*** and ***Soil*** – ***2D*** analysis program) is a general-purpose finite element analysis program for tunnel and support design, underground excavations, surface excavation, slope stability, embankments, dynamic analysis, foundations, consolidation and groundwater seepage (Rocscience, 2019). Its counterpart, RS3 (***Rock*** and ***Soil*** – ***3D*** analysis program) exhibits the same capabilities in 3D mode.

2.4.3.2 Boundary Element Method (BEM)

In this method, only the boundary of the opening is divided into elements. The boundary element analysis requires only one-dimensional elements unlike in finite element analysis, whereas in a two-dimensional analysis, 2D finite elements (e.g. triangular elements) are required (Stacey, 2018). Boundary element analysis offers the advantage of being quick in data preparation where there is a challenge of unavailability of powerful computers. The technique is based on well-known solutions in the theory of elasticity which are:

1. Boussinesq's solution – this defines the stresses and displacements below a flat surface due to the application of a point force perpendicular to that surface (Podio-Guidugli and Favata, 2014a).
2. Flamant's solution – this gives the stresses and displacements below a flat surface due to a line force applied perpendicular to that surface (Podio-Guidugli and Favata, 2014b).
3. Kelvin's solution – this is a 3D situation and provides the stresses and displacements anywhere within the infinite elastic solid due to a point force acting at some point within that solid (Podio-Guidugli and Favata, 2014c).

2.4.3.3 Finite Difference Method (FDM)

This method differs from the finite element analysis in that it takes a different approach to which a solution of the equilibrium questions is arrived upon. A general fact is that, what can

be done by FDM can also be done by FEM and the reverse holds. The cycle of calculations basically follows the steps indicated in Figure 2.11.

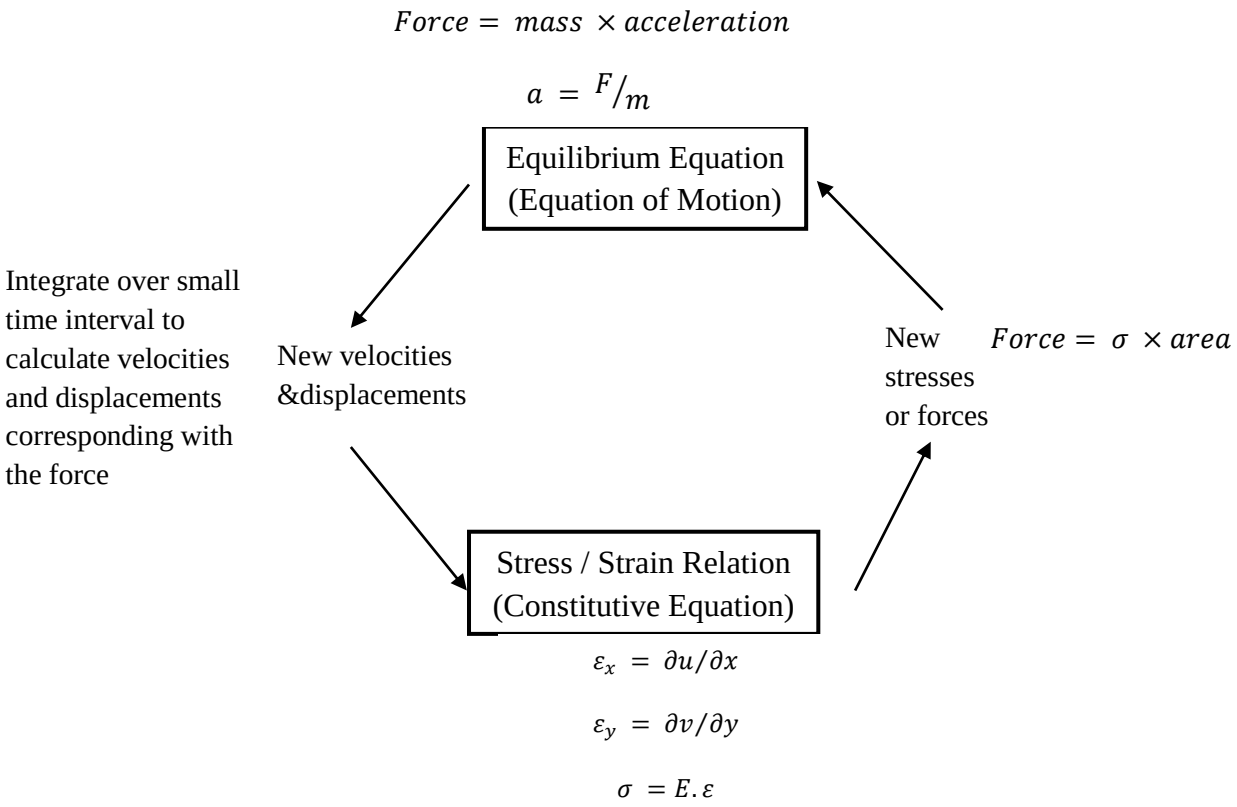

Figure 2.11: Basic calculation cycle in FDMs (after Stacey, 2018)

The technique considers the concept that when an excavation is made in the rock mass, the equilibrium of the stresses is disturbed. This results in changes in the strain, hence displacement within the rock mass. Generally, this change in stress and strain occurs instantaneously in an elastic rock mass. However, using FDMs this change is a gradual, iterative process until the forces and displacements in the rock mass are again in equilibrium (Stacey, 2018).

2.5 Design and Analysis of Crown Pillar Stability

In recent years, extensive research has been carried out to study the issues influencing ground stability on coinciding open pit and underground mining operations especially during transition from the former to the latter method. Transition from open pit to underground or vice versa is associated with crown pillars being created between the pit bottom and the underground excavation roof. A crown pillar is defined as a horizontal plug of rock of variable geometry that is situated above the uppermost underground working of a mine (Henning, 2007). The reason why crown pillars are left is to isolate the surface and underground excavations. This isolation will ensure the integrity of the open pit mining

equipment, personnel safety and prevents inflow of surface water into the underground workings (Xu et al., 2019). Bakhtavar, Oraee and Shahriar (2010) defined the minimum crown pillar thickness as the minimum rock cover, measured vertically, above the highest point of the underground workings which provides an acceptable factor of safety against crown pillar failure during mining activities. Generally, the stability of crown pillars improves with increasing crown pillar thickness. However, the thicker the crown pillar, the more the ore that is sterilised and the reverse holds. This crown pillar thickness is influenced by several factors. Among them are the geological condition, in-situ stress state, rock mass quality, mining method and sequence, pillar geometry as well as specific mine operational standards.

2.5.1 Crown Pillar Failure Mechanisms

Carter (2014) argued that there are five principal crown pillar failure mechanisms that have been observed from numerous failure cases that have been experienced in the past. It was observed that these failure mechanisms are clearly distinctive and each of them has to be analysed differently from the other. Bar et al. (2018) argued that these crown pillar failure mechanisms are dependent on:

- Ground conditions;
- Size and geometry of underground excavations;
- Initial and changing stress regime; and
- External factors such as rainfall, seismicity and blasting.

Bar et al. (2018) defined these crown pillar failure mechanisms, (see Figure 2.12), as follows:

1. Plug failure - this is a failure mechanism associated with steeply dipping, well defined continuous discontinuities. At low confining stresses, for example, when overburden is removed during open pit mining, effective friction on the discontinuities reduces to initiate downward sliding of a block or plug.
2. Chimneying failure mechanism which occurs in weak rocks with low cohesion.
3. Caving – this failure mechanism requires large spans and low confining stresses to propagate. It can be due to persistent discontinuities or general disturbances of the rock mass.
4. Unravelling – this requires a blocky rock mass, typically with at least three joints, which under high stresses can be reasonably stable. However, at low confinement, wedges form and fall into the void.

5. Delamination – this is a crown pillar failure mechanism which manifest in thin or laminated rock strata by allowing separation between the layers (i.e. bedding planes, foliations or continuous joints).

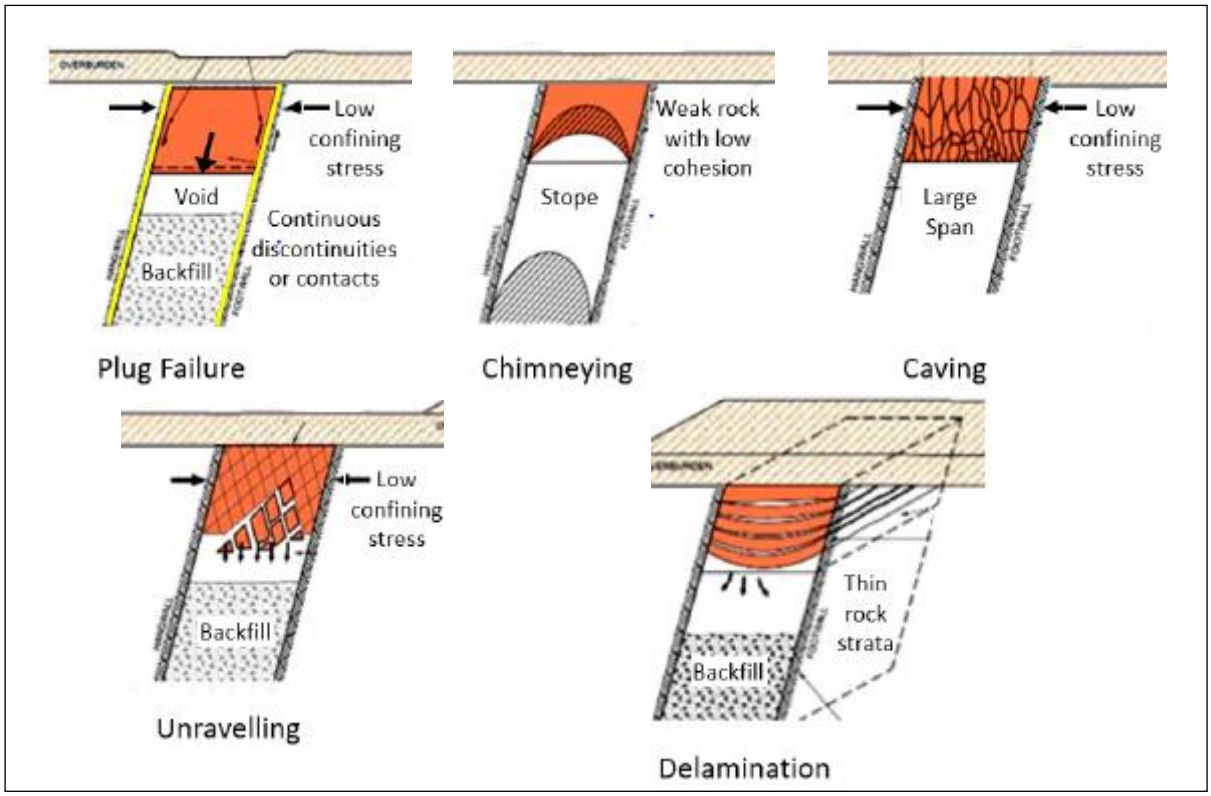

Figure 2.12: Crown pillar failure mechanisms (adopted from Bar et al., 2018)

2.5.2 Stability Assessment of Crown Pillar Thickness

Bar et al. (2018) mentioned that in order to assess stability of crown pillars, three approaches can be used, which are:

1. Empirical methods based on rules of thumb and/or rock mass quality and the scaled span method.
2. Structural analysis and cavability assessments.
3. Numerical modelling.

Numerical methods can be used to simulate the feasibility of various crown pillar thicknesses based on the predicted displacements and stresses. By simulating different crown pillar thicknesses, the response of underground workings and pit slopes can be better understood thereby making easier decisions to identify an appropriate crown pillar thickness (Xu et al., 2019). However, Xu et al. (2019) argued that numerical methods can give optimal results in the determination of crown pillar thickness but these results are mainly controlled by specific economic environment which is very difficult to predict. The major challenge with numerical

modelling approaches is that they are still lagging behind when dealing with analyses and designing of crown pillars, where there is great variability in rock mass properties. Choice of the appropriate input data and proper constitutive models to be incorporated in the numerical model still remains a challenge.

Other than the use of numerical analyses, various empirical methods for the determination of stable crown pillars have been developed with some based on rules of thumb. Among these approaches is the Scaled Span approach which is a method that provides an effective means for empirically sizing a rock crown pillar over a near-surface excavation (Carter, 2014). This approach evolved with an idea of developing a better relationship that would describe the crown pillar geometry with respect to rock mass quality. The first step in the determination of a safe crown pillar thickness is to calculate the scaled span of the crown pillar using the formula shown in Equation [2.18].

$$\mathbf{C_s = S\left(\frac{\gamma}{T(1+S_R)(1-0.4\cos\theta)}\right)^{0.5}} \qquad \mathbf{[2.18]}$$

Where, C_s is the scaled span, (m);

S is the crown pillar span, (m);

γ is the rock mass weight, (t/m^3);

S_R is the span ratio S/L; in this case L is the crown pillar strike length; and

θ is the dip angle of the ore body

The second step in this approach is to determine the critical span which is given by Equation [2.19].

$$\mathbf{S_c = 3.3Q^{0.43}[Sinh(Q)]^{0.0016}} \qquad \mathbf{[2.19]}$$

Where, S_c is the critical scaled span and Q is the Q-value from the Q-system.

The safety factor of the crown pillar can then be calculated using Equation [2.20] below.

$$\mathbf{F_c = \frac{S_c}{C_s}} \qquad \mathbf{[2.20]}$$

It should be noted that C_s reflects the mined geometry, whereas S_c reflects the rock mass quality. If C_s is higher than S_c, the value of F_c will be less than 1 thereby implying an

increased likelihood of failure happening. The probability of failure of the crown pillar of varying thicknesses can then be calculated using Equation [2.21].

$$\mathbf{P_f = 1 - erf\left[\frac{2.9F_c - 1}{4}\right]} \qquad \textbf{[2.21]}$$

Tao et al. (2018) suggested that a relationship between the different crown pillar thickness, the safety factor of the pillar and the probability of failure can be put on a plot. The critical safety thickness with a low probability of failure can then be determined from the plot. Carter (2014) emphasized that the scaled span approach is based on the principle that, as the size of an underground excavation increase, so does the degree of failure risk and the likelihood of collapse of that structure's crown. However, if the excavations are made in a high-quality rock mass, the possibility of experiencing failure is significantly reduced. Influence of structures such as large faults on crown pillar stability must be well considered as these can take control of the back-break angle from the viewpoint of assigning Q-values especially for the purpose of using the Scaled Span approach (Carter, 2014). Depending on the angle of the fault structure relative to the ore zone geometry as well as the stoping zone, these structures may influence the calculation of the crown pillar span. When determining the Q-value for the rock masses forming the crown pillar, ideally the water condition (J_w) and stress conditions (SRF) are set at unity, that is, $J_w = 1$ and SRF = 1, implying dry conditions and normal confinement respectively. However, in-situations where, for example, there is an excavated open pit which has accumulated water, J_w cannot be considered as unity but rather set to a lower value to account for adverse groundwater conditions. Moreover, a de-stress state may occur due to the mining of the open pit closer to underground workings, therefore SRF should be adjusted to account for this stress change thus resulting in a lower value of Q.

2.6 Ground Control

The understanding of ground instabilities and precise prediction of rock mass behaviour provides a basis for the design of appropriate ground control systems. Miners involved in room and pillar mining of PGMs and chrome indicated that the common support systems in such mines employ 1.5m to 1.6m resin bolts in conjunction with 4m to 6m long cable anchors (Pickering et al., 2010). The main challenge being faced is that of the lack of roof bolters that are capable of installing long cable anchors that are longer than the stoping width. This limitation has caused the installation of cable anchors to be done manually thus leading to high exposure of the operators.

If ground instabilities are left uncontrolled to within acceptable limits, catastrophic ground failure may occur which leads to loss of human life and equipment as well as sterilisation of mineral resources. To this end, it therefore becomes imperative to implement proper ground control methods to achieve safe working environment as well as create excavations which can stand for their intended lifespan. Good ground control involves proper excavation design and the systematic installation of suitable support of openings during excavation to prevent ground or strata instability occurring at a mining or tunnelling operation (WorkSafe New Zealand, 2016). However, this research will only focus on optimising excavation dimensions as a ground control strategy.

2.7 Chapter Summary

Guided by the research objectives, the review on literature focused on the issues concerned with ground instabilities encountered on interacting mining operations during transition from open pit to underground mining or vice versa. The review brought out that extensive research that has been done has mainly dealt with ground instability issues on mining activities involving steeply dipping ore bodies. Most of the case studies used in the previous researches were involved in transition from open pit to underground caving mining methods. However, this research introduces a case study which is different from the ones previously studied in that the underground operations are approaching a mined out open pit and the deposit is fairly shallow dipping. As a result, it is the opinion of the author that this research be done and, therefore, this scenario will be addressed in the subsequent chapters of this research report.

The review also focused at the common rock mass classification systems which can be used to characterise the rock masses. The major finding on the relook of these classification systems being that, each system has some inherent limitations. Hence the need to use two or more systems in characterising rock masses in order to get a, closer to reality, prediction of rock mass behaviour. A thorough study of the numerical modelling techniques also brought out the suitability of the finite element method in the modelling of rock masses affected by high stress redistributions such as the scenario in the current case study. Crown pillar failure mechanisms were reviewed with the goal of finding the most likely failure mechanism that would be incurred in the case under this study. Approaches to deal with the determination of stable crown pillar thickness were also explored. Review of current literature indicated that, when using empirical methods, the aspect of probability of failure should be considered in trying to determine a stable crown pillar.

3 CASE STUDY – ZIMBABWE PLATINUM MINES (ZIMPLATS MINES)

3.1 Background of the Mine

Zimplats Mine is a wholly owned subsidiary of Zimplats Holdings Limited which in turn is a subsidiary (87% shareholding) of the South Africa based and listed company Impala Platinum Holdings Limited (Implats). Zimplats Mines operations are concentrated on the Great Dyke in Zimbabwe. It is engaged in the business of producing platinum group of minerals. Its operations consist of ore production from its four underground operations up to the production of PGM-furnace matte which in turn is dispatched for refinery in South Africa.

Zimplats took over BHP's share of the then Hartley Mine in 2000 after the latter had closed Hartley Mine after failing to meet targets in the preceding year (Zimplats Holdings Limited, 2017). In 2001, Zimplats established an open-pit at Ngezi after an investment from its major shareholder Implats. During the period spanning from 2003 to 2005, Implats increased its shareholding to 87% and subsequently engaged in expansion project in 2006. According to Zimplats Holding Limited (2018), the expansion project resulted in an increase in ore production and concentrator capacity to about 4.2Mtpa. In 2010, the mine engaged in the development of its 4th underground operation, Bimha Mine, thereby ramping up production to 6.2Mtpa. Zimplats Mine experienced a major ground collapse at Bimha Mine in 2014 and its redevelopment was commenced in the subsequent year, 2015, coupled with resuscitation of open-pit operations which had been stopped. In 2018, Bimha Mine was brought back to full capacity thereby enhancing the group's overall production.

3.2 Location and Operations

The four underground mines which are currently being operated by Zimplats Mines are all situated in the Hartley Geological Complex which is part of the Great Dyke. The operations are located approximately 170km south-west of the capital city, Harare. The mining operations are accessed via a 77km tarred road off-shooting from the Harare-Bulawayo highway. Figure 3.1 is the map of Zimbabwe showing the position of the Hartley geological complex which hosts Zimplats Mines as well as some other PGM geological complexes situated along the Great Dyke. Figure 3.2 is a zoom into the Hartley geological complex which depicts the sub-deposits (hosting the Zimplats underground mines) within the complex. Among the underground mines shown on Figure 3.2 is Portal 2, Rukodzi Mine, which is specifically used as the case study mine in this research.

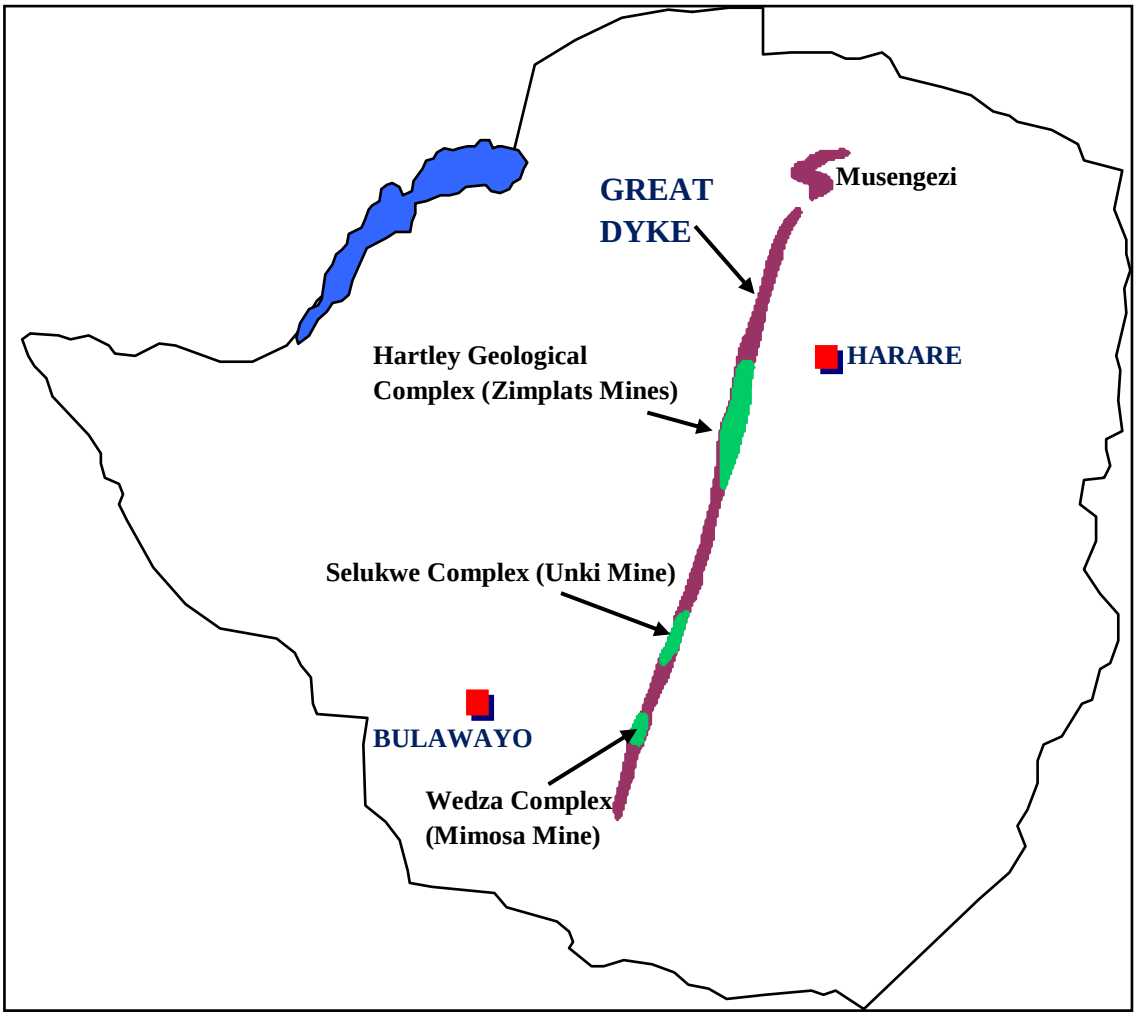

Figure 3.1: Geological complexes on the Great Dyke (Zimplats Holdings Limited, 2014)

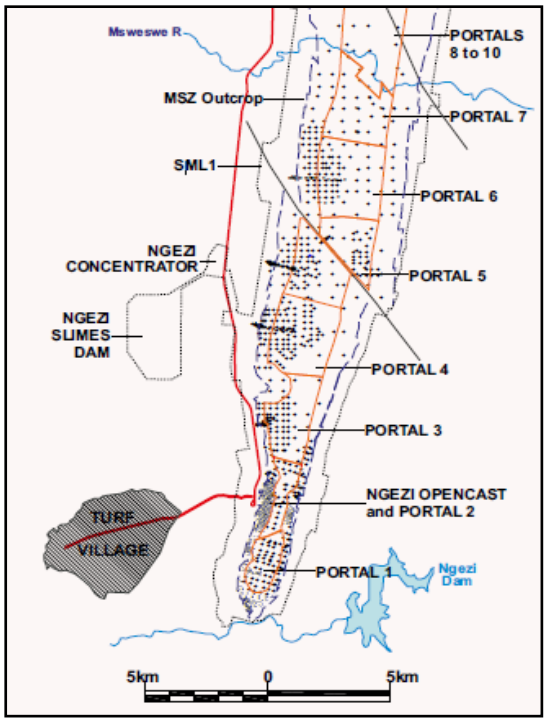

Figure 3.2: Sub-deposits within the Hartley Complex (Zimplats Holdings Limited, 2014)

3.3 Climate and Vegetation

According to Zimplats Holdings Limited (2005), the mining operations are situated in the area with an altitude of approximately 1200m above sea level. This altitude subjects the region to a temperate climate with daily maximum temperatures in the range of 20-30°C. The summer season in the region spans from November to April. The summer season is usually fairly wet, with an average rainfall of 760mm per annum. The winter season is generally from May to August with some intermittent frost being experienced. Exceptionally wet or dry seasons are not unusual, but winter rainfall is very limited. The most prevalent wind direction in this mining area is from the north-east.

The mining project area is located entirely on State land and consists of poor-quality agricultural land that traditionally has been used for cattle grazing and light subsistence agriculture (Zimplats Holdings Limited, 2005). Generally, the light woodland cover in the area is not of significant conservation importance as similar woodland is found extensively throughout Zimbabwe.

3.4 Geology

The deposit is located within the Sebakwe Sub Chamber of the Great Dyke of Zimbabwe. Initial exploration in the area have proved the existence of PGMs in economic quantities over a narrow zone (ranging from 2 to 3 metre width) at the base of a sulphide rich horizon that is found within large parts of the Great Dyke (Zimplats Holdings Limited, 2005). This zone is commonly known as the Main Sulphide Zone (MSZ).

3.4.1 Regional Geology

The Great Dyke is an elongate mafic to ultra- mafic layered intrusion trending the NNE-SSW direction across the Zimbabwe Archaean Craton. The dyke is highly elongate, slightly sinuous, 550km long, with a maximum width of 12km. The dyke developed as a series of initially discrete magma chamber compartments, which joined up as the chambers filled. The chambers coalesced below the Main Sulphide Zone (MSZ) and so before erosion took place, the MSZ would have been continuous along the length of the Dyke (Zimplats Holdings Limited, 2005). The Dyke is divided into two major successions, a lower ultramafic sequence dominated from the base upwards by cyclic repetitions or band units of dunite, harzburgite and bronzitite (pyroxenite), and an upper mafic sequence consisting mainly of gabbro and gabbronorite. However, much of the mafic sequence has been removed by erosion.

The MSZ is preserved in a continuous zone stretching 90km from Lake Manyame to Ngezi Dam known as the Hartley Complex. The Hartley Complex straddles two sub-chambers, Darwendale and Sebakwe and Zimplats operations lie towards the south of the Sebakwe Sub-chamber. The MSZ lies in ultramafic (pyroxenite), which is 5 to 50 metres below the contact between the mafic and ultramafic sequences. The MSZ is a lithologically continuous layer between 2 and 10 metres thick that forms an elongated basin as shown in Figure 3.3. Layers of igneous rocks within the basin dip at between 5° and 20° near the margins and flatten out near the centre to form a flat-lying floor.

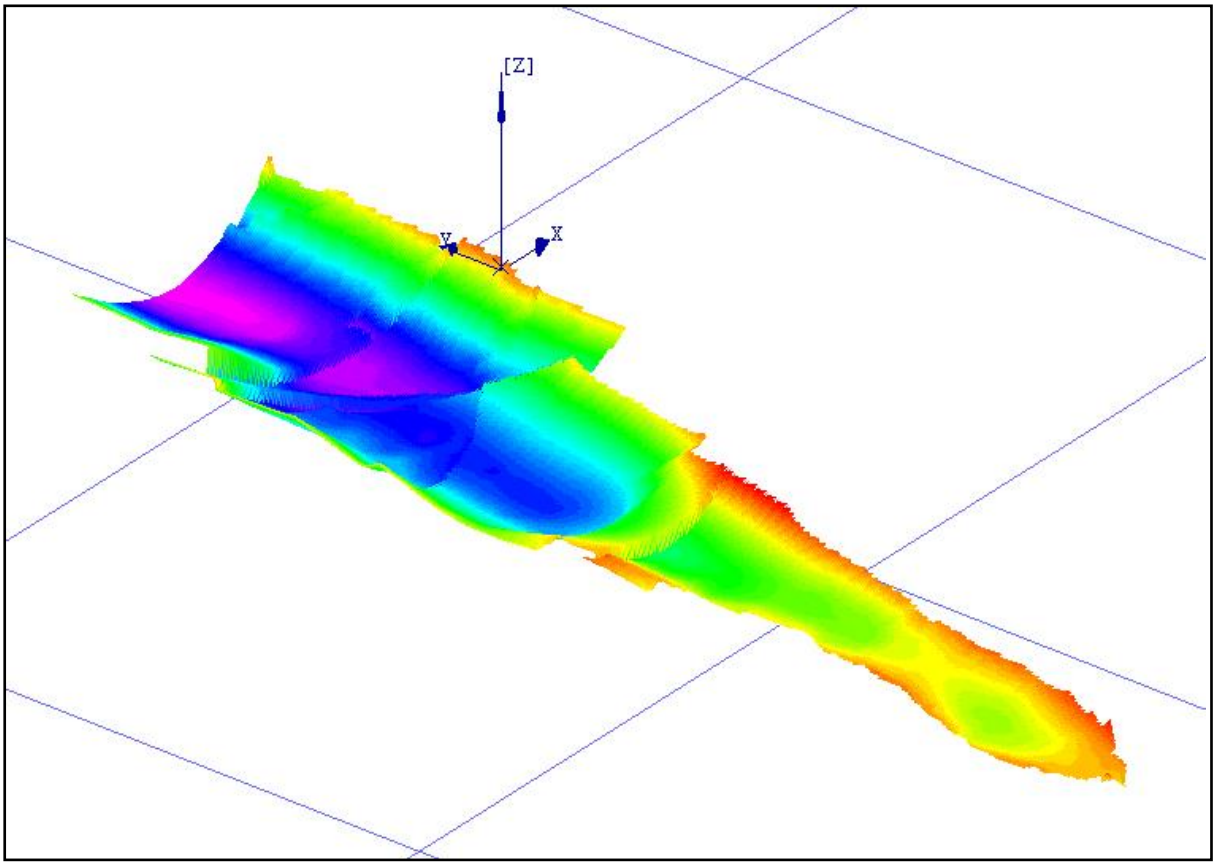

Figure 3.3: 3D view of the synformal and faulted shape of the MSZ (Zimplats Holdings Limited, 2005)

Typically, the MSZ consists of a 2-10-metre-thick zone containing 2-8% of iron - nickel - copper sulphides disseminated in pyroxenite (Zimplats Holdings Limited, 2005). The base of this nickel - copper - rich layer is overlapped by a 1-5-metre-thick zone composed of precious metals such as platinum, palladium, gold and rhodium. Considerable amounts of iridium, ruthenium and osmium also exist within the deposit. The principal sulphide minerals are pyrrhotite, chalcopyrite and pentlandite. The platinum group element (PGE) mineralization

cannot be visually delineated, but is spatially linked to the peak sulphide zone in a consistent manner allowing its location to be identified from the sulphide peak.

3.4.2 Local Geology

Portal 2, Rukodzi Mine operations are concentrated on the keel of the Dyke so, the dip throughout the mine span is mostly near horizontal ranging up to 7 degrees. Mineralisation is disrupted in places by barren, coarse-grained bronzitite lenses that are localized. At Rukodzi Mine, barren bronzitite typically occurs in lenses near the top of the PGE sub-zone.

The feasibility study by Zimplats Holdings Limited (2005) indicated that, in the gabbronorite and pyroxenite, open spaced fractures are filled by hydrothermal minerals (quartz - carbonate) and associated alteration minerals (chlorite - talc - amphibole). It is further highlighted that some of the fractures have been filled by intrusive dolerite, aplite, granite or pegmatoid. Many of the narrow aplite dykes and sills contain crushed fragments of quartz and feldspar indicating cataclastic deformation in or adjacent to faults and shears. In the gabbronorite, the joint fill is usually quartz - carbonate - chlorite whilst in the pyroxenite, the fill is commonly amphibole - chlorite - carbonate - talc - serpentinite. These different types of fill reflect the different wall rock geochemistry and consequent alteration patterns caused by hydrothermal circulation through fractures.

Generally, extensive faulting has modified the synformal shape of the MSZ. There are two major faults within the Portal 2 mining area. There is the Gwazana Fault trending 115^{o} and it lies 360m north of the Portal 2 declines. Exploration drilling has shown that this fault dips 45^{o} to the north and has a 6-12m up throw to the north. Area fault zone is 1-6m wide. The existence of this fault in the Portal 2 area has resulted in displacements being changed to approximately 6m downthrown to the north. On the southern side of the Portal 2 decline, (a distance of approximately 130m), there is another fault with an 11m up throw. There are also other numerous smaller faults both reverse and normal with displacements from a few centimetres to a few metres that have been mapped in the area.

3.5 Mining Method

The reef at Rukodzi Mine dips towards a central axis in a synform plunging gently to the north and it flattens near the axis. The dip on the eastern and western extremities of the deposit is variable, but is generally less than 7°. The east-west extent mineralisation ranges from 500m to 1km on the northern side of the Rukodzi Mine area. It is on these outcrops,

where open pit mining has been employed both on the eastern and western sides. Mechanised room and pillar at a stopping width of 2.5m has been employed in the underground mining area. Access to the underground operations is by twin declines which have been developed starting from the pit bottom of the western pit and advancing towards the eastern. The eastern and western pits have been mined to depths of approximately 50m. Figure 3.4 is a schematic cross-section view showing the interactions between the underground excavations and the open pit excavations. Some of the portions of the open pit have been backfilled, whereas some portions have got some water accumulations. The room and pillar pattern is designed in such a way that 7.0m wide panels in stopes and 6.0m wide panels in permanent roadways are created. In stopes, the in-situ pillars are 4.0m x 4.0m, whereas those supporting the roadways are slightly larger, taking up dimensions of 5.0m x 5.0m.

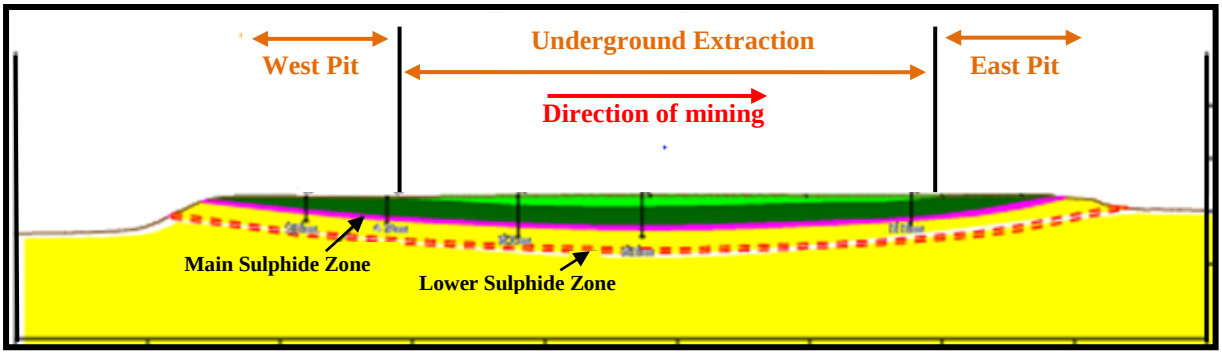

Figure 3.4: Schematic of underground and open pit excavation boundaries

Production drilling in the underground operations is done using low profile jumbos with a single boom, achieving an average advance of 3.0m per blast. Pumpable emulsion is the main explosive used for column charging. Blasted ore is mucked using 10 tonne Toro LHDs. The LHDs load the ore into EJC433 low profile 30 tonne dump trucks which haul the ore to the crusher at the surface.

Support drilling is by mechanised roof bolters which drill holes for the installation of 2.0m mechanical anchor bolts as well as 6.0m cable anchors. The mechanical anchors are grouted over a length of 1.8m and a face plate installed on a 1.0m x 1.0m grid pattern in roadways. Strapping in drives is also practised coupled with shotcreting on areas which have bad ground in order to enhance the support system. In short life areas such as stopes, 2.0m mechanical anchor bolts are installed on a pattern dependent on the ground classification and 6.0m cable anchors are installed where necessary.

4 METHODOLOGY

4.1 Introduction

This chapter highlights the methods used for collection of relevant data to this research. A description of how the data on the rock mechanical properties was processed is presented in this chapter. The assumptions which were made on the validity of the collected data are also incorporated in this section. A detailed description of how the numerical models were developed in RS2 and RS3 is also presented in this chapter.

4.2 Data Collection

The author made a visit to Zimplats Mine for a period of two weeks with the intention of collecting relevant data for the research. This gave chance to the author to have an appreciation of the mining operations at the area of focus of this research. The chief rock engineer authorised the accessing of the mine's geotechnical database as well as some technical reports covering some geotechnical aspects of Rukodzi Mine.

The database provided data which was mainly comprised of the laboratory results for the rock mechanical properties, whereas the technical reports had information about the mining parameters. The data was based on the results of widespread laboratory testing carried out to determine the rock mechanical properties for Rukodzi Mine. On instances where the data was not available specifically for Rukodzi Mine, data from the nearby Ngwarati Mine and Mupfuti Mine was adopted. The laboratory tests were done by ROCKLAB on behalf of Zimplats Mine and these include:

- Triaxial strength testing;
- Uniaxial compressive strength (UCS) testing; and
- Brazilian tensile strength testing.

The adoption of rock mechanical properties data from Ngwarati Mine and Mupfuti Mine was assumed to be valid since these mines were operating in the same geological environment as Rukodzi Mine. Furthermore, the idea of adopting this external data was enhanced by the fact that the underground operations for all these three mines were being carried out at almost similar depths, that is, approximately ±250m below the surface.

Apart from accessing the database and technical reports, the author also managed to visit the underground operations in order to have an appreciation of the ground condition variations as excavations advance towards the near surface areas. It should be noted that the visit could not

be done in the southern section of the mine, as was intended by the author, where the underground excavations were mined towards the mined out open pit. This was due to the inaccessibility of the area, since operations in that section had since been stopped due to ground instability issues. The decision to visit this alternative area was reached upon based on the assumption that, the ground behaviour and the inherent ground features that could be observed in this particular area were almost similar to those experienced in the area bound by the open pit excavations and underground excavations.

During the underground visit the author managed to note the prevailing mining parameters such as the bord and pillar dimensions both in roadways and stopes. It also allowed the observation of some geotechnical features such as some joints filled with some clayey material, low angled oxidised shear zones and joints.

4.2.1 Core Logging Data

Core logging data was extracted from the results of the previously logged horizontal boreholes which include one from the southern section and another one from the northern section. Data representing the northern section rock mass was extracted from borehole, 75N278E. Borehole 75N278E was drilled in a horizontal orientation in a direction towards the east in such a way that it intercepted the rock mass bounded by the underground and the eastern pit excavations. Its results were used to assess the variations in the rock mass conditions. The location of this borehole is illustrated on Figure 4.1 (one of the areas encircled in red).

4.2.2 Structural Mapping Data

Structural mapping on the pit slopes could not be carried out as was intended in the initial stages of this research. The mapping was foregone due to the inaccessibility of the pit slopes since some portions of the open pit had been backfilled and some portions had water accumulations. It was also noticed that there was no data from structural mapping that had been recorded in the geotechnical database as was the case with core logging data. The intent to carry out structural mapping was to get some input values for the parameters used in the calculation of RQD values using Palmstrom's equation (Equation 2.3 mentioned in Chapter 2).

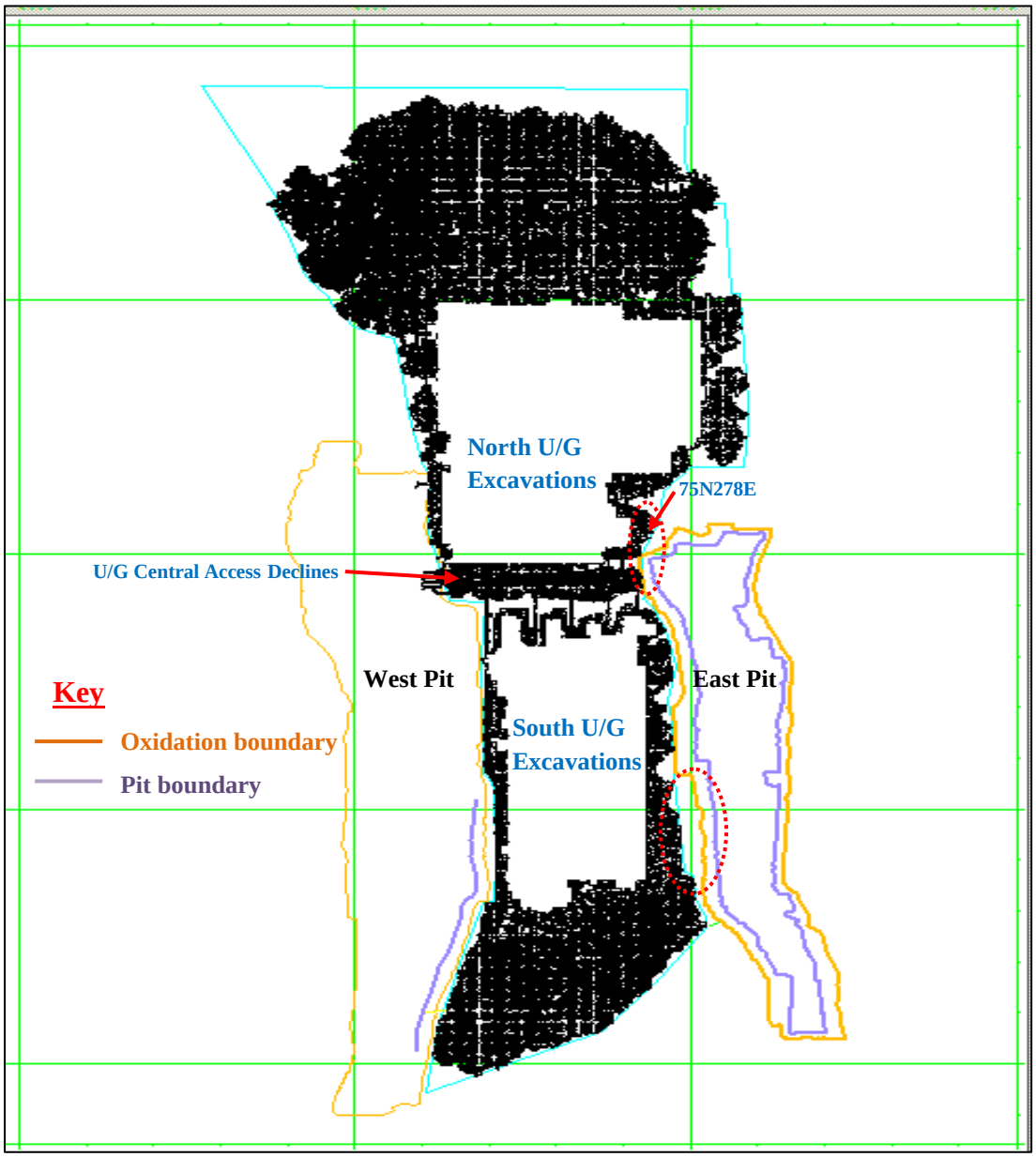

Figure 4.1: Plan of underground and open pit interactions at Rukodzi Mine

4.2.3 Rock Mass Classification

The Q-system was solely used to quantify the rock mass quality due to the fact that the data that was available provided the input values for deducing the Q-values. It is also worth noting that the RQD values incorporated in the calculation of Q-values were based on Deere's method of calculation. The Q-values were derived from the core logging results of borehole 75N278E. The Q-values were of great importance in quantifying the quality of the rock mass encompassing the area of concern for this research. The use of results from the two boreholes rather than one was done deliberately so as increase the sample results. Hence, guaranteeing a good representation of the area under study.

The Q-values were derived by inputting average values for the parameters used in the equation for calculating Q-values, that is, Equation 2.4 mentioned in Chapter 2. The availed results for borehole 75N278E comprised of input parameter values to a depth of approximately 95m. These input parameters included the RQD, J_n, J_r, J_a, J_w and SRF. The author opted to group the borehole depth into classes (span of rock mass) of 15m intervals for the sole purpose of reducing the bulkiness of the data. Thus, average values for RQD, J_n, J_r, J_a, J_w and SRF were calculated for each class. For example, for a class ranging from 0m to 15m, the average RQD value corresponding to this class was obtained by averaging the RQD values for spans of 0m to 3m, 3m to 6m, 6m to 9m, 9m to 12m and finally 12m to 15m. The same technique was used for the derivation of the average RQD values for the other classes that are, 15m to 30m, 30m to 45m, 45m to 60m, 60m to 75m and finally 75m to 95m. This technique was applied for getting the average values for all the other input parameters used in the calculation of Q-values except for the values of the parameter J_n, the joint number. For the J_n values, the most frequent J_n value in the range was selected. For example, on the drill core range spanning from 15.35m to 30.35m, the most frequent J_n value was 9. Thus, a J_n value of 9 was assigned for that segment of the core and this was so for all the other segments.

4.3 Numerical Modelling

For this research, RocScience modelling codes, RS2 version 10.0 and RS3 version 3.0 were used to analyse the rock mass behaviour. It is important to note that, the choice of the modelling codes was rather based on availability more than its capabilities in comparison to the other computer packages. Permission to use the modelling codes was granted from RocScience since the University of the Witwatersrand was a subscriber to the RocScience Education Program.

4.3.1 Modelling Input Parameters

4.3.1.1 Failure Criterion Input Parameters

Hoek and Brown (1997) suggested that when the slope or underground excavation is large and the block sizes are small in comparison, the rock mass can be treated as a Hoek-Brown material. From the field observations, it was seen that there were some considerable number of small rock blocks formed by intersecting joints. Thus, the rock mass hosting the larger part of the excavations was modelled as Hoek-Brown material. The use of this failure criterion necessitated the derivation of the values for the Hoek-Brown parameters such as the:

- σ_{ci} – the intact rock uniaxial compressive strength;
- m_b, the value of the Hoek-Brown constant m for the rock mass; and

- *s* and *a*, constants which depend upon the characteristics of the rock mass.

There was need to first estimate the GSI and m_i values for the rock mass in order to determine the values for m_b and *s*. The study of the vertical borehole core logged data provided, coupled with the field visits by the author enabled the understanding and observation of the rock mass physical appearance. Hence, the estimation of GSI values using the GSI chart introduced by Hoek et al. (1997) was possible. Estimation of the GSI value was further validated by the use of the equation proposed by Hoek et al. (2013), which correlates the GSI system with the Q-system. This equation incorporates some of the parameters that are used in the calculation of the Q-value. These parameters include the joint roughness, Jr, joint alteration, Ja and rock quality designation, RQD as shown in Equation [3.1]. According to Hoek and Brown (1997), the values of the intact rock uniaxial compressive strength, σ_{ci} and the Hoek-Brown constant, m_i, can be determined from the triaxial strength test results. Thus, upon estimating the GSI value and obtaining the m_i value, the values for the constants m_b, *s* and *a*, for the rock masses were calculated using the inbuilt GSI calculator in the numerical modelling codes.

$$\boldsymbol{GSI = \frac{52J_r/J_a}{1+J_r/J_a} + \frac{RQD}{2}} \qquad \textbf{[3.1]}$$

Both the rock mass and the backfill were modelled as elastic materials. For the backfill, only the uniaxial compressive strength, σ_{ci} m_b, *s* and *a*, values were input in the models without the need to estimate its GSI value since it does not fall within the types of material defined in the GSI chart.

4.3.1.2 In-situ Stress Considerations

In-situ stress measurements were recently carried at Bimha Mine and Mupfuti Mine. However, Mupfuti Mine in-situ stress results were deliberately adopted in the models of this research due to the fact that, it is closer to Rukodzi Mine operations. It is worth noting that the obtained in-situ stress results were disputed to be a bit on the higher side than what was being anticipated and it was argued that, these values might have incorporated some mining induced stresses. Nevertheless, the author deliberately chose to adopt the results as they were, given that the focus of this research was on prediction of ground behaviour. Hence, adoption of these high stress values would induce some sense of conservativeness to the design engineer when deciding the type of support required.

The in-situ stress measurements at Mupfuti mine were done at 92N29 panel which is about 160m below surface and the values for the principal stresses and their directions (adopted from *Appendix C*) were as follows:

σ_1 = 8.4MPa at 322^o from North;

σ_2 = 7.5MPa at 67^o from North; and

σ_3 = 5.3MPa at 231^o from North.

Considering an average density value of 3250kg/m^3 (see Table B-1 in *Appendix B*) of the websterite-bronzitite rock unit and gravitational loading (g) of 9.81m/s^2, the in-situ vertical stress (σ_v) can also be calculated using Equation [2.1] mentioned in Chapter 2.

Using Equation [2.1], the vertical in-situ stress value obtained for a point which is 160m below ground surface is around 5.1MPa. It should be noted that even though the overburden material was not homogenous, the calculation assumed material homogeneity for simplicity in modelling. The value obtained from the calculation corresponds well with the value of σ_3 obtained from the in-situ stress measurements. Since, the calculated value of σ_v and that of σ_3 were almost similar coupled with the fact that the vertical stress was smaller than σ_1 and σ_2, then σ_3 was considered to be acting vertically, whereas σ_1 and σ_2 were considered to be horizontal stresses. It is worth noting that σ_1 and σ_2 (also denoted as σ_H and σ_h respectively) were considered as the in- and out-of-plane horizontal stresses respectively. Thus, the stress ratios K_H and K_h incorporated in the RS2 and RS3 models were determined using Equations [3.2] and [3.3] respectively:

$$K_H = {}^{\sigma_H}/_{\sigma_v} \qquad \textbf{[3.2]}$$

$$K_h = {}^{\sigma_h}/_{\sigma_v} \qquad \textbf{[3.3]}$$

4.3.2 RS2 Numerical Modelling

A 2D model was set-up in RS2 Version 10.0 in order to analyse the behaviour of the ground around open pit and underground excavations. The analyses focused on the stresses and deformation around the underground and pit excavations. A 2D model was created based on the geometry shown in Figure 4.2 (which is a schematic plan view representative of the sections encircled in red on Figure 4.1). The model depicts the excavations as seen through cross-sectioning line A-A and its model geometry in RS2 is shown in Figure 4.3.

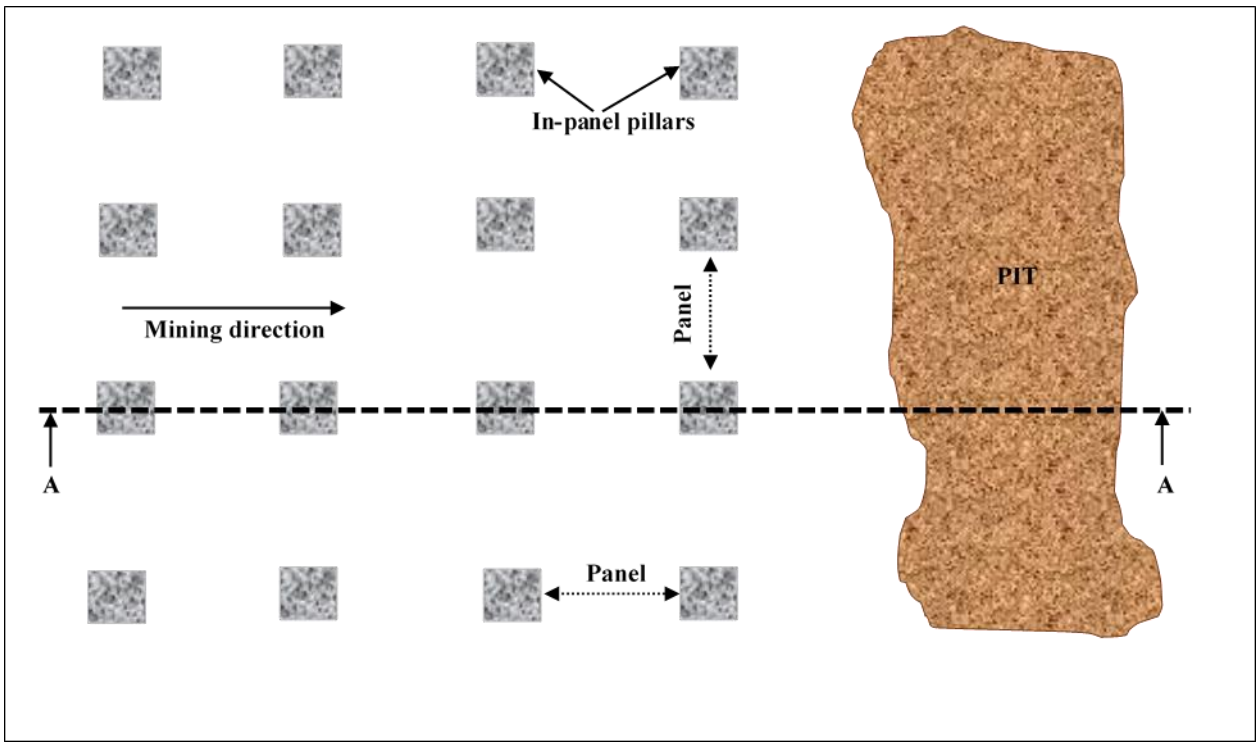

Figure 4.2: Schematic plan view of the underground excavations interacting with the pit

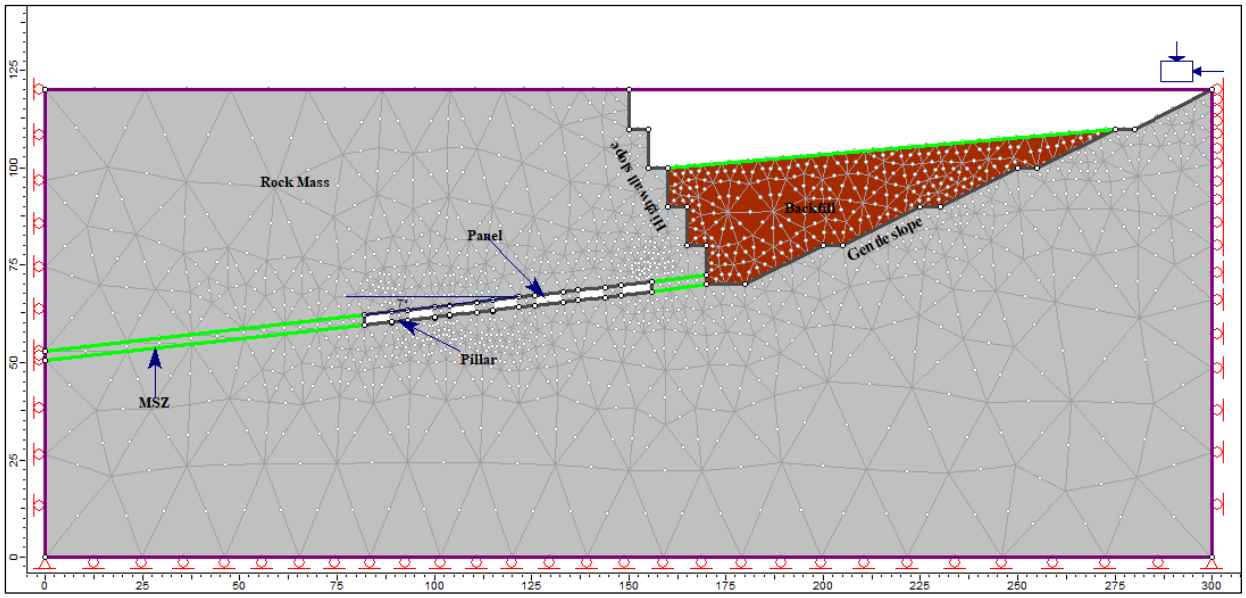

Figure 4.3: RS2 model of underground and open pit excavations

4.3.2.1 RS2 Model Geometry Setup

The model was created in such a way that the mining excavations were bound inside a rectangular external boundary with a length of 300m and a width of 120m. The excavations consisted of underground stopes of 4m-square in-situ pillars separated in between by ventilation holings/panels with a pillar to pillar distance of 7m and a mining height of 2.5m.

The pit was modelled in such a way that the highwall on the reef side was steep and the outcrop sidewall was gentle. The highwall side was modelled with a bench angle, bench height and bench width of 90^o, 10m and 5m respectively. The pit was mined to an ultimate depth of 50m. Though not truly representing the actual angle on the ground, a bench angle of 90^o on the pit highwall side was deliberately used in order to reduce the overall span of the pit in the model. The underground stopes were below but not directly underneath the pit, that is, to one side of the pit highwall as shown in Figure 4.3. Most of the excavation geometry dimensions were based on the real mining parameters used on the actual ground.

4.3.2.2 Multi-staging of Excavations in RS2

The concept of multi-staging excavations, inherent in the RS2 code, was adopted so as to simulate the way the excavations were carried out on the actual ground. Thus, in the first scenario, the sequence was such that the open pit was excavated in the first stage followed by backfilling of the open pit in the second stage then the excavation of underground stopes in the subsequent seven stages. Staging of the underground stopes was such that, the excavating process started on the panel which was furthest away from the pit highwall then a pillar was left in between this first panel with the one that followed. The sequence of excavating proceeded in such a manner towards the pit highwall side. As mentioned earlier, the excavation of the underground stopes followed a continuous and shallow dipping (0^0 to 7^0 dip) reef towards the pit highwall side. In order to analyse the effect of water ponding on the stresses and displacements, another scenario was set-up using the same model as the one for scenario 1. In this second scenario, the model was subjected to some evenly distributed loads due to water ponding, *see the model on Appendix E5*. The choice of the stages at which evenly distributed loads were applied was based on the idea that the occurrence of water ponding condition would only happen after some considerable time of mining.

4.3.2.3 Meshing and Boundary Conditions

The segments forming up the external boundary were variably restrained depending on the intended behaviour anticipated for the excavations which were to be created in the model. The bottom external boundary was restrained in the y-direction such that there would be free movement in the x-direction only. The vertical segments of the external boundary were restrained in the x-direction thereby allowing free movement in the y-direction only. The top segments of the external boundary were set as a free boundary to portray the ground surface upon which the open pit was excavated. Graded mesh type was selected such that the discretization density of the mesh elements was allowed to increase around the surface and

underground excavations. To enhance a finer delineation of the damage zones around the excavations, a 6 Noded Triangle mesh element type was selected.

4.3.3 RS3 Numerical Modelling

It was mentioned in the previous chapter that the case study mine used the bord and pillar mining method. Bord and pillar mining is associated with creation of wide-open panels which are left in-between an array of pillars. It is with no exception that in this case study, underground panels were formed as underground mining progressed towards the mined-out pit. In general, numerical simulations involving underground tunnels (in this case, referred as panels) requires 3D modelling to study the stress distribution around the panel face. However, in this study, 3D modelling was done in order to see how stresses were distributed on the in-panel pillars. Furthermore, 3D modelling allows for detailed examination of stress concentrations around the edges and ends of excavations (Sundar et al., 2016). To this point, 3D modelling using the finite element RS3 Version 3.0 was done.

4.3.3.1 Multi-staging of Excavations in RS3

Just like in RS2 modelling, the multi-staging function was also employed in the 3D models in an endeavour to replicate the order in which the excavations were done on the actual ground. Only the model sequence followed in scenario 1 of the 2D models was adopted. In this scenario, the pit was excavated first followed by backfilling of the bottom three pit benches and lastly, the excavation of underground panels. Progressive mining of underground panels was modelled in such a way that model slices of 3m were used to simulate the advance per blast on the last half part of the advancing panels.

4.3.3.2 RS3 Model Geometry Setup

A rectangular box was created to form an external boundary of the model. The box was created with a length of 300m along the y-direction, width of 200m along the x-direction and depth of 120m along the z-direction. Schematic geometries were created for both the underground and open pit excavations although RS3 Version 3.0 code has an option to import geometries from other CAD (computer-aided design) based software packages. The non-availability of already modelled geometries, as well as for the sake of simplicity, led the author opted to create the model out of schematic geometries that closely mimic what is on the real ground.

The open pit geometry was made up of consecutively stepped irregular prisms. The pit was patterned in such a way that a steep highwall on the side of approaching underground panels

and a gentle slope on the opposite side were created as shown in Figure 4.4. The option of plotting polylines, inbuilt in the RS3 code, enabled the creation of the pit geometry by initially drawing an irregular polyline followed by extruding it to a depth of 10m along the z-direction. Thus, subsequent plotting and extruding of the polylines resulted in coupled polygons which formed up the pit benches. The underground panels were created by selecting some 3D primitive box geometry option inbuilt in the RS3 Version 3.0 code. These 3D prisms were created with dimensions that represented the real parameters on the actual ground. Thus, they were 7m wide and 2.5m high to represent the actual panel length and panel width respectively. The mining direction was taken to be parallel to the y-axis. Thus, the prisms were segmented into 3m slices along the y-direction in order to mimic the actual advance per blast. In order to truly represent what was on the actual ground, the panels were inclined at about 7^0 from the horizontal so that the excavations would follow a continuous and inclined reef.

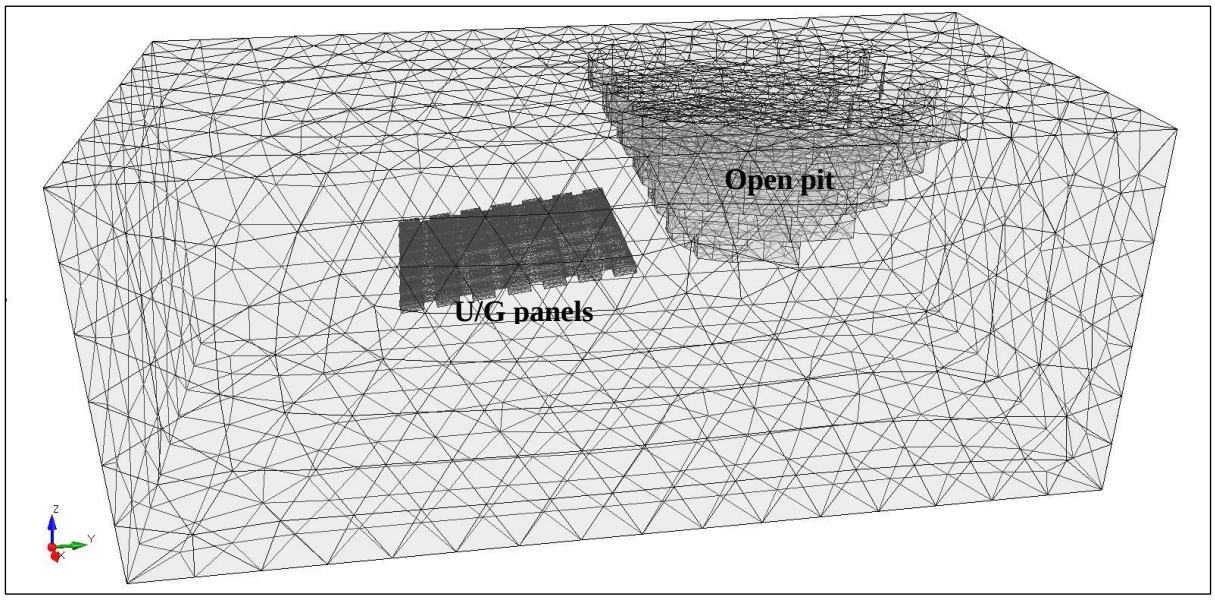

Figure 4.4: 3D model representing the underground and open pit excavations

4.3.3.3 Meshing and Boundary Conditions

Two different mesh types are available in RS3, which are the graded and uniform meshes. The graded mesh type is most appropriate to use when dealing with subsurface excavations that integrate clearly defined excavation boundaries while uniform meshing is suitable for surface excavations where boundaries are not openly defined. However, this research involved both subsurface and surface excavations and the author opted to use the graded mesh type such that the discretization density of the mesh elements was allowed to increase around excavations. The 4-noded Tetrahedron and 10-noded Tetrahedron solid element types

are available in RS3. Though the 10-noded Tetrahedron element type would give more accurate results, the graded 4-noded tetrahedron was used in this study in order to simplify the computation. As for the boundary conditions, the Auto Restrain (surface) option inbuilt in RS3 was selected. This option allows for the top surface to be kept free from any restraints to allow displacement in this surface. The bottom and side surfaces were fully restrained in all directions so that the model remains stable under loading.

4.4 Stability Analysis of the Intermediate Pillar

Stability analyses of the rock mass intermediate the underground and pit excavations were done. Initially, this intermediate rock mass was imagined as ground that would form a classic crown pillar in-between underground and pit excavations. However, upon studying the precepts of crown pillar geometry and failure mechanisms, the author observed that the case under study would not involve the formation of a well-defined crown pillar. It is worth recalling that a crown pillar is defined as a horizontal plug of rock of variable geometry that is situated above the uppermost underground working of a mine. The location of the underground excavations relative to the pit excavations would not create a classic crown pillar since the underground excavations were not directly underneath the pit. Rather, the author resorted to call this (rock mass in-between underground and pit excavations) as the intermediate pillar.

It was highlighted in the earlier chapter that there are basically three approaches that can be used for stability analysis of pillars. Among these approaches are empirical analysis, structural analysis or numerical modelling. Meanwhile, the geometry of the pillar would not permit the use of the Scaled Span Method discussed in detail in Chapter 2. Hence, the author opted to analyse the stability of the intermediate pillar using a numerical modelling approach. Therefore, a 2D finite element analysis using the model created in RS2, as described in Section 4.3.2, was done. The analyses focused on the strength factor of the rock mass; forming the intermediate pillar, surrounding the pit highwall side and that in the hanging walls of the underground panels in the close proximity to the crown pillar. The analyses were done for the models with intermediate pillar widths of 15m and 6m. The decision to end the analyses with a model having an intermediate pillar width of 6m was premised on the guidelines provided by Section 54 subsection (1) of the *Mining (Management and Safety) Regulations (SI 109 of 1990)* of Zimbabwe. It stipulates that in metalliferous mines, continuous pillars of not less than six meters in width should be left standing in-between separate mining excavations. It is noteworthy that major concern was on the stability of the

rock mass in the hanging wall of the underground panels because this is where operations were still active.

4.5 Chapter Summary

A detailed description of the research approaches taken in order to satisfy the objectives of this research has been highlighted in this chapter. Rock mechanical properties data from laboratory tests was extracted from the mine's geotechnical database. The data comprised of results from laboratory tests such as the triaxial strength test, UCS test and Brazilian strength test. Numerical values for the rock mechanical properties as well as the in-situ stress values were used as input data in the numerical models. Core logging data was used in the Q-system with the aim of establishing the quality of the rock mass in-between underground and pit excavations. This chapter also highlighted a detailed description of how the numerical models were built in Rocscience packages, RS2 and RS3. In 2D modelling, two scenarios were modelled to represent the interactions between the underground and open pit excavations. The first scenario represented some underground excavations approaching a backfilled pit. Whereas, the second scenario represented some underground excavations approaching a backfilled pit coupled with some water ponding. Three-dimensional modelling was done with the sole purpose of getting an insight of how the stresses would be distributed on the in-panel pillars. The last section of this chapter provides a description of the approach used in doing a stability analysis of the intermediate pillar.

5 RESULTS AND DISCUSSION

5.1 Introduction

This chapter highlights the results of the rock mass characterisation through the use of rock mass classification systems. It is also in this chapter where numerical modelling results and their interpretations are presented. The last section of the chapter concludes by a stability analysis of the pillar intermediate the underground and pit excavations.

5.2 Rock Mass Characterisation

For this study, the Q-system was the main classification system used to classify the rock mass between the open pit and the underground excavations. The Geological Strength Index (GSI) was also partly used for providing estimates of the strength and rock mass deformation properties incorporated in the numerical models.

5.2.1 Rock Quality Tunnelling Index, Q

The rock mechanics team at the mine provided the underground geotechnical borehole core logging results which enabled the rock mass characterisation. The data from borehole 75N278E was used to calculate the Q-values. These Q-values were used to bring out the quality of the intermediate rock mass between the underground excavations and the eastern pit. RQD values calculated using Deere's equation, highlighted in Figure 2.4, were used in the derivation of Q-values using Equation [2.4] mentioned in Chapter 2. Table 5.1 shows the input values *(extracted from Table A-1 and Table A-2 in Appendix A)* adopted for estimating the Q-values based on 75N275E borehole core logging results.

Table 5.1: Estimation of Q-values from Borehole 75N278E

Hole ID 75N278E										
Depths		**Interval (m)**	**RQD**	**J_n**	**J_r**	**J_a**	**J_w**	**SRF**	**Q-value**	**Ground Class**
From (m)	**To (m)**									
0.00	15.35	15.35	83	9	1.5	4	0.66	4	**0.57**	**D**
15.35	30.35	15	93	4	2	2	0.75	2.5	**7.00**	**B**
30.35	45.97	15.62	91	4	1.5	1	0.75	2.5	**10.24**	**A**
45.97	61.46	15.49	94	4	2	1	0.75	2.5	**14.10**	**A**
61.46	78.14	16.68	77	6	2	2	0.75	2.5	**3.85**	**C**
78.14	94.48	16.34	43	9	2	3	0.75	2.5	**1.43**	**C**

Allocation of the ground class type was based on the class ranges of Q-values shown in Table A-2 in *Appendix A.* It can be observed that the sampled area exhibits a variation in the rock

classification type whereby the ground classes vary from A to D. The ground classification system is such that class A is very good ground, whereas class D is very poor ground. Justifications of the parameters used in the calculation of Q-values are provided in below.

5.2.2 Rock Quality Designation (RQD)

RQD-values depicted in Table 5.1 are considerably high in five of the segments of the drill core except for the last segment. From 0mm to 15.53m, the RQD value is slightly lower than those for the subsequent three segments. This may be attributed to idea that some blast induced fractures might have been misconstrued as natural joints in the identification of drill core pieces incorporated in the calculation of RQDs. Thus, the RQD value for the segment closer to the periphery of the excavation surface might have been slightly distorted. Though there is possibility of a biased RQD value on the first segment, it is not to a very large extent since blasting only has an impact up to a 2m depth from the excavation periphery (NGI, 2015). There is a decrease in the RQD value from 61.46m to 78.14m, most probably due to an interception of a weak zone. From 78.14m to 94.48m, the RQD value is significantly low thereby implying further extension of a well-defined weak zone. Usually weak zones are areas with highly foliated rocks or rocks with well-developed schistosity. There is a direct relationship between RQD value and Q-value. Thus, holding other parameters constant, the higher the RQD the higher the Q-value and the reverse holds.

5.2.3 Joint Set Number, J_n

The J_n values were assigned depending on the number of joint sets and random joints intercepted within each of the drill core ranges. J_n values allocated to each segment of the drill core were selected from Table A-2 in *Appendix A.* The first segment of the drill core was assigned a considerably higher value of 9 as compared to the other segments. In general, the higher the number of joint sets intercepted by the drill core, the higher the assigned value of J_n. The higher number of joint sets intercepted by the drill core in the first segment may be attributed to the earlier mentioned idea that some blast induced fractures might have been misconstrued as natural joints forming some substantial joint sets. However, as the borehole extends further away from the excavation surface, where there is minimum impact of blasting, few joint sets were intercepted. An average of two joint sets were intercepted in the subsequent segments of the drill core. Hence, a J_n value of 4 was consistently assigned to the subsequent segments. When the was drill core considered to have intercepted two joint sets coupled with random joints, a J_n value of 6 was assigned. It is worth noting that the number of joint sets intercepted by the drill core depends on the orientation of the borehole. In the

case were a borehole is drilled parallel to the joints then a smaller number of joint sets are intercepted. However, if the borehole is drilled perpendicular to the joints then a higher number of joint sets are intercepted. This means that there is a possibility of assigning J_n values which are quite different. Thus, careful consideration must be taken when assigning J_n for a particular rock mass.

5.2.4 Joint Roughness Number, J_r

The J_r values fell within the range of 1.5 up to 2 such that the intercepted joints could largely be described as rough or irregular planar joints as well as smooth undulating joints. It is common knowledge that the greater the joint roughness, the higher the joint friction. Thus, very rough joints, joints with no filling or joints with only a thin and hard mineral filling are favourable to ground stability. The J_r values shown in Table 5.1 can be considered to be moderately rough, thus their influence on the Q-value is not too significant.

5.2.5 Joint Alteration Number, J_a

J_a values are highly dependent on the thickness and strength of infill of the clayey minerals in the joints. The J_a values which ranged from 1 to 4 for the drill core segments suggests that the joints alterations varied from being unaltered to slightly altered joint walls. For the first and the last segments of the drill core, slightly higher J_a value of 4 were assigned. The slightly higher values on these segments suggests that there was interception of joints with some joint filling or small clay fraction greater than 3mm in thickness. This corroborates well with the supposition that was mentioned earlier that this portion of the borehole might have intercepted a weak zone.

5.2.6 Joint Water Reduction Factor, J_w

Joint water pressure reduces the normal stress on the joint walls and cause rock blocks to shear more easily. The joint water may soften or wash out the mineral infill and thereby reduce friction on the joint planes. The assigning of J_w values was based on the observations that were made during the field survey as well as from guidance gathered from literature. During the field survey, some water could be seen dripping from the support boreholes. In addition, some low angled oxidised shear zones and joints were noticed thereby exposing that the rock mass was partially oxidised. It was mentioned in Chapter 2 that when mining involves excavations with water accumulations, the J_w cannot be considered as unity but rather set to a lower value to account for adverse groundwater conditions. Thus, the assigned J_w values for this drill core ranged from 0.66 to 0.75. According to NGI (2015), J_w values for underground excavations which are near the surface may vary with the seasons and amount

of precipitation. Thus, the J_w values are subject to variability depending on the climatic seasons.

5.2.7 Stress Reduction Factor, SRF

A consistent SRF value of 2.5 was assigned to this drill core. The value is acceptable since the underground excavations are close to the surface where low stresses and open joints are frequent in massive competent rock. Additionally, assigning of this value can be supported by the fact that for shallow excavations, there are high chances of the intercepting single weakness zones with or without clay or disintegrated rock.

5.3 Field Survey Observations

An underground visit to the peripheral areas of the southern section of the mine exposed the author to quite a number of variations in ground conditions. It was noticed that as the underground excavations approach the extreme limb parts of the deposit, the rock mass becomes partially oxidised. The rock mass towards the demarcated 30m oxidation zone on the southern section of the mine was highly flooded with low angled oxidised shear zones and joints. This confirmed the suggestion that these are inherent structures which had developed some years ago not due to mining activities. Thus, the fact that shallow mining areas are associated with high prevalence of natural joints is vindicated. These natural joints pose as ready weakness planes. Any ground opening activity in these shallow areas can cause loss of ground confining stress. Consequently, joint surface coherence is lost thereby rendering instabilities to the underground excavations. Low angled structures pose a challenge to support design in that reinforcement elements such as rock bolts or cable anchors must be long enough to be able to pin the weak rock mass slabs to the upper stable layers.

Another issue which was quite prevalent in these upper ore zones was the existence of a considerable amount of water within the rock mass. Water could be noticed dripping from the boreholes which were housing some roof bolts. This corroborates with the assigned J_w values of 0.66 or above as was mentioned in the Q-system rock mass quality analysis. Structures with water dripping from them were very common and signs of oxidation occurring in joints were clearly showing. These water saturations experienced in the near surface underground excavations fortify the hypothesis that if open pit mining is done in the vicinity of underground excavations, the adverse water effects on ground stability would be aggravated. This is due to the fact that the pit would accommodate some water accumulations especially from rainfall water, thereby increasing water saturation within the rock mass. High water

prevalence is not a desirable thing in mining areas because water aids in increasing pore pressure as well as washing away of infill material between discontinuities hence weakening the rock mass.

Fragmentation quality showed to have deteriorated as underground excavations approached near surface zones (±50 metres below ground surface). This was validated by the existence of high brows and over-breaks in stope panels. This is due to the high frequency of low angled oxidised fractures within this zone. Thus, for instance, if there was an open pit ahead, the brows and over-breaks would have been even worse since open pit excavations would have induced some rock mass relaxation. This would result in some zones being highly stressed and some incurring very low compressive to tensile stresses. It is those areas that are under very low compressive or tensile stresses that incur failure by ravelling of blocks in the panel roofs. Hence, high brows and over-breaks cold be noticed in stope panels. It is common knowledge that the creation of excavations in the rock mass implies some stress unloading condition. Hence, rock mass confinement is lost and consequently, the discontinuities inherent in the rock mass are rendered weak.

5.4 Numerical Modelling Input Parameters

Table B-1 in *Appendix B* depicts some of the material properties of the rock unit (composed of websterite and bronzitite) incorporated in the modelling exercises. As mentioned in the previous chapter, these values were based on the results of extensive testing done by ROCKLAB on behalf of Zimplats Mines.

5.4.1 Failure Criterion Input Parameters

The triaxial test results were used together with the Hoek-Brown GSI chart to derive the input parameter values for the Hoek-Brown failure criterion incorporated in the numerical modelling codes. The GSI value was calculated using Equation [3.1] which correlates GSI values to parameters used in the calculation of Q-values. In order to be consistent with the rock mass rating obtained in the Q-system, the average values for the input parameters *(adopted from Table 5.1)* relevant to Equation [3.1] were used and a GSI value of 64 was obtained. The GSI value was also calculated using Jr, Ja and RQD values from the drill core segment which had the worst RQD value of 43.27 and from that, a GSI value of 42 was obtained. Taking a more conservative approach, the GSI value of 42 was the one used in the numerical models.

Four samples were put under triaxial tests and the set of values for σ_1 and σ_3 were input in the formulae (shown in Appendix B2) to determine σ_{ci} and m_i values. The σ_{ci} and m_i values for the rock mass were obtained from the spreadsheet presented on Table B-2 in *Appendix B.* Upon inputting the GSI, σ_{ci} and m_i in the inbuilt GSI calculator in RS2 code, the peak parameter values m_b, a, and s for the rock mass were obtained as shown in Table 5.2 *(extract from Appendix D).* The rock mass elastic modulus and Poisson's ratio values shown in Table 5.2 are averages derived from the seven UCS test results shown in Table B-1 in *Appendix B.* Accompanying, the average values for the elastic modulus and Poisson ratio are the standard deviations (*numbers in brackets*) calculated using the sample standard deviation formula shown in Table 5.2. It is worth noting that there were no strength test data available for the estimation of the parameter values for backfill material. Hence, the author resorted to adopt values suggested for backfill material in the inbuilt RS2 examples.

Table 5.2: Generalised Hoek-Brown parameter values

Rock Mass		
Mechanical Properties		**Generalised Hoek-Brown parameter values**
Parameter	**Value**	**Peak**
σ_{ci} (MPa)	215	m_b = 1.17
Poisson's ratio	0.24 (0.01)	*s = 0.0016*
GSI	42	*a* = 0.51
m_i	9.25	
Elastic modulus (GPa)	148 (11)	
Backfill Material		
σ_{ci} (MPa)	7.5	m_b = 1
Poisson's ratio	0.15	*s = 0.001*
Elastic modulus (GPa)	2	*a* = 0.5
$SD = \sqrt{\frac{\Sigma(\chi-\bar{\chi})}{N-1}}$ Where, *SD* is the Standard Deviation, $\bar{\chi}$ is the sample mean and *N* is the number of samples.		

5.4.2 In-situ Stress Input Values

As highlighted in the previous chapter, the in- and out-of-plane stress ratios incorporated in the models were calculated based on the in-situ stress results measured at the nearby Mupfuti Mine at 160mbgs. The stress ratios were calculated as follows:

In-plane stress ratio $\quad K_H = 8.4/5.3 = 1.58$

Out-of-plane stress ratio $\quad K_h = 7.5/5.3 = 1.42$

The Field Stress option in the RS2 code was selected as this allowed for defining of the stress field conditions prior to excavations.

5.5 2-Dimensional Modelling

Analyses of the principal stress distributions and total displacements around the underground and open pit excavations were performed using the RS2 modelling software. Modelling results for models representing the two scenarios highlighted in the previous chapter are presented and discussed in this section.

5.5.1 Scenario 1 Model Contour Results

Figures 5.1 to 5.4 shows modelling results for the principal stress (σ_1) distributions around the underground and pit excavations. Figure 5.1 and 5.2 shows the principal stress distributions when the pit is excavated and when the pit is backfilled respectively. The stress contours show that excavation of the pit result in redistribution of stress such that the rock mass in the vicinity of the pit surfaces is subjected to low compressive stresses ($\sigma_1 \leq 0.3$MPa). Zones which are under tensile stresses can be noticed underneath the pit surfaces both on the highwall side and gentle slope side. However, backfilling slightly increases confinement stresses on the pit surface such that the rock mass underneath it incurs some slight increase in the compressive stresses.

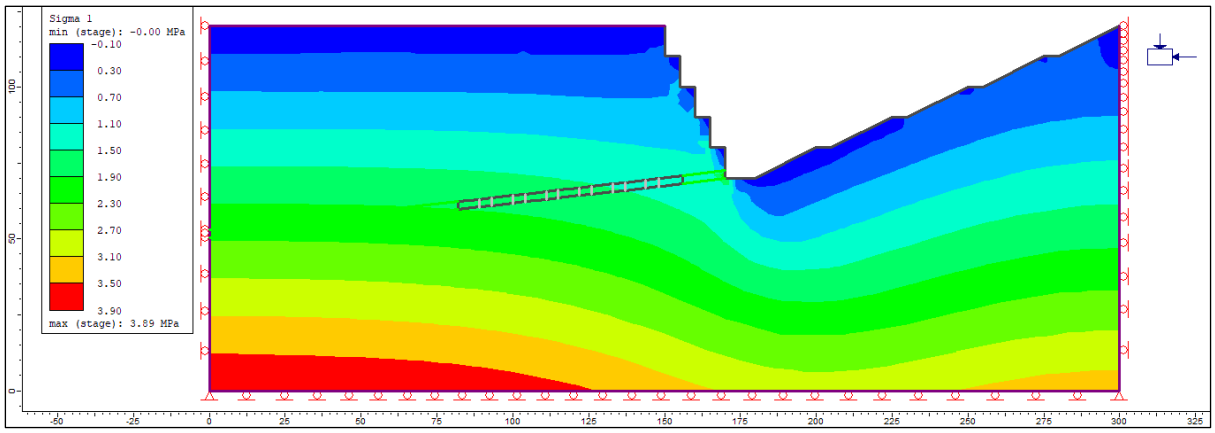

Figure 5.1: Stress (σ_1) when the pit is excavated

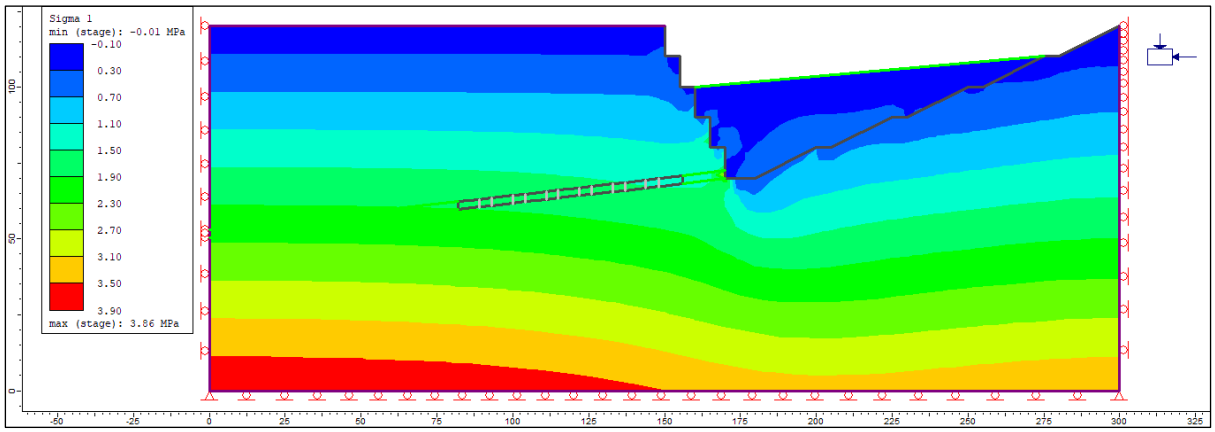

Figure 5.2: Stress (σ_1) when the pit is backfilled

Figures 5.3-5.4 shows the stress distributions when subsequent underground excavations are mined out. When the underground panels are mined out, stress redistributions cause some significant relaxation in the panel hanging walls. Figure 5.3 and 5.4 reflects that excavation of the underground panels result in enlargement of zone experiencing very low compressive stresses (σ_1 <1Mpa) as well as tensile stressed zones in the hanging wall and footwall of the panels. This zone is quite remarked in the hanging wall and footwall of the panel which is close proximity to the pit highwall side as seen on Figure 5.4.

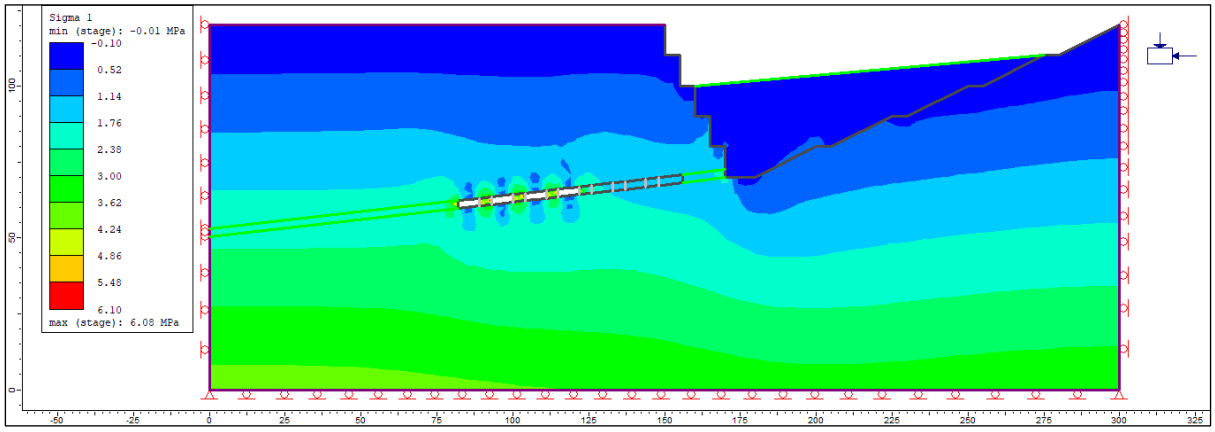

Figure 5.3: Stress (σ_1) when the first underground panel is excavated

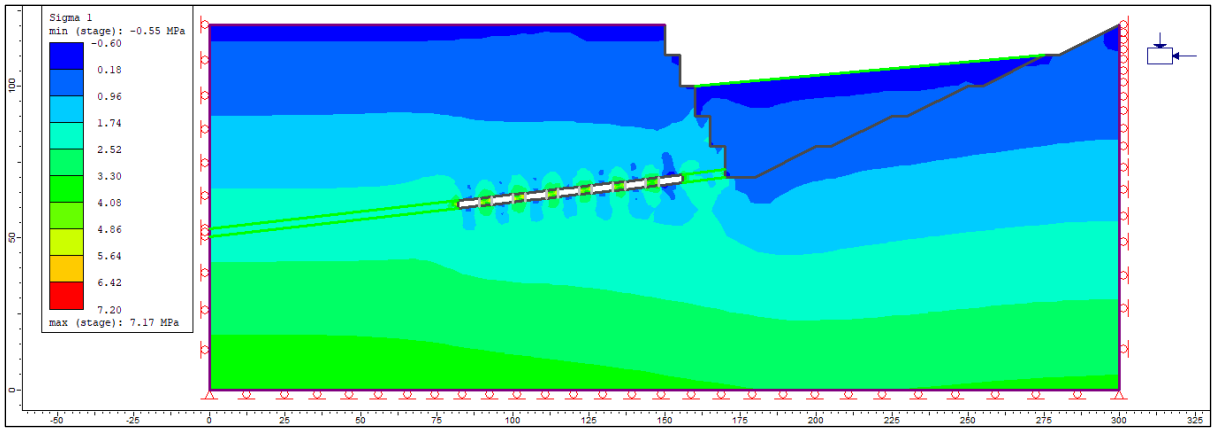

Figure 5.4 Stress (σ_1) when the seventh underground panel is excavated

Although there are zones of very low compressive stresses and tensile stresses in the panel roofs and footwalls, some substantial compressive stressing can be observed on the in-panel pillars. This is valid since creation of excavations in the rock mass result in stress redistributions in the surrounding rock mass thereby causing some areas to be considerably stressed and some being relaxed. Thus, in this case, stress redistribution result in slightly stressed in-panel pillars.

Analyses to determine the total displacements around the excavations were done and the results are shown in Figures 5.5 – 5.8. The results depict some very small displacements (≤4mm) at all stages. The small displacements signify some elastic behaviour thereby proving that no failure has happened in the rock mass. This is expected since the stresses experienced were very low (≤7MPa) when compared to the substantially high UCS value of 215MPa used in the models.

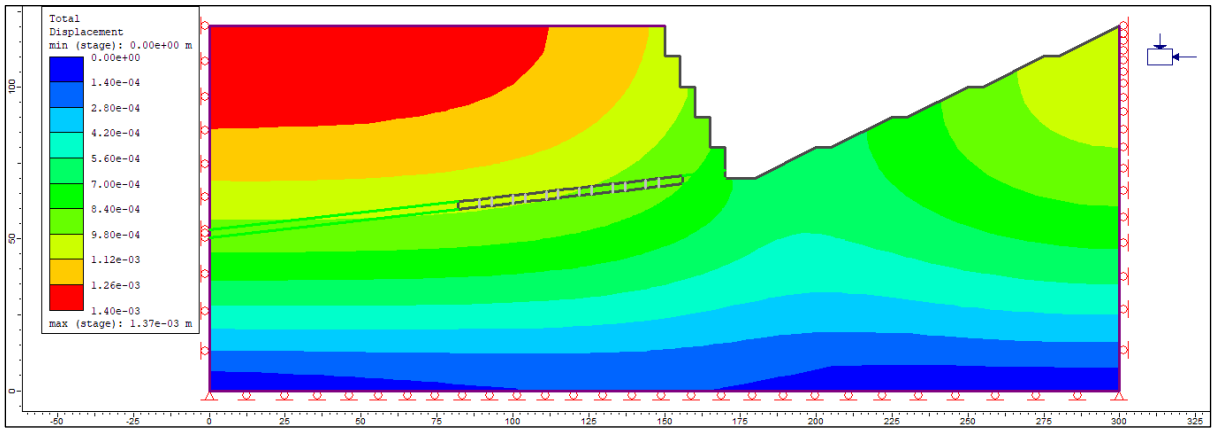

Figure 5.5: Total displacements when the pit is excavated

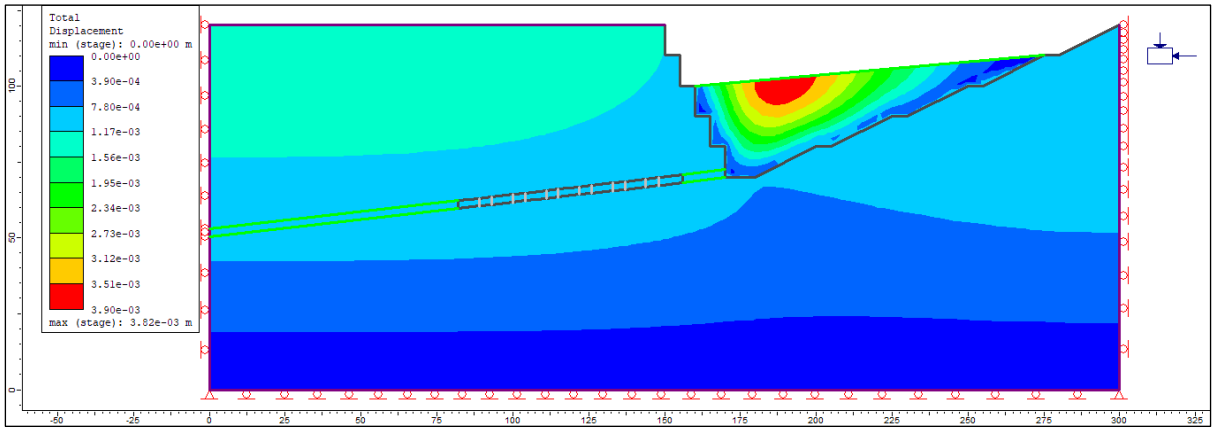

Figure 5.6: Total displacements when the pit is backfilled

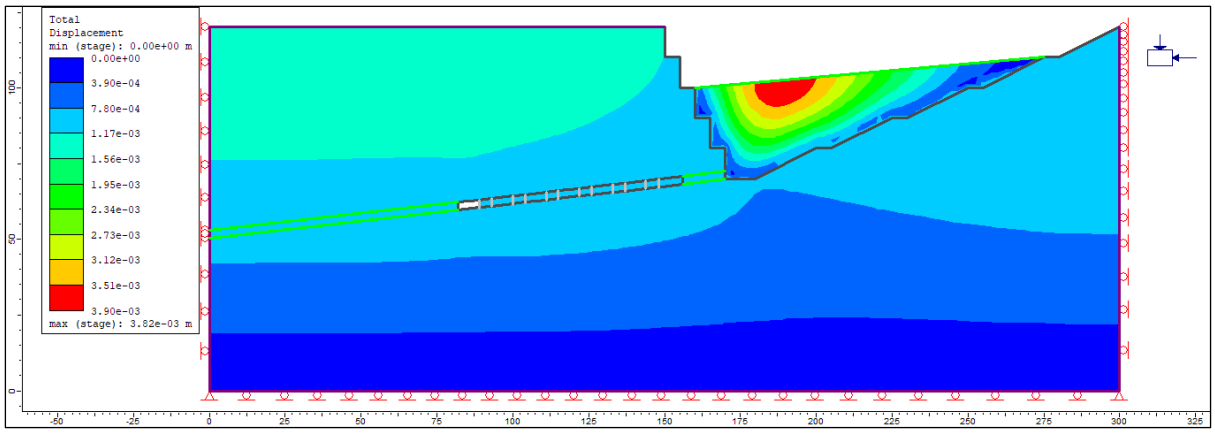

Figure 5.7: Total displacements when the first underground panel is excavated

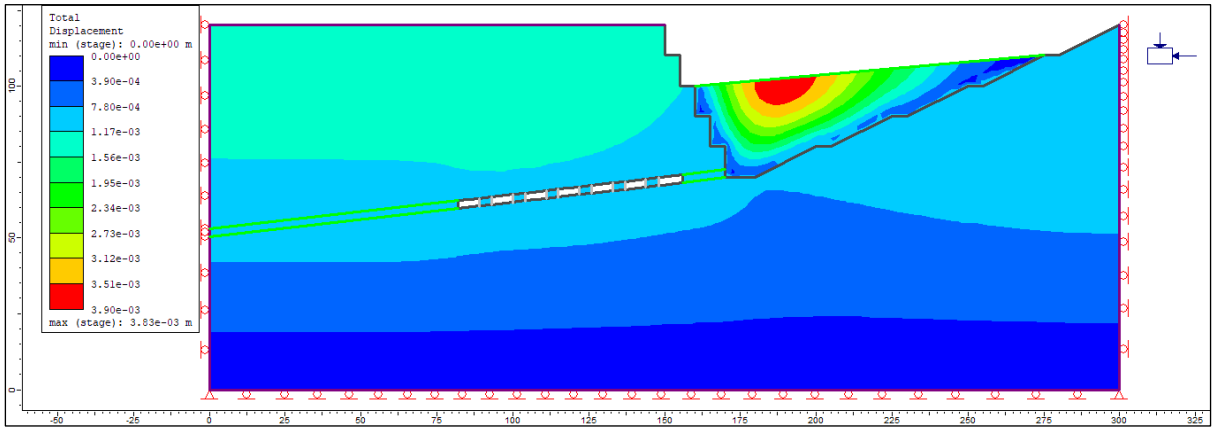

Figure 5.8: Total displacements when the seventh underground panel is excavated

5.5.2 Scenario 2 Model Contour Results

Particular attention was also put on analysing the effect of water accumulation on the pit. The same model in scenario 1 was used in this second scenario. The only difference was that, in the second scenario, there were evenly distributed loads on the backfill due to water ponding. Figures 5.9 and 5.10 show the chart results for stress (σ_1) and total displacements at stage 9 respectively.

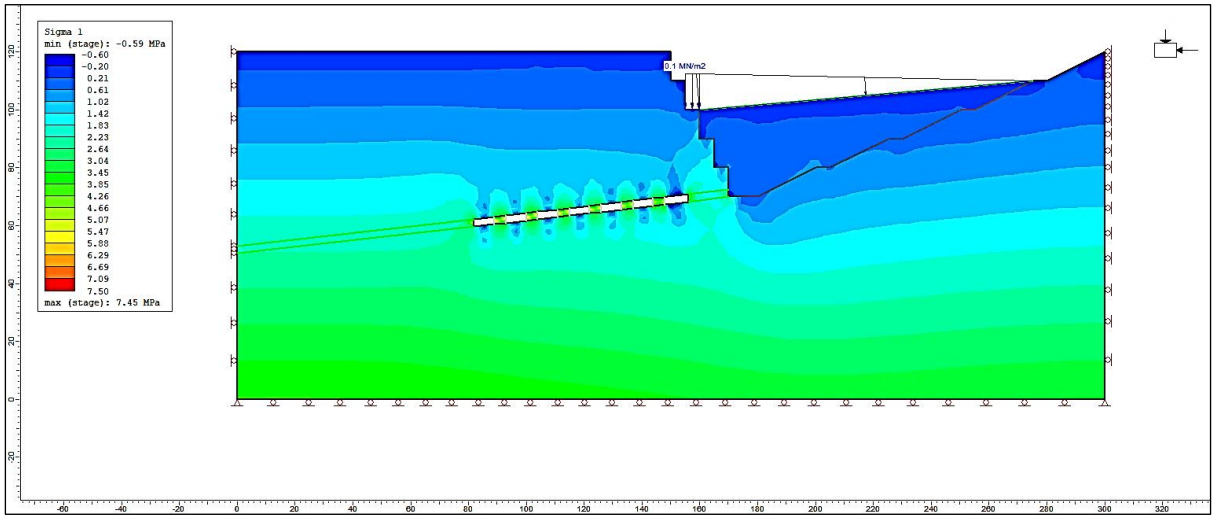

Figure 5.9: Stress (σ_1) distributions on excavations involving water ponding

Generally, the excavations are surrounded by a rock mass that is experiencing very low compressive stresses and even tensile stresses *(zones in dark blue)*. Almost similar to the stress results observed in scenario 1, zones of very low stresses are quite remarked in the middle sections of the panels' hanging wall and footwall. The small displacements recorded on the model exhibits some elastic behaviour in the rock mass. This could be attributed to the fact that discontinuities were not incorporated in the models. They were deliberately left out of the models because of infinite number of variations of joint orientations, lengths and positions that happen in the rock mass. However, the effect of water cannot be ignored

because it is on these discontinuities where significant deformation is usually noticed especially when the rock mass is saturated with water.

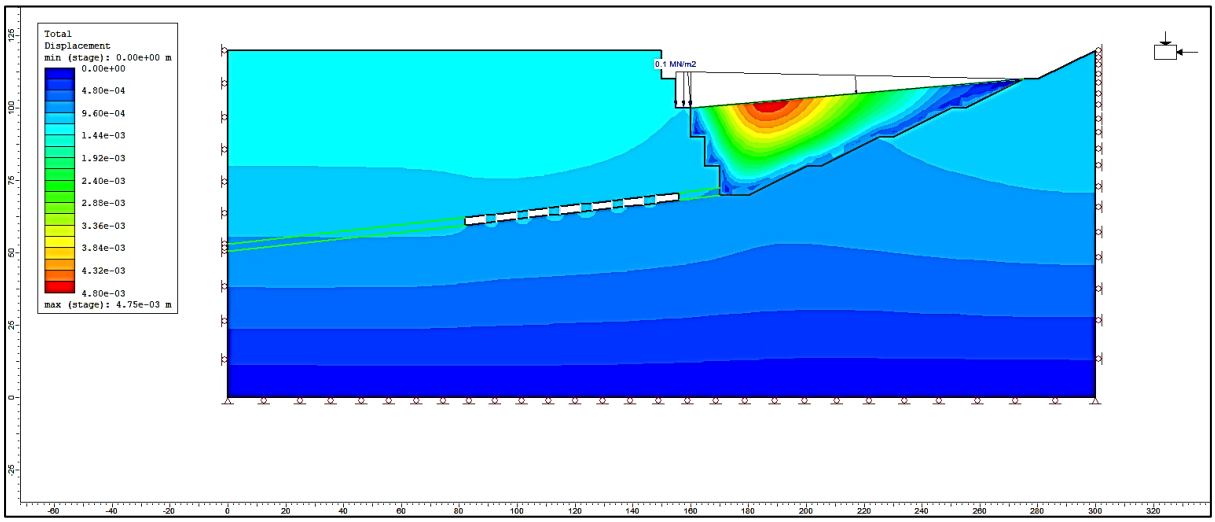

Figure 5.10: Total displacements on excavations involving water ponding

5.5.3 Discussion of 2D Results

Queries to determine the values for the principal stresses and total displacements around the underground and open pit excavations were run on the models for the two scenarios and these are shown in *Appendix E*. Two material queries were used, with the first one placed in the hanging walls of the underground panels. The starting point for this first query was at the top left corner of the panel furthest from the pit highwall side. Its termination point was just above the panel in the close proximity to the intermediate pillar. The second query was placed along the pit highwall side and its starting point was closer to the surface while its termination was somewhere within the intermediate pillar. The placements for the material queries was premised on the postulation that these zones were the most active and critical to the stability of both underground and pit excavations. For instance, on underground panels, the hanging wall is vulnerable to falls of ground due to very low horizontal stresses. On the other side, the pit highwall side is susceptible to stress relaxation which may enhance sliding of blocks along weakness planes. Furthermore, chances of pit slope failure were likely to be increased by the presence of water in the pit which cause the weakening of rock masses especially along discontinuities.

Largely, very low compressive stresses (σ_1<3MPa) were incurred in the rock mass surrounding the underground and pit excavations. On the underground panels, zones which were experiencing low compressive stress and even tensile stresses were those in the middle sections of the panel hanging walls. These zones of low compressive stresses and tensile

stresses were quite enlarged for the panels in the close proximity of the pit highwall side. The low compressive stresses will cause strata relaxation in the panel hanging walls which, in turn, will increase the likelihood of falls of ground in the panels. Falls of ground in these shallow excavations are inevitable due to the fact that the rock mass is normally flooded with discontinuities which induce blocky conditions. Additionally, near surface excavations are associated with low confining stresses due to less overburden. Thus, if the compressive stresses are very low or if tensile stresses are experienced, then there will be lack of block confinement. This lack of confinement will result in falls of ground in the underground working areas.

Similar to the principal stresses, the total displacements were significantly low (<4mm) such that they resembled some linear elastic deformation behaviour in the rock mass. This may be attributed to the probable exaggeration of the rock mass stiffness since discontinuities were not incorporated in the numerical models though there are a very important factor. It was mentioned earlier that the discontinuities were deliberately left out of the models because of infinite number of variations of joint orientations, lengths and positions. It is commonly known that discontinuities influence the extent to which a rock mass deforms. They form the planes of weaknesses upon which significant displacements can occur. Although, the RS2 model could not bring out significant deformation in the rock mass, the field observations confirmed the presence of discontinuities in the rock mass. Thus, structurally controlled failure both on the pit and underground excavations cannot be ruled out and support strategies to counter them must be put in place.

Analyses of the models involving water ponding showed a slight enlargement of the zone experiencing low compressive stresses as well as tensile stresses *(see Figures 5.4 and 5.9).* This zone was quite remarked especially on the panel in the close proximity to the pit highwall side. A slight increase in the total displacements was noticed on the model involving water ponding on the pit excavations. Though the increases in the rock deformation with the introduction of water ponding were so minute, it gives an impression that the presence of water in mining areas increases the chances of rock deformation of especially when it is a blocky rock mass.

Failure on the underground panels was of major concern since the workings were still very active unlike on the pit slope where operations were now dormant. Thus, any failure on the pit slope, whether be it by plane, wedge or toppling mechanism, would not be of catastrophic significance to the underground mining operations. The only concern associated with pit

slope failure would be that which wold cause water inrushes into the underground excavations. Thus, stability of the pillar in-between the underground and pit excavations needed to be carefully considered. It is this pillar that would act as a plug to stop water inrush into the active underground workings.

5.6 3-Dimensional Modelling

Bord and pillar mining involves creation of pillars which are critical for the stability throughout the life of the mine. Hence, 3D modelling was solely done in order to get an insight on how the in-panel pillars would be stressed. Knowledge of the stresses exerted on the pillars helps the rock engineer to come up with the appropriate pillar dimensions that ensure an acceptable factor of safety.

5.6.1 3D Stress Results

Figure 5.11 shows the stress contour for the model at the initial stage. It is worth noting that the initial stress contour serves as a benchmark of how the stress is distributed before any excavation is cut in the rock mass. A quick check of the validity of the model can be done by, for example, randomly choosing a point on the model and note down the stress value that has been automatically computed by the system. Thereafter, proceed to calculate the vertical stress (ρgh) and compare it with the system calculated value. For validity of the model, the values should be approximately the same.

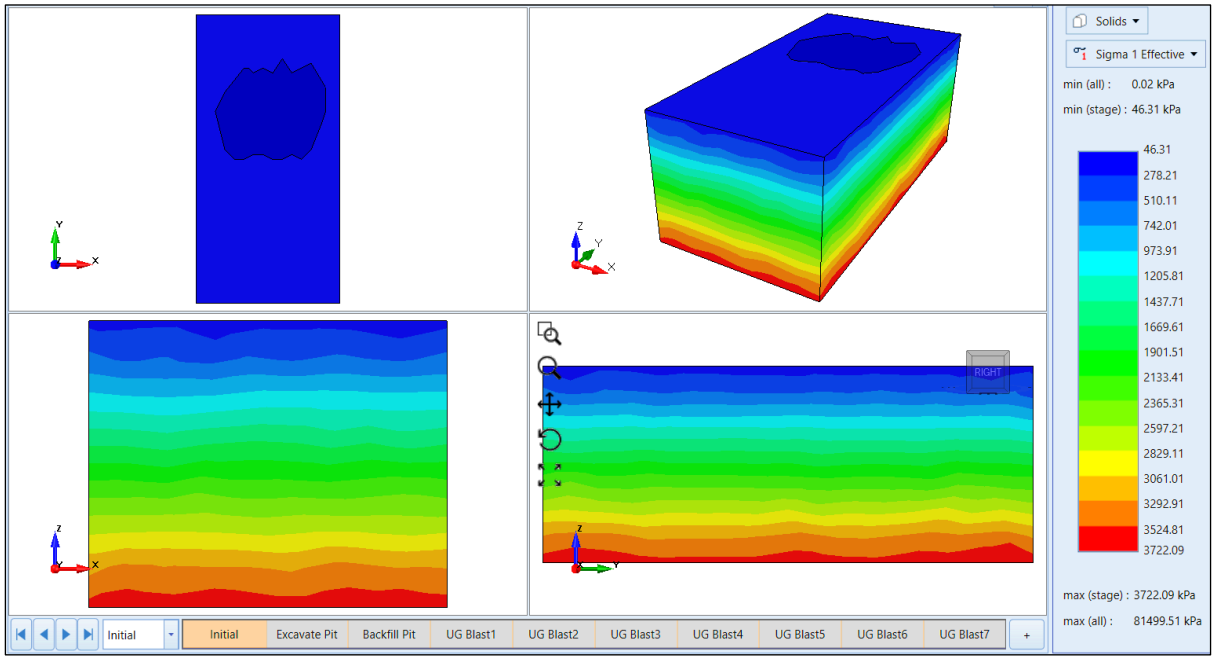

Figure 5.11: Initial stress contour

Thus, for example, assuming homogeneity and with a material density of 3200kg/m^3 *(used in the model)* at a point located at 120m below the surface, the resultant vertical stress would be

3.76MPa. This value is close to the maximum effective stress value of approximately 3.72MPa obtained in the model on Figure 5.11, *(i.e. zone in deep red).* Hence, the model was considered to be valid for further use in the subsequent analyses when more excavations were made in the rock mass. Figures 5.12– 5.14 shows the contour results where stress distributions are observed around the excavations at various stages of mining.

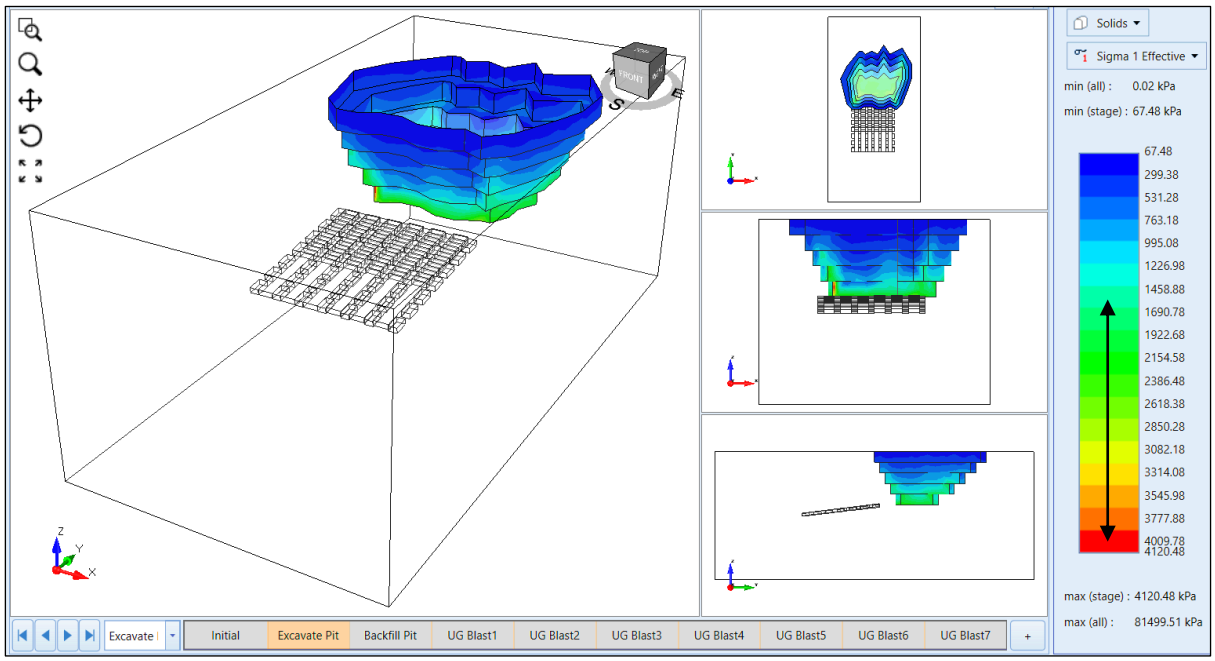

Figure 5.12: Stress distributions when the pit is excavated

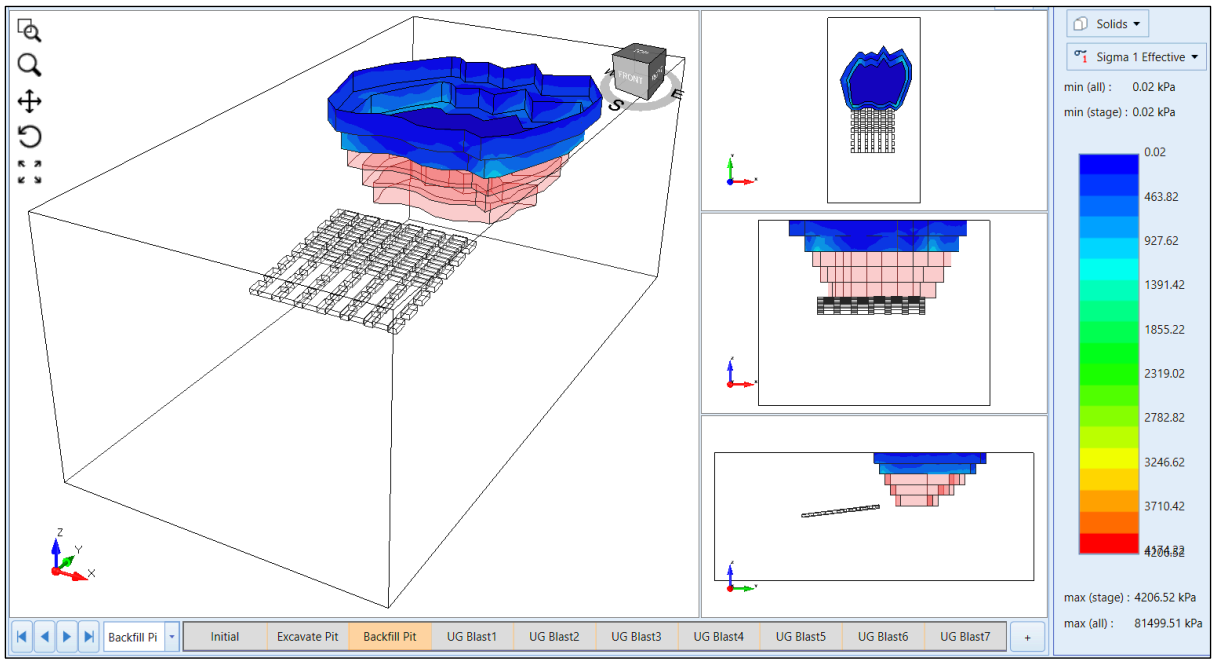

Figure 5.13: Stress distributions when the pit is backfilled

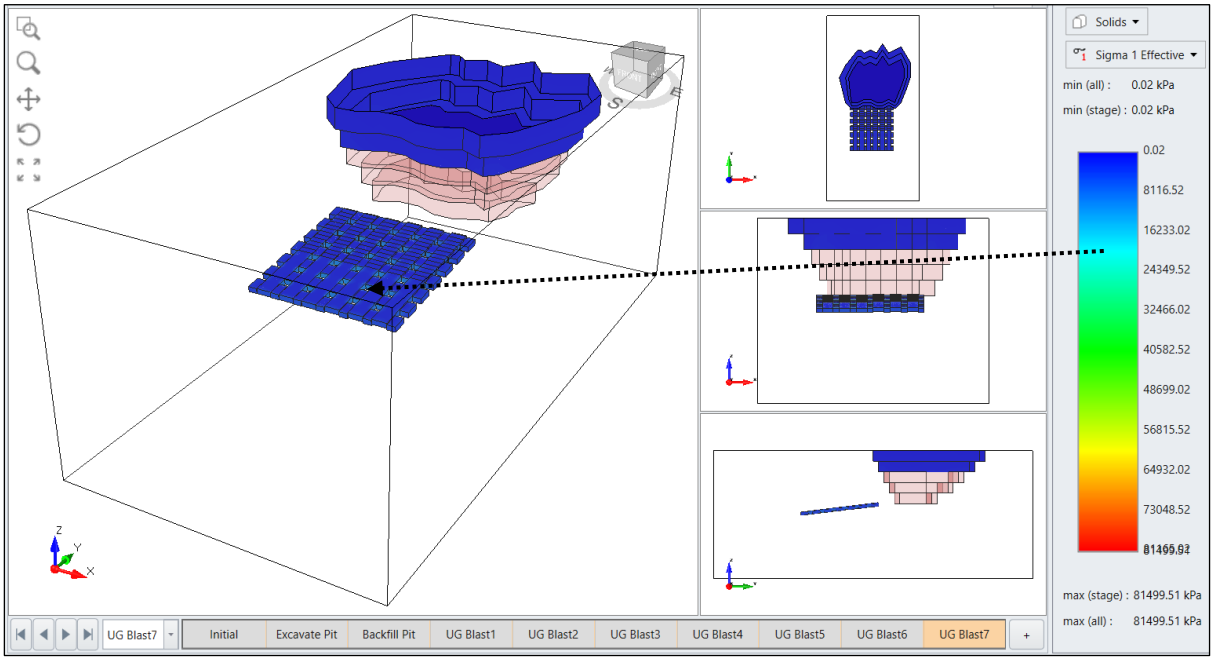

Figure 5.14: Stress distribution after the seventh blast on the underground panels

Figures 5.12 - 5.14 shows that the principal stresses (σ_1) around all excavations are significantly low. When the pit is excavated, the pit surfaces at the bottom benches exhibit some isolated areas of moderate stress concentrations ranging from 1.5MPa to 4MPa *(see zones with colours corresponding to the region highlighted by an arrow on the contour legend of Figure 5.12).* When the pit is backfilled, the stresses were significantly reduced to less than 0.02MPa on the pit surfaces above the backfill level.

The stresses around the underground panels were substantially low. However, a closer look at Figure 5.14 shows that the in-panel pillars were experiencing some substantial stresses as high as ±20Ma *(see area indicated by an arrow on Figure 5.20)*. It is common knowledge that as more excavations are made, stresses are redistributed to the rock mass surrounding the excavations. That is why the in-panel pillars were considerably stressed. In other words, the stress concentration in the pillars increased as more excavation openings were being created.

5.7 Comparison of 2D and 3D Modelling

It was mentioned earlier that 3D modelling was done for the sole purpose of accounting for the stress distribution on the in-panel pillars. Three-dimensional modelling enables comprehensive examination of the stress concentrations around the ends and edges of excavation. It was observed that 3D modelling predicted substantial pillar stresses exerted on the in-panel pillars than those obtained in the 2D models. The 2D modelling showed maximum in-panel pillar stresses of around ±6MPa, whereas 3D modelling showed pillar stresses as high as ±20MPa. Three-dimensional stress results proved to be more realistic since

it considers the tributary load exerted on the pillars due to overlying strata. In tabular bord and pillar mining, it is common that a pillar will not only sustain the area above it but also an overlap area beyond the pillar surface. Thus, 3D modelling managed to consider the tributary load which was not the case with 2D plane strain analysis.

5.8 Intermediate Pillar Stability Analysis

The strength factor tension results obtained from the 2D model are shown on Figures 5.15 and 5.16. The 2D model incorporating a backfilled pit coupled with water ponding was used. In order to account for the possible blocky conditions associated with these near surface excavations, an analysis of the strength factor with ubiquitous joints was run in RS2. This allowed for investigation of possible tensile failure in the intermediate pillar as well as along the pit highwall slope. Figure 5.15 shows the strength factor results when the intermediate pillar width is 15m. It can be clearly seen that a zone with a tensile strength factor of approximately 3 constitutes a larger portion of the intermediate pillar. A strength factor of 3 is considerably good such that pillar failure is unlikely to happen.

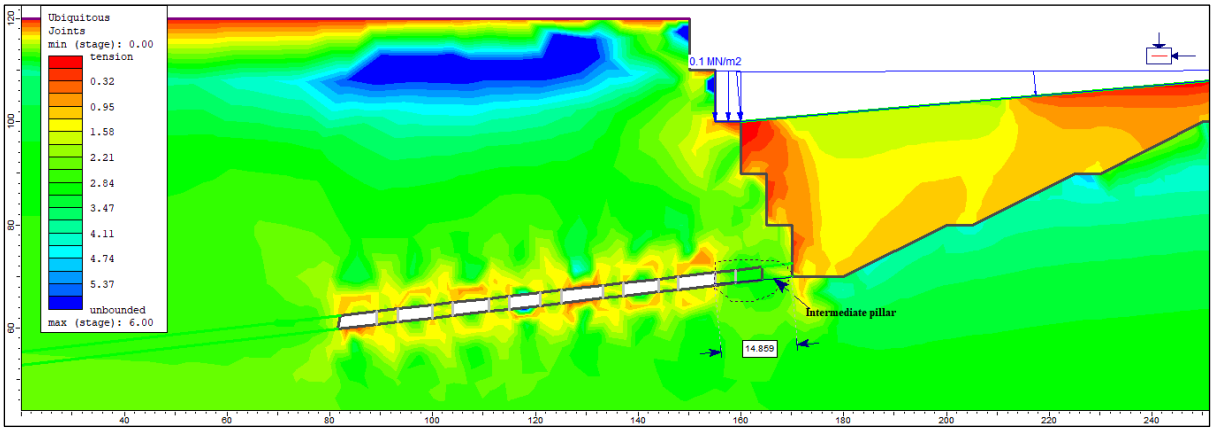

Figure 5.15: Strength factor results when the intermediate pillar width is 15m

Further excavation of the underground panels close to the proximity of the pit highwall side indicates a significant decrease in the strength factor of the rock mass constituting the intermediate pillar. For instance, on Figure 5.16 where the intermediate pillar width has been reduced to about 6m, a zone with a strength factor less than 1 constitutes the middle portion of the pillar. This signifies that pillar weakening leading to tensile failure is inevitable on the intermediate pillar. Therefore, there should be no further reduction of the pillar width as this will pose a danger of water inrush into the underground workings in the event that the pillar fails. In addition, the rock mass in the vicinity of the pit highwall slope showed zones of very low strength factors (i.e. S.F $\leq$ 1; *orange and red zones*).

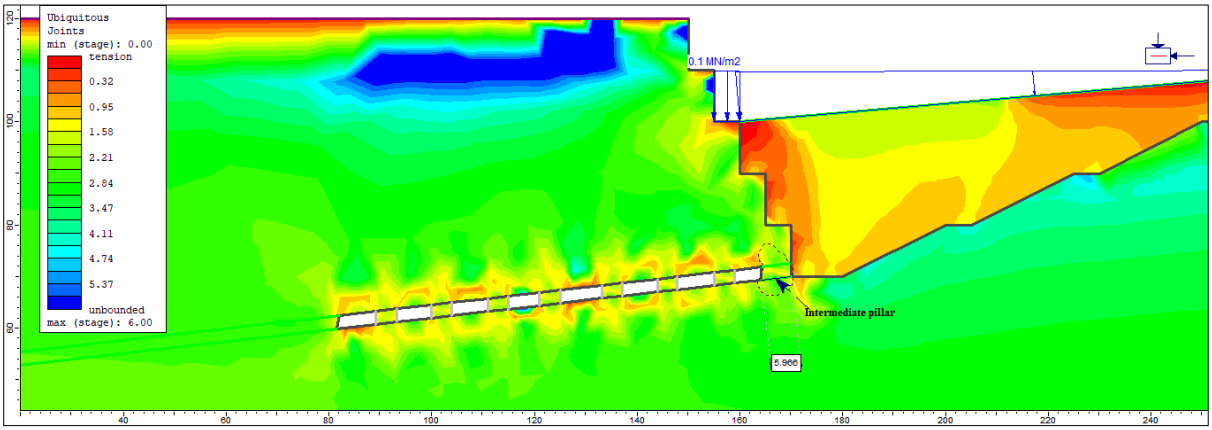

Figure 5.16: Strength factor results when the intermediate pillar width is 6m

Figure 5.17 shows the effects of the minor principal stresses on the excavations. Particular attention was on the effect of these stresses in the hanging walls of the underground panels.

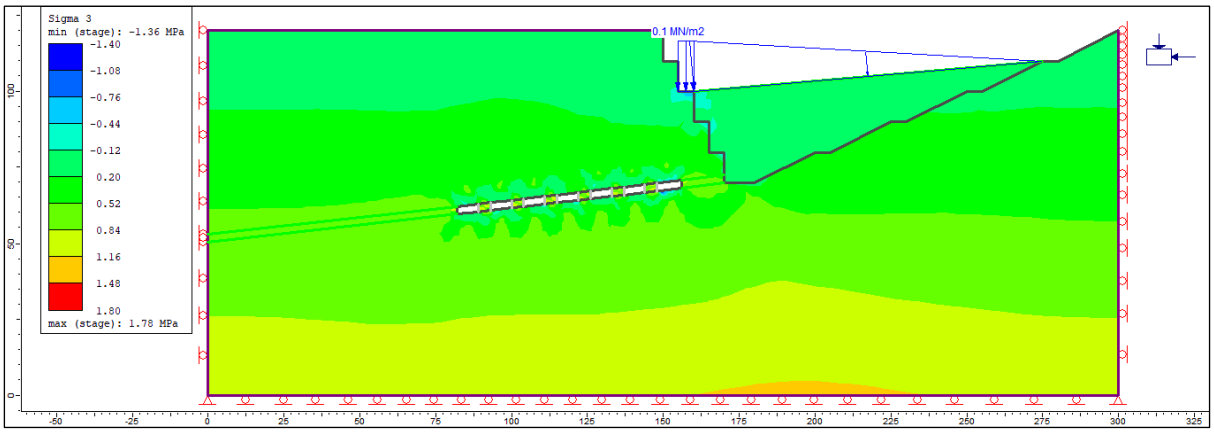

Figure 5.17: Minor principal stresses on the excavations

It can be seen from Figure 5.17 that the minor principal stresses upon the hanging walls are largely in the tensile range *(light blue zones)*. These tensile stressed zones are very sensitive to gravitational fallouts of blocks and wedges especially in the hanging walls of the underground panels. Dislodging of the blocks is even more enhanced when there is invasion of water in the rock mass as it will reduce the normal stress on the discontinuities.

Ozbay et al. (1995) mentioned that the major purpose for leaving barrier pillars is to control the tensile zone and to increase strata stiffness so as to avert possible pillar runs in stopes supported by non-yield pillars. Thus, there is need to leave an intermediate pillar which has a sufficient strength factor such that regional failure is avoided. However, the ore extraction process should be economically viable. Therefore, the intermediate pillar should be as slender as possible so that not much of the resource is sterilised in the pillar.

Terbrugge et al. (2009) argued that, a good mining excavation is that which fails just after the last truckload has left the mine. If it is such a case, it implies that the rock engineer would not have been too conservative in the design of the pillar. Hence, a maximum possible amount of ore would have been extracted. To this end, an optimum intermediate pillar width would be the one which is moderately slender but, also having a considerably low probability of failure. A pillar with such characteristics should be the one settled for by the rock engineer.

5.9 Chapter Summary

The chapter starts with the classification of the rock mass intermediate the underground and pit excavations. In general, the RQD values were very high signifying some substantial rock mass intactness. However, it is worth noting that RQD values are dependent on the orientation of the drill hole. For example, a drill core extracted parallel to the discontinuities is bound to give a high RQD value, whereas the one extracted across the discontinuities will give a low RQD value. It was observed that misconstruing of blast induced fractures as natural joints is possible especially of the segments extracted closer to the excavation surfaces. This might have been the reason why the first segment of the drill core had a slightly lower RQD value than those for the subsequent segments. Though the RQDs were very high, the obtained Q-values were slightly on the lower end mainly due to the influence of low J_w values. However, the ground intercepted by the drill core can be considered to be of fair quality if one is to classify it using the ground classification system based on the Q-value ranges used at the case study mine.

Field observations exposed that the rock mass near the surface is partially oxidised and awash with natural joints. These natural joints form planes of weakness which render instability to mining excavations. This confirmed the general understanding that near surface excavations are more prone to structurally controlled than stress induced failure. During the field survey, some water could be noticed dripping from the support boreholes. This observation corroborates well with the assignment of slightly low J_w (i.e. 0.66 - 0.75) which were used in the calculation of the Q-values. Structurally controlled failure was also evident as seen by the presence of high brows and over-breaks in the underground panels.

Two-dimensional modelling showed that excavation of the pit resulted in low confinement of the rock mass underneath it. However, backfilling increased the rock mass confinement. Excavation of more underground panels closer to the pit resulted in the enlargement of the zones experiencing low compressive stresses and some under tensile stresses. Total displacements on all the stages were very low (≤4mm) indicating some elastic behaviour in

the rock mass. Two-dimensional modelling without the incorporation of discontinuities made the rock mass to appear as very intact such that little deformation was observed. It is commonly known that water reduces the joint cohesion and washes away the infill material thereby weakening the rock mass. Leaving out of discontinuities from the models further distorted the results of the weakening effect imposed by water on the rock mass.

Three-dimensional modelling was done for the sole purpose of showing out how the stresses were distributed on the in-panel pillars. Three-dimensional modelling showed some substantial pillar stressing of ±20MPa, whereas 2D modelling predicted pillar stresses of around ±6MPa. The difference is attributed to the fact that 3D analysis considers the tributary load upon the pillars which is not the case with 2D plane strain analysis. In other words, 2D analysis underestimates the pillar load. It was also observed that the strength factor of a intermediate pillar decreases as the pillar width decreases. The rock mass in the hanging walls of the underground panels had very low strength factors especially on the panel closest to the pit highwall. In addition, 2D analysis showed that the minor principal stresses in the hanging walls were largely tensile in nature. The tensile conditions cause the panel hanging walls to be susceptible to falls of ground.

6 CONCLUSIONS AND RECOMMENDATIONS

6.1 Overview of the Research

The main goal of this research was to predict the ground instabilities encountered by interacting underground and open pit excavations. The study was anchored on a case study which involved underground mining excavations which were advancing towards a mined out open pit. It was hypothesized that the foregoing open pit mining excavations would cause ground disturbance such that when underground panels were to be mined in the vicinity of the pit, there would be high prevalence of rock mass failure in the underground workings. Characterisation of the rock mass between the underground and pit excavations was done using the Q-system. In order to get a clear understanding of how the rock mass behaves as underground mining excavations advance towards the pit, simulations were done using 2D and 3D FEM numerical modelling. Various numerical models were built to represent two different scenarios which include:

- Underground excavations interacting with a backfilled open pit; and
- Underground excavations interacting with an open pit which was backfilled as well as water ponded.

Lastly, a stability analysis of the intermediate pillar was done using a 2D FEM model created in RS2. After carrying out all the necessary analyses, the following conclusions and recommendations were reached upon.

6.2 Conclusions

Upon carrying out rock mass characterisation, it was evident that the water condition in the rock mass has a high influence on the quality of the rock mass. Although, the rock mass appeared to be very intact judging from the obtained RQD values, the resultant Q-values were low due to the low J_w values. The low J_w values which were assigned corroborated well with what was observed in the field survey, that is, water could be seen dripping from the support boreholes. It is logical to suggest that the dripping water which was noticed could be water that might have been accumulated on the pit. Furthermore, blasting activities on the pit might have caused further opening and extension of natural joints in the rock mass thereby creating pathways for water to permeate through the rock mass.

The presence of high brows and over-breaks in panels proved the issue that is always raised that near surface excavations are associated with structurally controlled failure. The near surface rock mass is usually partially oxidised and awash with natural discontinuities as was

observed from the field survey. The natural geological structures create blocks and zones which are highly distressed which in turn create huge irregularities in the state of stress of the rock mass.

Two-dimensional modelling showed that near surface excavations are associated with very low compressive stresses and tensile stressed zones in the rock mass. It was observed from 2D analysis that less overburden result in lower stresses around the excavations. It is these very low stresses which increase the risk of fallouts and progressive failure especially on the underground panels. In addition, very low stresses around excavation are detrimental in that they promote opening up of geological structures such as faults and joints. An open discontinuity above an underground panel can cause creation of distressed zones in the panel roof so that a bearing arch above the panel cannot be formed. Generally, it can be concluded that a panel at a shallow depth result in a larger area experiencing tensile stresses than that for a panel at a greater depth. It is commonly known that the tensile stresses cause plastic deformation in rock masses. The very small displacements observed on the excavations from 2D analysis indicate some linear elastic behaviour in the rock mass. This may be attributed to the exaggeration of the rock mass stiffness since discontinuities were not incorporated in the models.

Three-dimensional modelling brought out the issue of how stresses are distributed in the third dimension. Understanding of pillar stresses is of paramount importance especially when modelling bord and pillar mines as it helps in the design of stable pillars. Three-dimensional modelling effectively accounted for the tributary load sustained by the in-panel pillars which was not the case with 2D plane strain analysis. Two-dimensional analysis underestimated the pillar stresses at around 6MPa, whereas 3D analysis predicted pillar stresses of around 20MPa.

The intermediate pillar stability analysis using a 2D model showed that as more underground excavations are made in the vicinity of the pit highwall side the strength factor of the intermediate pillar is reduced. In other words, the smaller the pillar width the more prone it is to failure. Hence, there is need to always balance the extraction ratio with the pillar strength. Pillar strength is a function of rock material strength and the pillar geometry. Thus, the pillar should be wide enough to sustain the imposed stresses on it. From the minor principal stress analysis, it was seen that the rock mass surrounding the underground panels was largely under tensile stresses. Usually plastic deformation is due to tensile stresses. It can thus be concluded that, in shallow excavations, the stresses and displacements developed and the size

of the plastic zone around underground panels are not only dependent on the mechanical properties of the rock but also on the position of those panels relative to other nearby excavations.

6.3 Recommendations

The research has brought out the adverse effects of water on the rock mass quality. Water inflows into mining excavations are not desirable because it increases the pore pressure as well as washing away of infill material between discontinuities thereby weakening the rock mass. A mined out open pit can be a source of water accumulations especially during the rainfall season. With time, the accumulated water will permeate through the inherent natural discontinuities thereby weakening the rock mass. In addition, blasting activities on the pit may cause further extension and opening up of natural joints in the rock mass. To this point, if pit mining has preceded underground board and pillar mining then the pit must be backfilled to increase the rock mass confinement. However, the backfill can sometimes accommodate water accumulation in the pit such that a danger of water or mud rush can be imposed on the active underground workings. Therefore, a strict monitoring program must be put in place to monitor the water accumulations on the pit. Consistent dewatering of the pit should be adhered to so as to reduce the risk imposed by possible water inrushes in the event that the intermediate pillar fails.

It was earlier mentioned that, if well calibrated, numerical models play an important role in the understanding and prediction of rock mass behaviour. It is important to recall that the choice of the numerical modelling packages used in this research was rather based on availability more than their capabilities in comparison to the other computer packages. Therefore, more detailed numerical modelling using commercial packages such as MAP3D, which is specifically developed for modelling bord and pillar excavations, should be used to enhance the understanding of the rock mass behaviour.

REFERENCES

Baczynski N.R.P 2000, 'STEPSIM4 "step-path" method for slope risks.' *Proceedings of the International Conference on Geotechnical and Geological Engineering (GeoEng2000)*, Melbourne, Australia, November 2000. Techtonic Publishing Co., Lancaster, pp. 86-92.

Bakhtavar E., Oraee K., and Shahriar K., 2010, 'Determination of the optimum crown pillar thickness between open pit and block caving'. *29th International Conference on Ground Control in Mining*, Dept. of Mining Engineering, College of Engineering and Mineral Resources, Morgantown, West Virginia, USA, pp. 325-332.

Bar N., DuPlessis P., Nicoll S., Welideniya S., Ryan C. and McAllister P., 2018. 'Risk management strategies for open pit mining through historic underground workings'. *ISRM International Symposium-10th Asian Rock Mechanics Symposium*, Singapore.

Barton N., Lien R., and Lunde J., 1974, 'Engineering classification of rock masses for the design of tunnel support.', *Rock Mechanics*, vol 6, no. 4, pp. 189-236.

Bieniawski Z.T., 1973, 'Engineering classification of jointed rock masses.', *The Civil Engineer in South Africa*, vol 15, pp. 335-343.

British Geological Survey., 2011, *Natural ground stability*, Nottingham, viewed 02 August 2018, <https://shop.bgs.ac.uk/GeoReports/examples/S004.pdf>.

Carter T.G., 2014, *Rocscience*, Guidelines for use of the scaled span method for surface crown pillar stability assessment. Ontario, pp 1-34, viewed 31 March 2019, <https://rocscience.com/documents/pdfs/library/Trevor_Carter_2014.pdf.>.

Castro L.A.M., and McCreath D.R., 1997, 'How to enhance the geomechanical design of deep openings.', *In Proceedings of the 99th CIM Annual General Meeting,Vancouver*, Canadian Institute of Mining, Montreal, Canada, pp. 1-13.

Corkum A., 2017, RS2 (Phase2) Overview tutorial-tunnelling, viewed 27 March 2019, <https://www.youtube.com/watch?v=2n3RPCputKo>.

Deere D. U. and Deere D. W. 1988, 'The Rock Quality Designation (RQD) Index in practice. Rock classification systems for engineering purposes', American Society for Testing and Materials, ASTM STP 984, Louis Kirkaldie, Ed. Philadelphia, pp. 91-101.

Deere, D., Hendron, A., Patton, F ,and Cording, E. 1967, 'Design of surface and near surface construction in rock. In failure and breakage of rock', *Proceedings of the 8th U.S. Symposium on Rock Mechanics-Failure and Breakage of Rock*, American Institute of Mining, Metallurgical and Petroleum Engineers, New York, pp. 237-302.

Diering J.A.C., and Stacey T.R., 1987, 'Three-dimensional stress analysis: a practical planning tool for mining problems.', *Proceedings of the Twentieth International Symposium on Application of Computers and Mathematics in Mineral Industries*, SAIMM, Johannesburg, South Africa.

Eberhardt E., Woo K., Stead D., and Elmo D., 2015, 'Transitioning from open pit to underground mass mining: Meeting the rock engineering challenges of going deeper', *Proceedings of the International Symposium on Rock Mechanics*,Canada Institute of Mining, Montreal, Canada.

Edison Investment Research., 2012, *Mwana Africa*, viewed 06 August 2018, <https://www.edisoninvestmentresearch.com/?ACT=18&ID=7175&LANG=>.

Gay N.C. 1975, 'In-situ stress measurements in Southern Africa', *Tectonophysics*, vol 1-4, no. 29, pp. 447-459.

Guler G., Quaye G.B., Jager A.J., Schweitzer J.K., Grodner M., Reddy N., Andersen L., Milev A., and Wallmach T., 1998, 'A methodology for the definition of geotechnical areas within the South African gold and platinum stoping horizons', SIMRAC Project Report GAP 416, SIMRAC, Johannesburg, South Africa.

Hammah R. E., and Curran J. H. 2009, 'It is better to be approximately right than precisely wrong:Why simple models work in mining geomechanics', *Proceedings of the International Workshop on Numerical Modeling for Underground Mine Excavation Design*, Asheville, North Carolina, USA, pp. 55 - 63.

Heidbach O., Rajabi M., Reiter K., and Ziegler M.O. (2016): World Stress Map. GFZ Data Services, viewed 14 June 2021, <https://doi.org/10.5880/WSM.2016.002>

He M.C., Feng J.L. and Sun X.M. 2007, 'Stability evaluation and optimal excavated design of rock slope at Antaibao open pit coal mine, China', *International Journal of Rock Mechanics & Mining Sciences*, vol 45, pp. 289-302.

Henning J.G., 2007, 'Review of crown pillar investigations in a Historic Mine Camp', *1st Canada-US Rock Mechanics Symposium-Rock Mechanics Meeting Society's Challenges and Demands*, American Rock Mechanics Association, Vancouver, Canada, pp. 1441-1445.

Hoek E., and Brown E.T., 1997, 'Practical estimates of rock mass strength', *International Journal of Rock Mechanics and Mining Sciences*, vol 34, no. 8, pp. 1165-1186.

Hoek E., and Brown E.T., 1980, *Underground excavations in rock*, 1st edn, CRC Press, London.

Hoek E., Carter T.G., and Diederichs M.S. 2013. 'Quantification of the Geological Strength Index chart', *ARMA* 13-672, *47th US Rock Mechanics/Geomechanics Symposium*, San Francisco, June 23-26.

Holley K., Skayman P., and Zhiwei H. 2006, 'Geotechnical design for open pits at Tanjianshan, China', *International Symposium on Stability of Rock Slopes in Open Pit Mining and Civil Engineering, Southern African Institute of Mining and Metallurgy*, Johannesburg, South Africa, pp. 483 - 508.

Hume D. C. 2011, 'Numerical validation and refinement of emperical rock mass modulus estimation', MSc Thesis submitted to the Department of Geological Sciences and Geological Engineering at Queen's University, Department of Geological Sciences & Geological Engineering, Kingston, Ontario, Canada.

Jarosz A., and Wanke D., 2003, 'Use of InSAR for monitoring of mining deformations', *Proceedings of FRINGE 2003 Workshop*, Frascati, Italy.

Laubscher D.H. 1990, 'A geomechanics classification system for the rating of rock mass in mine design', *Journal of the Southern African Institute of Mining and Metallurgy*, vol 90, no. 10, pp. 257-273.

Li S.J., Feng X.T., Li Z.H., Chen B.R., Zhang C.Q., and Zhou H., 2012, 'In-situ monitoring of rockburst nucleation and evolution in the deeply buried tunnels of Jinping II Hydropower Station.', *Engineering Geology*, no. 137-138, pp. 85-96.

Li, S.J., Feng, X.T., Wang, C.Y., and Hudson J.A., 2012, 'ISRM Suggested Method for Rock Fractures Observations Using a Borehole Digital Optical Televiewer'. *Journal of Rock Mechanics and Rock Engineering*, vol 46**,** pp. 635–644.

Martin C.D., Kaiser P.K., and McCreath D.R. 1999, 'Hoek-Brown parameters for predicting the depth of brittle failure around tunnels.', *Canadian Geotechnical Journal*, vol 36, no. 1, pp. 136 - 151.

Mining (Management and Safety) Regulations 1990. SI 1990/109. Harare: Printflow.

MOSHAB. 2000, 'Open pit mining through underground workings', Guideline, Department of Industry and Resources, Western Australia, East Perth, Western Australia.

NGI., 2015, 'Using the Q-system - Rock mass classification and support design'. Handbook.

Nguyen P.M.V., and Niedbalski Z., 2016, 'Numerical modelling of open pit (OP) to underground (UG) transition in coal mining', *Studia Geotechnica et Mechanica*, vol 38, no. 3, pp. 35-48.

Ozbay M.U., Ryder J.A., and Jager A.J. 1995, 'The design of pillar systems as practised in shallow hard-rock tabular mines in South Africa', *Journal of the Southern African Institute of Mining and Metallurgy*, vol 95, no. 1, pp. 7-18.

Paillet F.L., Barton C., Luthi S., Rambow F., and Zemanek J., 1990, *Borehole Imaging*, SPWLA Reprint Series edn, Society of Professional Well Log Analysts, Texas.

Palmstrom A. 1982, 'The volumetric joint count–a useful and simple measure of the degree of rock mass jointing', *Proceedings of the 4th Congress of International Association of Engineering Geology*, New Dehli, pp. 221-228.

Pickering R.G.B., Du Plessis A.G., and Annandale G., 2010, 'Hard-rock room and pillar mining best practice industry workshop', *The 4th International Platinum Conference, Platinum in transition 'Boom or Bust',* The Southern African Institute of Mining and Metallurgy, Sun City, South Africa, pp. 231-238.

Podio-Guidugli P., and Favata A., 2014a, The Boussinesq Problem. 'In: Elasticity for Geotechnicians. Solid Mechanics and Its Applications', vol 204. Springer, Cham, viewed 15 June 2021, <https://doi.org/10.1007/978-3-319-01258-2_5>

Podio-Guidugli P., and Favata A., 2014b, The Flamant Problem. 'In: Elasticity for Geotechnicians. Solid Mechanics and Its Applications', vol 204. Springer, Cham, viewed 15 June 2021, <https://doi.org/10.1007/978-3-319-01258-2_4>

Podio-Guidugli P., and Favata A., 2014c, The Kelvin Problem. 'In: Elasticity for Geotechnicians. Solid Mechanics and Its Applications', vol 204. Springer, Cham, viewed 15 June 2021, <https://doi.org/10.1007/978-3-319-01258-2_6>

Reutech Mining., 2019. An Intergrated Solution Approach, Underground Mining, viewed 14 June 2021, <https://www.reutechmining.com/solutions/?gclid=CjwKCAjw_JuGBhBkEiwA1xmbRfflAd32q_PALC1hAqYflC2_enQvCJ7Rkx_CTA1hG2vQldi8rFQJvRoC8uUQAvD_BwE#underground>

Rocscience, 2019a. 'RS2 Version 10.0'.

Rocscience, 2019b. 'RS3 Version 3.0'.

Sepehri M., Apel D. B., and Hall R. A. 2017, 'Prediction of mining-induced surface subsidence and ground movements at a Canadian diamond mine using an elastoplastic finite element model', *International Journal of Rock Mechanics and Mining Sciences*, vol 100, pp. 73-82.

Severin J., Eberhardt E., Ngidi S., and Stewart A., 2009, 'Importance of understanding 3-D kinematic controls in the review of displacement monitoring of deep open pits above underground mass mining operations', *Proceedings of the 3rd CANUS Rock Mechanics Symposium*, Toronto, Canada.

Stacey T.R. 2018, 'Numerical modelling techniques in rock engineering', Lecture Notes, School of Mining Engineering, University of the Witwatersrand, Johannesburg.

Stacey T.R., and Swart A. H. 2001, 'Evaluation of the stability of underground excavations', in *Practical Rock Engineering Practice for Shallow and Opencast Mines*, SIMRAC, Braamfontein, Johannesburg.

Stacey T.R., and Wesseloo J., 1998, 'In-situ stresses in mining areas in South Africa', *Journal of the Southern African Institute of Mining and Metallurgy*, vol 98, no. 7, pp. 365-368.

Swart A.H., Stacey T.R., Wesseloo J., Joughin W.C., le Roux K., Walker D., and Butcher R., 2000, 'Investigation of factors governing the stability/instability of stope panels in order to define a suitable design methodology for near surface and shallow mining operations', Minerals and Energy, SRK Consulting, OTH 501, Johannesburg.

Swindells C.F., Adhikary D.P., Coulthard M.A., Wang C., Ganeswaren R., and Golosinski T.S. 2000, 'Further research into methods of analysing the stability of deep open pit mines',

Project Report, Australian Centre of Geomechanics, University of Western Australia, Crawley,Western Australia.

Tao Z., Li M., Zhu C., He M., Zheng X., and Yu S., 2018, 'Analysis of the critical safety thickness for pretreatment of mined-out areas underlying the final slopes of open-pit mines and the effects of treatment', *Shock and Vibration*, Article ID 1306535, 8 pages.

Terbrugge, P., Contreras L., & Steffen O., 2009. 'Value and risk in slope design'. *Proceedings of the Slope Stability Conference*, Santiago, Chile, pp. 9-11.

WorkSafe New Zealand., 2016, *Ground or strata instability in underground mines and tunnels*, Wellington, New Zealand, viewed 08 August 2018, <https://worksafe.govt.nz/topic-and-industry/extractives/guidance-position-statements/ground-or-strata-instability-in-underground-mines-and-tunnels/>.

Xu S., Suorineni F.T., An L., Li Y.H., and Jin C.Y., 2019, 'Use of an artificial crown pillar in transition from open pit to underground mining', *International Journal of Rock Mechanics and Mining Sciences*, no. 117, pp. 118-131.

Zimplats Holdings Limited., 2005, 'Zimplats Holdings Limited Intergrated Annual Report'.

Zimplats Holdings Limited., 2012, Mineral Resources and Ore Reserves Statement and JORC Code, viewed 03 September 2018, <https://www.zimplats.com/data/2018/09/Zimplats_Ore_Reserves_Statement.pdf>.

Zimplats Holdings Limited., 2014, 'Zimplats Holdings Limited Intergrated Anual Report'.

Zimplats Holdings Limited., 2017, 'Zimplats Holdings Limited Intergrated Annual Report'.

Zimplats Holdings Limited., 2018, 'Zimplats Holdings Limited Intergrated Annual Report'.

APPENDIX A: Borehole Core Logging Data

Table A-1: Core logging data for Borehole # 75N275E

ZIMPLATS EXPLORATION GEOTECHNICAL LOG SHEET

Page 1 of 2

Hole ID: MSP 003 **75N278E** | **Survey Orient:** | **Core Diameter:** HQ

Location: Rukodzi | **Logged by :** 10.11.15

DEPTHS			MECHANICS											GENERAL		DISCONTINUITIE	Q-RATING CALCULATIONS								
From(m)	To (m)	Interval (m)	Core recovery (m)	Core Recovery (%)	RQD (m)	RQD (%)	Rock type	Mining position	Average Dip	Joint Volume (Jv)	RQD (Palmstrom)	RQD (Palmstrom Corrected)	Oxidation	Presence of Water	UCS Comment	Fract. Type	RQD Final (Deere) - Length >10cm	RQD Final (Palmstrom) - 115-3.3Jv	Joint Set Number (Jn)	Joint Roughness (Jr)	Joint Alteration (Ja)	Joint Water (Jw)	Stress Reduction Factor (SRF)	Q- Value (Deeres RQD)	Q- Value (Palmstroms RQD)
0.00	3.35	3.35	3.35	100%	3.35	100	0.00	HW	78	3.28	104	100	HOX	Y	Weak	J	100	100	20.00	1.50	1.00	0.25	4	0.47	0.47
3.35	6.35	3.00	3.04	101%	3.04	101	BRZ	HW	42	1.00	112	100	HOX	Y	Weak	J	101	100	20.00	2.00	1.00	0.25	4	0.63	0.63
6.35	9.35	3.00	3.00	100%	1.17	39	BRZ	HW	47	2.33	107	100	HOX	Y	Weak	J	39	100	20.00	0.50	2.00	0.25	4	0.03	0.08
9.35	12.35	3.00	3.00	100%	2.62	87	BRZ	HW	53	2.67	106	100	HOX	Y	Weak	J	87	100	20.00	1.50	1.00	0.25	4	0.41	0.47
12.35	15.35	3.00	2.98	99%	2.68	89	BRZ	HW	88	5.00	99	99	POX	S	Strong	J	89	99	9.00	1.50	1.00	0.75	2.5	4.47	4.93
15.35	18.35	3.00	2.95	98%	2.91	97	BRZ	HW	36	0.33	114	100	POX	S	Strong	J	97	100	2.00	2.00	4.00	0.75	2.5	7.28	7.50
18.35	21.35	3.00	3.03	101%	2.90	97	0.00	HW	72	1.67	110	100	POX	S	Strong	J	97	100	9.00	1.50	1.00	0.75	2.5	4.83	5.00
21.35	24.35	3.00	3.05	102%	2.68	89	0.00	HW	72	5.67	96	96	POX	S	Strong	J	89	96	9.00	1.50	1.00	0.75	2.5	4.47	4.82
24.35	27.35	3.00	2.97	99%	2.51	84	0.00	HW	56	4.00	102	100	POX	S	Strong	J	84	100	9.00	2.00	1.00	0.75	2.5	5.58	6.67
27.35	30.35	3.00	3.03	101%	2.88	96	0.00	HW	56	2.00	108	100	POX	S	Strong	J	96	100	9.00	1.50	1.00	0.75	2.5	4.80	5.00
30.35	33.35	3.00	2.85	95%	2.65	88	BRZ	HW	53	1.67	110	100	POX	Y	Strong	J	88	100	9.00	0.50	1.00	0.25	2.5	0.49	0.56
33.35	36.35	3.00	2.45	82%	1.14	38	BRZ	HW	31	0.33	114	100	POX	Y	Strong	J	38	100	2.00	1.50	1.00	0.25	2.5	2.85	7.50
32.98	33.89	0.91	0.91	100%	3.00	330	BRZ	HW	68	13.19	71	71	POX	Y	Strong	J	330	71	9.00	1.50	1.00	0.25	2.5	5.49	1.19
33.89	36.89	3.00	3.00	100%	2.95	98	BRZ	HW	55	5.33	97	97	POX	Y	Strong	J	98	97	9.00	1.50	1.00	0.25	2.5	1.64	1.62
36.89	39.89	3.00	3.00	100%	3.00	100	BRZ	HW	60	8.67	86	86	POX	Y	Strong	J	100	86	9.00	2.00	1.00	0.25	2.5	2.22	1.92
39.89	42.12	2.23	2.23	100%	3.00	135	BRZ	HW	51	5.38	97	97	POX	Y	Strong	J	135	97	9.00	1.50	1.00	0.25	2.5	2.24	1.62
42.12	43.99	1.87	1.87	100%	2.73	146	BRZ	HW	57	6.95	92	92	POX	Y	Strong	J	146	92	9.00	1.50	1.00	0.25	2.5	2.43	1.53
43.99	44.82	0.83	0.83	100%	3.00	361	BRZ	HW	47	8.43	87	87	POX	Y	Strong	J	361	87	9.00	2.00	1.00	0.25	2.5	8.03	1.94
44.82	45.97	1.15	1.15	100%	3.00	261	BRZ	HW	60	11.30	78	78	POX	Y	Strong	J	261	78	9.00	2.00	1.00	0.25	2.5	5.80	1.73
45.97	47.62	1.65	1.65	100%	2.34	142	BRZ	HW	66	5.45	97	97	POX	Y	Strong	J	142	97	9.00	2.00	1.00	0.25	2.5	3.15	2.16
47.62	49.28	1.66	1.66	100%	2.95	178	BRZ	HW	66	4.22	101	100	POX	Y	Strong	J	178	100	9.00	2.00	1.00	0.25	2.5	3.95	2.22
49.28	50.28	1.00	1.00	100%	2.85	285	BRZ	HW	66	9.00	85	85	POX	Y	Strong	J	285	85	9.00	2.00	1.00	0.25	2.5	6.33	1.90
50.28	52.30	2.02	2.02	100%	2.90	144	BRZ	HW	48	2.97	105	100	POX	Y	Strong	J	144	100	9.00	2.00	1.00	0.25	2.5	3.19	2.22
52.30	53.74	1.44	1.50	104%	3.00	208	BRZ	HW	51	2.78	106	100	POX	Y	Strong	J	208	100	9.00	2.00	1.00	0.25	2.5	4.63	2.22
53.74	57.15	3.41	3.41	100%	2.64	77	BRZ	HW	42	0.59	113	100	POX	Y	Strong	J	77	100	2.00	1.50	1.00	0.25	2.5	5.81	7.50
57.15	60.15	3.00	3.00	100%	2.92	97	BRZ	HW	47	2.33	107	100	POX	Y	Strong	J	97	100	9.00	2.00	1.00	0.25	2.5	2.16	2.22
60.15	61.46	1.31	1.40	107%	3.00	229	BRZ	HW	55	0.76	112	100	POX	Y	Strong	J	229	100	2.00	2.00	4.00	0.25	2.5	5.73	2.50
61.46	63.53	2.07	2.07	100%	2.10	101	BRZ	HW	47	0.97	112	100	POX	S	Strong	J	101	100	2.00	2.00	1.00	0.75	2.5	30.43	30.00
63.53	66.71	3.18	3.18	100%	2.70	85	BRZ	HW	48	1.89	109	100	POX	Y	Strong	J	85	100	9.00	2.00	1.00	0.25	2.5	1.89	2.22
66.71	67.71	1.00	1.00	100%	3.00	300	BRZ	HW	55	1.00	112	100	POX	Y	Strong	J	300	100	2.00	2.00	4.00	0.25	2.5	7.50	2.50
57.15	60.15	3.00	3.00	100%	2.92	97	BRZ	HW	48	1.67	110	100	POX	Y	Strong	J	97	100	9.00	2.00	1.00	0.25	2.5	2.16	2.22
60.15	61.46	1.31	1.40	107%	3.00	229	BRZ	HW	55	0.76	112	100	POX	Y	Strong	J	229	100	2.00	2.00	4.00	0.25	2.5	5.73	2.50
61.46	63.53	2.07	2.07	100%	2.10	101	BRZ	HW	47	1.93	109	100	POX	Y	Strong	J	101	100	9.00	2.00	1.00	0.25	2.5	2.25	2.22
63.53	66.71	3.18	3.18	100%	2.70	85	BRZ	HW	48	1.89	109	100	POX	Y	Strong	J	85	100	9.00	2.00	1.00	0.25	2.5	1.89	2.22
67.71	69.79	2.08	2.08	100%	2.52	121	BRZ	HW	48	6.73	93	93	POX	Y	Strong	J	121	93	9.00	3.00	1.00	0.25	2.5	4.04	3.09
69.79	72.79	3.00	3.00	100%	1.77	59	BRZ	HW	46	2.33	107	100	POX	Y	Strong	J	59	100	9.00	1.50	1.00	0.25	2.5	0.98	1.67
72.79	75.35	2.56	2.56	100%	2.06	80	BRZ	HW	55	0.78	112	100	POX	Y	Strong	J	80	100	2.00	2.00	4.00	0.25	2.5	2.01	2.50
75.35	78.14	2.79	2.79	100%	0.56	20	BRZ	HW	38	0.72	113	100	POX	Y	Strong	J	20	100	2.00	1.50	1.00	0.25	2.5	1.51	7.50
78.14	81.22	3.08	3.08	100%	0.87	28	BRZ	HW	40	0.32	114	100	POX	Y	Strong	J	28	100	2.00	1.50	4.00	0.25	2.5	0.53	1.88
81.22	82.32	1.10	1.10	100%	0.82	75	BRZ	HW	38	0.91	112	100	POX	Y	Strong	J	75	100	2.00	2.00	4.00	0.25	2.5	1.86	2.50
82.32	85.71	3.39	3.39	100%	2.73	81	BRZ	HW	66	2.36	107	100	POX	Y	Strong	J	81	100	9.00	2.00	4.00	0.25	2.5	0.45	0.56
85.71	88.71	3.00	3.00	100%	0.40	13	BRZ	HW	44	1.33	111	100	POX	Y	Strong	J	13	100	2.00	1.50	1.00	0.25	2.5	1.00	7.50
88.71	89.73	1.02	1.02	100%	1.44	141	BRZ	HW	85	1.96	109	100	POX	Y	Strong	J	141	100	4.00	2.00	1.00	0.25	2.5	7.06	5.00
89.73	93.51	3.78	3.78	100%	0.51	13	BRZ	HW	59	1.59	110	100	POX	Y	Strong	J	13	100	9.00	2.00	1.00	0.25	2.5	0.30	2.22
93.51	94.48	0.97	0.97	100%	0.90	93	BRZ	HW	80	2.06	108	100	POX	Y	Strong	J	93	100	4.00	1.50	4.00	0.25	2.5	0.87	0.94

Table A-2: Corresponding ratings for parameters used in the calculation of Q-value

JOINT SET NUMBER (Jn)		
JOINT SET	INITIAL	Jn VALUE
Massive, few random joints	0.5	1
One joint set	1	2
Two joint sets	2	4
Three joint sets	3	9
Four or more joint sets, random heavily jointed	4	15
Crushed rock	10	20

JOINT WATER (Jw)			
OXIDATION	INITIAL	COMMENT	Jw VALUE
Oxidised Rock	ROX	M	0.5
Fresh	FRS	N	1
Partially Oxidised Rock	POX	S	0.75
Highly Oxidised	HOX	Y	0.25
Soil	SOL	Y	0.25
NOTE: NO (N), SLIGHTLY (S), MODERATE (M), YES (Y)			

JOINT ROUGHNESS NUMBER (Jr)			
DESCRIPTION	COMMENT	VALUE	
Discontinuous joints	F	4	F
Slickensided (undulating/ planar)	K	0.5	K
Smooth (planar)	P	1	P
Rough or irregular (planar)	R	1.5	R
Smooth (undulating)	S	2	S
Rough or irregular (undulating)	V	3	V

STRESS REDUCTION FACTOR (SRF)	
DESCRIPTION	VALUE
No shear, faults	1
No fault/shear/Blocky ground/Curved joints	1.5
One shear/fault	2.5
Two faults not intersecting in block	3.5
One fault and Curved joints	4
Two faults and intersecting in block	7.5
Multiple faults/Wide shears mylonite zones	10

JOINT ALTERATION NUMBER (Ja)			
DESCRIPTION	CLASSIFICATION	COMMENT	VALUE
Zones or bands of disintegrated or crushed filling	Crushed rock	CR	12
Clayey Joint filling > 1cm	Extremely open	E	8
Joint filling > 1mm but <3mm	Moderately open	M	2
Joint filling > 3mm	Open	O	4
Slight infill coating < 1mm	Tight	T	1
Tightly healed, hard rockwall joints, no filling	Very tight	V	0.5

GROUND CLASS	
DESCRIPTION	CLASS
Q > 10	A
4 < Q < 10	B
1 < Q < 4	C
Q < 1	D

APPENDIX B: Rukodzi Mine Material Properties

Table B-1 Material Properties

Uniaxial Compressive Strength Test Results (Rukodzi Mine)

Specimen	Sample No	Depth from (m)	Depth to (m)	Density g/cm^3	UCS (MPa)	Poisson's ratio (v)	E (GPa)
1	CW91H/W0	200.25	200.75	3.24	222	0.23	143
2	CW91H/W0	208.40	208.50		247		
3	CW72H/W0	182.50	182.62	3.06	235	0.25	142
4	CW72H/W1	194.40	194.52	3.22	169	0.22	128
5	NG43H/W0	331.58	331.70	3.32	228	0.24	157
6	NG43H/W0	353.09	353.21	3.26	184	0.24	154
7	CC107H/W0	336.59	336.72	3.30	254	0.25	155
8	CC107H/W0	250.38	358.51	3.30	268	0.24	158
Average				**3.24**	**226**	**0.24**	**148**

Brazilian Tensile Strength Test Results (Ngwarati Mine)

Specimen	Sample No	Depth from (m)	Depth to (m)	Density g/cm^3	Mass (g)	Failure Load (kN)	Tensile Strength (MPa)
1	UTB-01A	72.60	72.95	3.05	129.8	22.7	12.65
2	UTB-01B	73.26	73.80	3.08	128.3	22.6	12.93
3	UTB-01C	75.04	75.45	3.06	141.0	24.3	12.60
Average				**3.06**		**23.2**	**12.73**

Triaxial Compressive Strength Test Results (Mupfuti Mine)

Specimen	Sample No	Depth from (m)	Depth to (m)	Density g/cm^3	σ_3 Confining Pressure (MPa)	σ_1 Strength (TCS) (MPa)
1	TCS-21	93.36	93.52	3.26	5	238.2
2	TCS-14	75.65	75.80	3.25	10	268.0
3	TCS-23	96.66	96.82	3.27	15	301.0
4	TCS-12	70.66	70.82	3.27	20	307.0

B2: Determination of σ_{ci} and m_i values

According to Hoek and Brown (1997) the following parameters and equations are used to derive values for the intact rock compressive strength, σ_{ci} and H-B constant, m_i:

$x = \sigma_3$ and $y = (\sigma_1 - \sigma_3)^2$. Where, σ_1 and σ_3 are the major and minor principal stresses recorded in the triaxial tests.

$$\sigma_{ci}{}^2 = \frac{\sum y}{n} - \left[\frac{\sum xy - (\sum x \sum y/n)}{\sum x^2 - ((\sum x)^2/n)}\right]\frac{\sum x}{n}$$

$$m_i = \frac{1}{\sigma_{ci}}\left[\frac{\sum xy - (\sum x \sum y/n)}{\sum x^2 - ((\sum x)^2/n)}\right]$$

And the coefficient of determination r^2 is given by:

$$r^2 = \frac{[\sum xy - (\sum x \sum y/n)]^2}{[\sum x^2 - ((\sum x)^2/n)][\sum y^2 - ((\sum y)^2/n)]}$$

Table B-2 Spreadsheet for the calculation of σ_{ci} and m_i

Parameter	x		y	xy	x(squared)	y(squared)
	5	238	54289	271445	25	2947295521
	10	268	66564	665640	100	4430766096
	15	301	81796	1226940	225	6690585616
	20	307	82369	1647380	400	6784652161
Total	**50**	**1114**	**285018**	**3811405**	**750**	**20853299394**

n	4
sigma σ(ci)	215
mi	9.25
r-squared	0.91

APPENDIX C: Zimplats Stress Measurements

Measurement name	Site 1 - Bimha South	Site 2 - Bimha North	Site 3 - Mupfuti
Location	22 S 17	44 N 14	92 N 29
Depth below surface (m)	175 m	243 m	161 m
Principal Stresses			
σ_1 *(MPa)*	**11.8**	**12.5**	**8.4**
Bearing (degrees from N)	28	317	322
Dip (degrees)	56	46	4
σ_2 *(MPa)*	**6.9**	**9.9**	**7.5**
Bearing (degrees from N)	119	71	67
Dip (degrees)	3	22	75
σ_3 *(MPa)*	**3.0**	**4.8**	**5.3**
Bearing (degrees from N)	211	178	231
Dip (degrees)	34	37	14
Stresses in Eastings-Northings-Vertical coordinate system			
σ_V *(MPa)*	**9.1**	**9.4**	**7.4**
Standard error (MPa)	0.5	0.8	0.1
σ_{NS} *(MPa)*	**6.1**	**7.3**	**7.3**
Standard error (MPa)	1.0	1.2	0.1
σ_{EW} *(MPa)*	**6.4**	**10.5**	**6.6**
Standard error (MPa)	0.5	0.4	0.2
τ_{NE} *(MPa)*	**-0.6**	**-0.5**	**-1.4**
Standard error (MPa)	0.4	0.4	0.1
τ_{EV} *(MPa)*	**1.9**	**-1.0**	**0.4**
Standard error (MPa)	0.3	0.3	0.1
τ_{VN} *(MPa)*	**3. 6**	**3.4**	**0.4**
Standard error (MPa)	0.6	0.6	0.1
Ave. standard error (MPa)	**±0.6**	**±0.6**	**±0.1**
Quality of measurement	Very good	Very good	Excellent

APPENDIX D: Hoek-Brown Parameters

Rock Mass

Material Color	
Initial Element Loading	Field Stress and Body Force
Unit Weight	0.032 MN/m3
Elastic Type	Isotropic
Poisson's Ratio	0.24
Young's Modulus	148000 MPa
Failure Criterion	Generalized Hoek-Brown
Material Type	Elastic
Compressive Strength	215 MPa
mb Parameter	1.16555
s Parameter	0.001589
a Parameter	0.509923
GSI Parameter	42
mi Parameter	9.25
D Parameter	0
Tensile Cutoff Type	0
Material Behaviour	Drained
Porosity Value	0.5
Static Water Mode	Dry

Backfill

Material Color	
Initial Element Loading	Body Force Only
Unit Weight	0.023 MN/m3
Elastic Type	Isotropic
Poisson's Ratio	0.15
Young's Modulus	2000 MPa
Failure Criterion	Generalized Hoek-Brown
Material Type	Elastic
Compressive Strength	7.5 MPa
mb Parameter	1
s Parameter	0.001
a Parameter	0.5
Tensile Cutoff Type	0
Material Behaviour	Drained
Porosity Value	0.5
Static Water Mode	Dry

APPENDIX E: RS2 Query Results

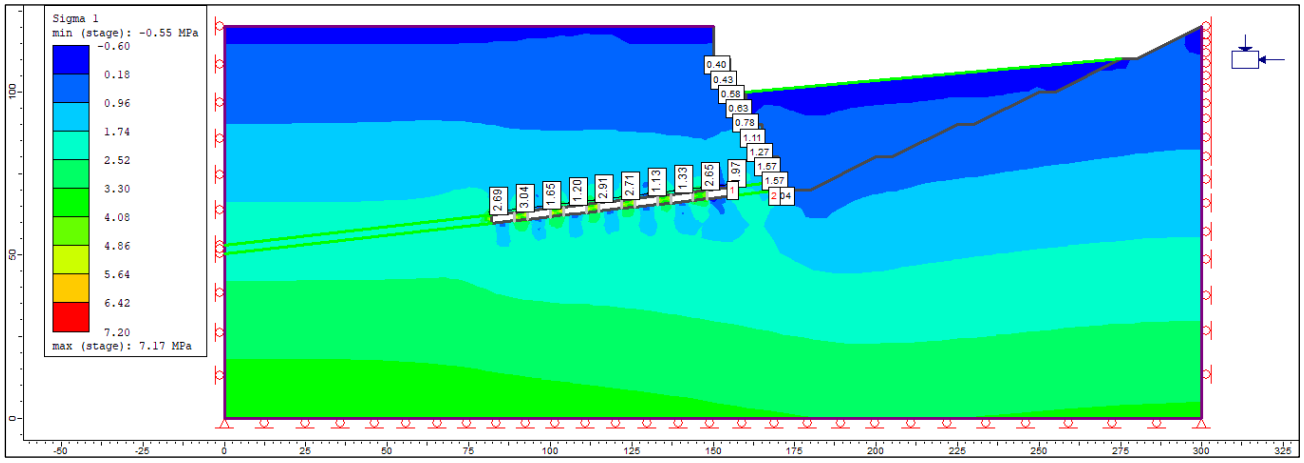

E1: Scenario 1 stress (σ_1) material queries

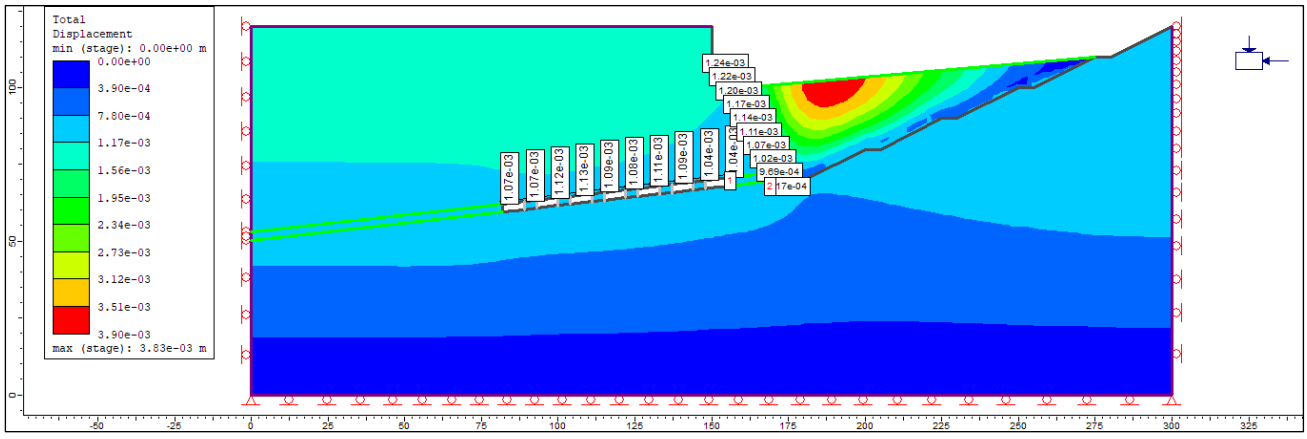

E2: Scenario 1 total displacements material queries

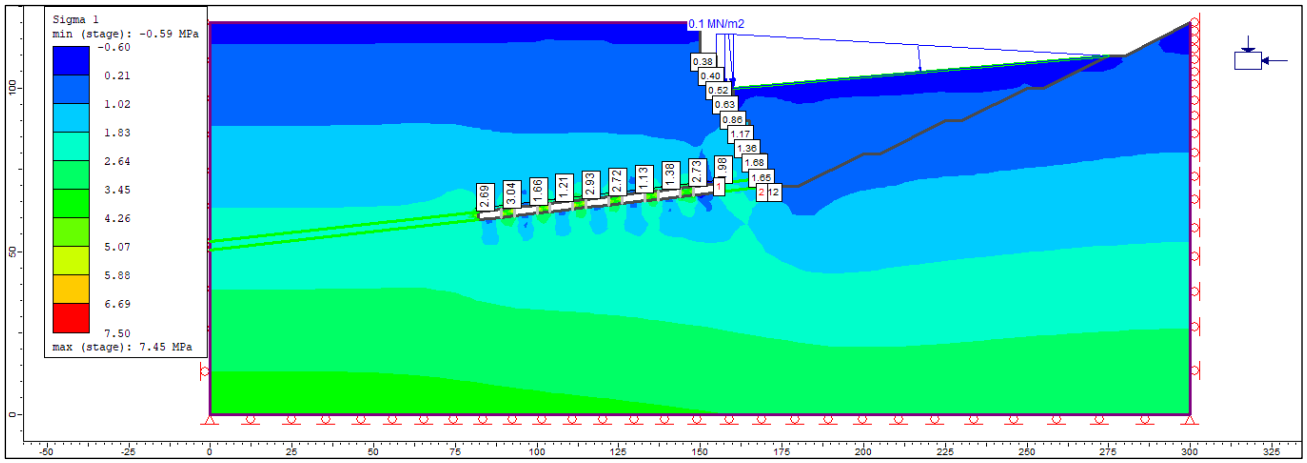

E3: Scenario 2 stress (σ_1) material queries

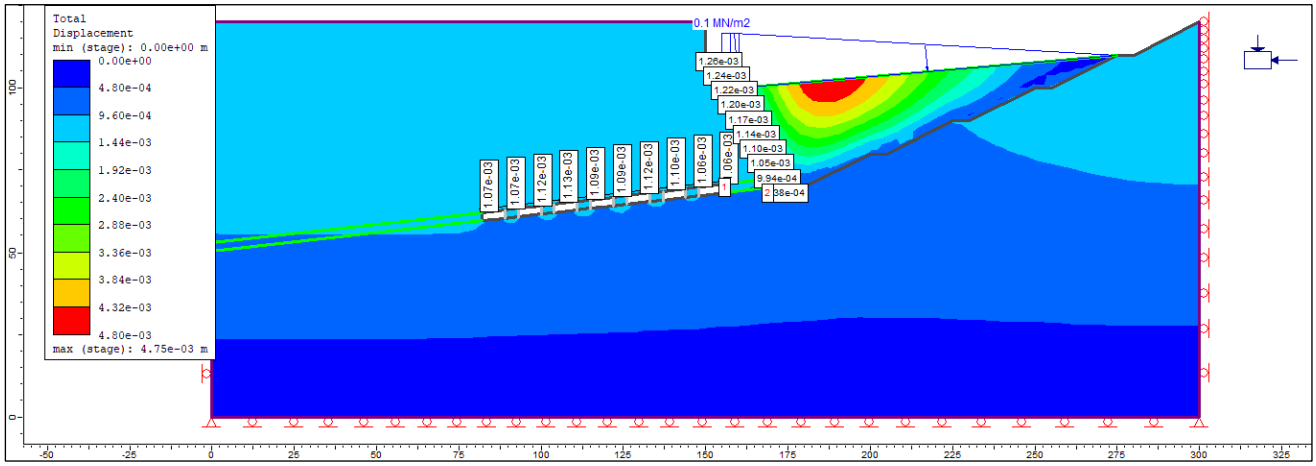

E4: Scenario 2 total displacements material queries

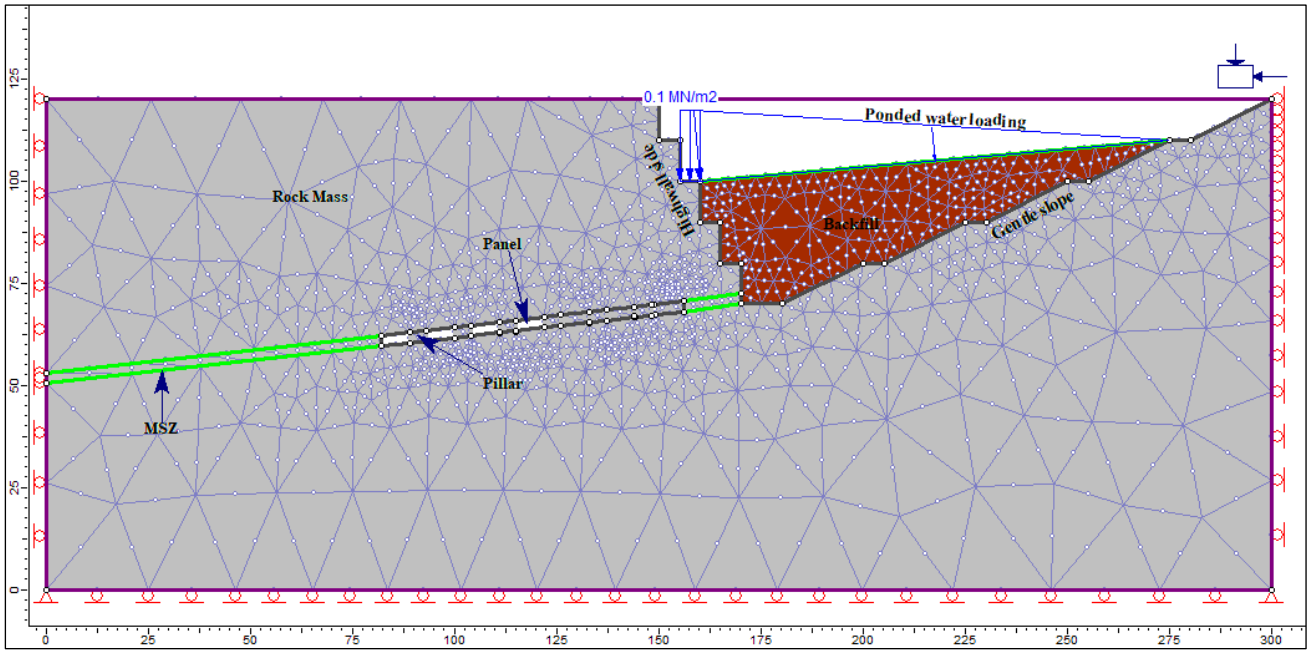

E5: Scenario2 RS2 model